

**Characterisation and validation of  
drug transport and GLP-1R function  
in primary porcine proximal tubular cells**

Inauguraldissertation

zur

Erlangung der Würde eines Doktors der Philosophie

vorgelegt der

Philosophisch-Naturwissenschaftlichen Fakultät

der Universität Basel

von

**Philipp Schlatter**

aus Basel Stadt, Schweiz

Basel, 2006

Genehmigt von der Philosophisch-Naturwissenschaftlichen Fakultät auf Antrag von

Prof. Jürgen Drewe

Prof. Jörg Huwiler

Basel, den 24.10.2006

Prof. Dr. H.-P. Hauri  
Dekan

## Acknowledgements

### Danksagung

Als erstes möchte ich mich bei meiner Frau und unseren Kindern bedanken, die mich während der Dissertation unterstützt und mit mir Freude und Frust geteilt haben. Meine älteste Tochter hat immer wieder nach dem Wohlbefinden der Nierenzellchen gefragt (manchmal war es keine gute Frage).

Die drei Jahre im Labor 411 sind im wahrsten Sinn des Wortes wie im Fluge vergangen. Zumindest habe ich es so empfunden. Dies habe ich vor allem der wirklich sehr guten Betreuung durch Jürgen und Heike zu verdanken. Den üblichen Problemen und Schwierigkeiten des Experimentierens, ohne die das Leben langweilig wäre, konnten sie mit vielen Ideen und Lösungen entgegenhalten.

Dank der guten Arbeitsatmosphäre war die Motivation selbst durch unvollständig (oder gar nicht?) funktionierende Experimente nicht totzukriegen. In ganz schlimmen Fällen waren es auch hier Jürgen und Heike, die aufbauten und einem wieder Hoffnung gaben. Vielen Dank!

Erstaunt und beeindruckt war und bin ich heute noch, dass Jürgen trotz seiner vielen Termine immer Zeit für uns findet und für die Schwierigkeiten Verständnis und Lösungen zeigte. Das ist nicht selbstverständlich, und ich weiss es sehr zu schätzen. Vielen Dank, Jürgen!

Uschi, ein Juwel, hatte für das Funktionieren des Labors gesorgt, damit der Materialschlacht die Munition (Pipetten, Platten, ...) nicht ausging.

Ich vermisse jetzt schon unsere gemeinsamen morgendlichen, von klassischer Musik begleiteten Nierenisolationen (16 Mal!).

Manisha hat diesbezüglich mit einem Alternativprogramm aufgewartet: Es gab Hirnisolationen. So manch einer wurde am Morgen etwas bleicher. Aber ich konnte durch ihr Projekt mit primären Zellen profitieren, da die Probleme oft ähnlicher Natur waren.

Christian war mit seiner mehrjährigen Erfahrung in Taqman und RT eine wunderbare Unterstützung, die ich oft in Anspruch nehmen konnte.

Marco hatte durch sein Beispiel gezeigt, wie man Effizienz und Schnelligkeit vereint, so wurde es nie zu ruhig im Labor.

Angelika und Birk, die "Neuen" im Bunde, haben das Labor vor dem Aussterben bewahrt und durch ihre frischen Ideen belebt.

Danken möchte ich auch den 410er für die gute Zeit, die wir verbringen konnten: Andrea, Anja, Bettina, Katri (durch sie konnte ich meine Finnischkenntnisse auf dem laufenden halten), Katarina, Michael, Priska und Saskia. Liliane und Markus waren bei der Betreuung der Diplomarbeit von Dorina Saurer eine grosse Hilfe, wenn es um HPLC ging.

Auch wenn TDM und Klips-Anfragen manchmal den Experimentierfluss unterbrachen, war es eine tolle Erfahrung. Hier möchte ich mich vor allem bei Alexandra für die Mühe und Geduld bedanken.

Vielen Dank auch an Jörg Huwylar für die Übernahme des Korreferates und Prof. Hamburger für den Prüfungsvorssitz meiner Dissertationsprüfung.

Unsere Wege trennen sich. Dieser Moment war abzusehen, doch er kam schneller als gedacht. Ich hoffe, dass wir auf die eine oder andere Weise noch Kontakt haben werden. Das Labor 411 wird mir in bester Erinnerung bleiben, vielen vielen Dank für alles.

## Abbreviations

ABC	ATP binding cassette
ACE	angiotensin converting enzyme
AST-120	oral charcoal adsorbent
ATP	adenosine-5'-triphosphate
AUC	area under the plasma concentration-time curve
AZT	azidothymidine alias zidovudine
BCRP	breast cancer resistance protein
BMDP	brain multidrug resistance protein
cAMP	cyclic adenosine monophosphate
cGMP	cyclic guanosine monophosphate
CHP	calcineurin B homologous protein
CT	threshold cycle
DOTATOC	somatostatin analogue: [1,4,7,10-tetraazacyclododecane-N,N',N'',N'''-tetraacetic-acid-D-Phe1-Tyr3 ]-octreotide
DPPIV	dipeptidylpeptidase IV
FITC	fluorescence marker
FTC	fumitremorgin C
P-gp	P-glycoprotein alias MDR1
GAPDH	glyceraldehyde-3-phosphate dehydrogenase
GLP-1R	glucagon like peptide receptor
GLUT	facilitative sodium independent sugar transporter
HEK	human embryonic kidney
HIV	human immunodeficiency virus
HK2	immortalised human proximal tubular cells
HKC	human kidney epithelial cell line
kDa	kilo Dalton
$K_M$	Michaelis constant
LLC-PK1	immortalised porcine proximal tubule cell line
MDCK	Madin-Darby canine kidney
MDR	multi-drug resistance
MK571	cysteinyl leukotriene 1 receptor antagonist

mRNA	messenger ribonucleic acid
MRP	multi-drug resistance associated protein
MTX	methotrexate
NBC	$\text{Na}^+ / \text{HCO}_3^-$ cotransporter
NBF	nucleotide-binding fold/domain
NHE	$\text{Na}^+/\text{H}^+$ exchanger
NSAID	non-steroidal anti-inflammatory drugs
OAT	organic anion transporter
OATP	organic anion transporting polypeptide
OCT	organic cation transporter
PAH	para-aminohippuric acid
$P_{\text{app}}$	apparent permeability coefficient
PDZ	post synaptic density protein, <i>Drosophila</i> disc large tumour suppressor and $\alpha$ -1 protein
PEPT	peptide transporter
PhIP	2-amino-1-methyl-6-phenylimidazo[4,5-b]pyridine, a dietary carcinogen
PHT	peptide and histidine transporter
PPPTC	primary porcine proximal tubular cell
RT-PCR	reverse transcription polymerase chain reaction
SGLT	sodium-dependent glucose cotransporter
SLC	solute carrier
SNP	single nucleotide polymorphism
T3	triiodothyronine
TEER	transepithelial electrical resistance
TM	transmembrane domain

## Table of contents

<b>Acknowledgements</b>	<b>3</b>
<b>Abbreviations</b>	<b>5</b>
<b>Table of contents</b>	<b>7</b>
<b>Summary</b>	<b>10</b>
<b>Aim of the thesis</b>	<b>13</b>
<b>1. Introduction</b>	<b>15</b>
1.1. Kidney – an overview	15
1.2. Transporters	16
1.2.1. ABCB1 (MDR 1) and members of ABCB	18
1.2.2. ABCC1-6 (MRP 1-6) and members of ABCC	19
1.2.3. ABCG2 (BCRP) and members of ABCG	21
1.2.4. SLC4A4 (NBC1)	22
1.2.5. SLC5A1/2 (SGLT1/2)	23
1.2.6. SLC9A3 (NHE3)	24
1.2.7. SLC15A1/2 (PEPT1/2)	25
1.2.8. SLC21A (OATP)	27
1.2.9. Overview of the SLC22A family	28
1.2.9.1. SLC22A1-3 (OCT 1-3)	28
1.2.9.2. SLC22A6-8, 11, 10 (OAT 1-5)	29
1.3. Proximal tubular cells – which species?	31
<b>2. Primary porcine proximal tubular cells as a model for transepithelial drug transport in human kidney</b>	<b>32</b>
2.1. Abstract	33
2.2. Introduction	33
2.3. Materials	36
2.4. Functional characterisation of transporters	36
2.4.1. Cell Culture	36
2.4.2. Transepithelial electrical resistance (TEER) measurement	37
2.4.3. Functional assays	38

2.4.4.	PCR	39
2.4.5.	Sequencing of slc15a1 (PEPT1) and slc22a8 (OAT3) PCR Products	40
2.4.6.	Confocal microscopy	40
2.4.7.	Statistical analysis	41
2.5.	Results	41
2.5.1.	Expression of transporters at mRNA level	41
2.5.2.	Sequencing	42
2.5.3.	Functional assay	43
2.5.4.	Uptake of fluorescein in viable cells	45
2.5.5.	Immunostaining	45
2.6.	Discussion	47
2.6.1.	Expression of transporters on mRNA level	47
2.6.2.	Protein expression	48
2.6.3.	Tightness	48
2.6.4.	ABCB1 (P-gp)	49
2.6.5.	ABCC1-6 (MRP1-6)	50
2.6.6.	Slc22a6/8 (OAT1/3)	50
2.6.7.	Slc15a1/2 (PEPT1/2)	51
2.6.8.	Slc5a1/2 (SGLT1/2)	51
2.6.9.	Transporters in other cell lines	52
2.6.10.	Final conclusion	52
<b>3.</b>	<b>Functional expression of BMDP in kidney</b>	<b>54</b>
3.1.	Abstract	55
3.2.	Introduction	55
3.3.	Methods	57
3.3.1.	Materials	57
3.3.2.	Cell Culture	57
3.3.3.	RT-PCR for BMDP standards	57
3.3.4.	Real-time Polymerase Chain Reaction (TaqMan® Assay)	58
3.3.5.	Sequencing of GAPDH and BMDP PCR products	59
3.3.6.	Confocal microscopy	59
3.3.7.	Western blot analysis	60



3.3.8.	Functional assays	61
3.3.9.	Statistical analysis	61
3.4.	Results	61
3.5.	Discussion	64
<b>4.</b>	<b>Glucagon-like 1 receptor expression in primary porcine proximal tubular cells</b>	<b>69</b>
4.1.	Abstract	70
4.2.	Introduction	71
4.3.	Materials and Methods	72
4.3.1.	Materials	72
4.3.2.	Cell Culture	72
4.3.3.	RT-PCR	72
4.3.4.	Real-time Polymerase Chain Reaction (TaqMan® Assay)	74
4.3.5.	Sequencing of SLC9A3 (NHE3), DPPIV, GLP-1R and GAPDH PCR products	74
4.3.6.	Confocal microscopy	75
4.3.7.	Immunohistochemistry	75
4.3.8.	Western blot analysis	76
4.3.9.	Functional assays	77
4.3.10.	Cytotoxicity assay	78
4.3.11.	Statistical analysis	78
4.4.	Results	78
4.5.	Discussion	81
<b>5.</b>	<b>Conclusions and outlook</b>	<b>87</b>
<b>6.</b>	<b>References</b>	<b>88</b>
	<b>Curriculum vitae</b>	<b>100</b>

## Summary

### Overview kidney

Kidney is, beside the liver, one of the most important organs for the elimination of waste products, toxins, drugs and their metabolites. Due to the anatomy of the kidney, ultra filtrate leaving the glomerulus passes first the proximal tubular cells. Therefore, these cells are exposed to high concentrations of xenobiotics which explains their high metabolic activity. This circumstance results sometimes in proximal tubular nephrotoxicity. In addition, various transmembrane proteins respectively transporters are responsible for the elimination or accumulation of drugs. This complex interplay is also responsible for drug-drug interactions.

Therefore, proximal tubular cells are an interesting tool to study drug transport in the kidney. These cells are mainly localised in kidney cortex which makes it easy to isolate them (Fig. 1.1). Further isolation procedures enables high purity of proximal tubular cells by excluding connective tissue cells, distal tubular cells and other undesirable cells (elucidated in detail in 2.4).

### Aim of the thesis

The aim of this thesis was to establish and validate a new in vitro model for drug transport in kidney by using primary porcine proximal tubular cells.

In a first step, primary porcine proximal tubular cells were isolated from pig kidney, which were retrieved freshly at the slaughterhouse. These isolated cells were investigated to verify their origin from proximal tubular cells. In a next step the cells were screened at mRNA, protein and functional level for functional expression of important drug transporters. Finally, it was investigated if this model can be used for screening of drug-drug interactions or for specific drug transporter properties.

### Expression of drug transporters

In cultured cells the following drug transporters were expressed (chapter 2.5 and 3.4)

A) at mRNA level:

- abcb1 (pMDR1)
- abcc1 (pMRP1)
- abcc2 (pMRP2)
- slc22a8 (pOAT3)
- slco1a2 (pOATP-A)
- slc15a1 (pPEPT1)

- slc5a2 (pSGLT2)
- slc4a4 (pNBC1)
- slc9a3 (pNHE3)
- abcg2 (pBCRP alias BMDP)

B) at protein level

- slc4a4
- abcb1
- abcc1
- abcc2
- abcg2

C) functionally

- abcb1: transport and uptake of digoxin, inhibition of digoxin transport and higher digoxin uptake with verapamil
- abcc1: uptake of methotrexate, higher methotrexate uptake with indomethacin and MK571
- abcc2: uptake of methotrexate, higher methotrexate uptake with MK571
- slc22a8: transport and uptake of fluorescein, inhibition of fluorescein transport and uptake with estrone sulfate
- slc15a1: transport and uptake of glycylsarcosine, inhibition of glycylsarcosin transport and uptake with benzylpenicillin
- slc5a2: uptake of glucose, inhibition of glucose uptake with phlorizin
- abcg2: uptake of mitoxantrone, higher mitoxantrone uptake with prazosin

Slc22a1 (pOCT1) and slc22a6 (pOAT1) were only expressed in freshly isolated cells but were down-regulated in culture. Freshly isolated proximal tubular cells showed functional activity of slc22a6 as uptake of fluorescein was inhibited with p-aminohippuric acid.

Confirmation of proximal origin

Several transporters are expressed exclusively in proximal tubular cells. This fact was used in order to confirm the origin of the proximal tubular cells with each isolation. Due to expression of slc15a1, slc5a2, slc4a4, slc9a3 and the enzyme dipeptidylpeptidase IV (DPPIV, see below) we confirmed, that our cells are indeed of proximal origin.

### BMPD expression

After validation of the above mentioned drug transporters, we searched for possible inhibitors of BMDP/pBCRP, that might influence elimination of known BCRP substrates such as the chemotherapeutics topo- and irinotecan and mitoxantrone. The tested drugs included various antiepileptic agents, non-steroidal anti-inflammatory drugs, proton pump inhibitor, caffeine, theophylline, thalidomide and dotatoc. Of all investigated drugs, only phenytoin was able to inhibit BMPD significantly in our model.

### GLP-1 effect in proximal tubular cells

Glucagon like peptide 1 (GLP-1) is an hormone, secreted after meal ingestion in the intestine. This peptide mediates satiety feelings and most importantly stimulates glucose dependent insulin secretion from pancreatic  $\beta$ -cells, thus lowering plasma glucose levels. Interestingly, GLP-1 also enhances renal sodium secretion in healthy volunteers. Therefore, we hypothesised that GLP-1 receptor (GLP-1R) is functionally expressed in proximal tubular cells. GLP-1R expression was confirmed at mRNA and protein level (chapter 4.4). More precisely, in kidney cortex the protein expression of GLP-1R seemed to be localised mainly in proximal tubular cells. Furthermore, we could show an inhibitory effect of GLP-1 on sodium re-absorption, indicating functional GLP-1R activity. In contrast to sodium re-absorption the re-absorption of glucose was not affected by GLP1.

## Aim of the thesis

Our objective was to establish and validate a new in vitro model for human drug transport in kidney. Though established cell lines of proximal tubular cells exist (e.g. LLC-PK1, HK-2, killifish renal tubules), they are either immortalised and often transfected or the assessment of functional bidirectional transport is not possible. With **primary** proximal tubular cells a more “in-vivo” like situation, where various drug transporters are expressed simultaneously, is established. We decided to use primary proximal tubular cells from pigs since this material is easy to obtain. Furthermore, pig seems to be physiologically more closely related to human than other species such as dog, rat, mouse and rabbit.

A first aim was to establish a cell culture model of primary proximal tubular cells from porcine. Therefore, fresh porcine kidneys were obtained from the slaughterhouse followed by an immediate isolation procedure. The origin from proximal tubular cells of these isolated cells had to be verified.

A next aim was to investigate if important drug transporters of proximal tubular cells are functionally expressed in our cell culture model. Therefore a screening of various known drug transporters had to be performed at mRNA and protein level. In addition, uptake and/or transport assays had to be carried out in order to show in-vitro functional activity of these proteins.

A next aim of the thesis was to investigate for the first time the functional expression of the porcine homologue of breast cancer resistance protein (BCRP/BMDP) in proximal tubular cells. Furthermore, we aimed at a functional discrimination of BMDP and P-gp activity. Therefore, cells had to be screened as mentioned above. For uptake assays specific substrates and inhibitors for BMDP and P-gp should be used.

Another aim was to investigate the functional expression of glucagon like peptide receptor in proximal tubular cells. Therefore, proximal tubules had to be screened for GLP-1R at mRNA and protein level. In order to measure sodium concentration with fluorescence, a method had to be established. Then the effect of GLP-1 in proximal tubular cells on sodium and glucose re-absorption had to be investigated.

With such an validated in-vitro model expressing various functional transporters simultaneously, it would be possible to predict tubular excretion rates, nephrotoxicity and

drug-drug interactions in an early stage of drug discovery and development more realistically.

# 1. Introduction

## 1.1. Kidney – an overview

In mammals, the kidney is a pivotal control organ for the homeostasis of fluids, electrolytes, proteins and glucose. Excess of water and substances results in enhanced excretion. However, a lack of water and electrolytes causes the kidney to enhance re-absorption, but maintaining the excretion of waste products, toxic products and drugs. In kidney, xenobiotics undergo three different processes: glomerular filtration, tubular secretion and tubular re-absorption. Secretion and re-absorption are mediated by transmembrane transport proteins of renal tubular epithelial cells and are therefore saturable [7]. As these processes often have to be maintained against concentration gradients, they are energy- respectively ATP-dependent. Proximal tubular cells are typically exposed to highest concentrations of xenobiotics, as the ultra filtrate leaves the glomerulus and flows (first) to the proximal tubule (Fig. 1.1). In addition, highest drug metabolising activity occurs in the kidney in proximal tubular cells explaining nephrotoxicity to be found often in these cells [10].

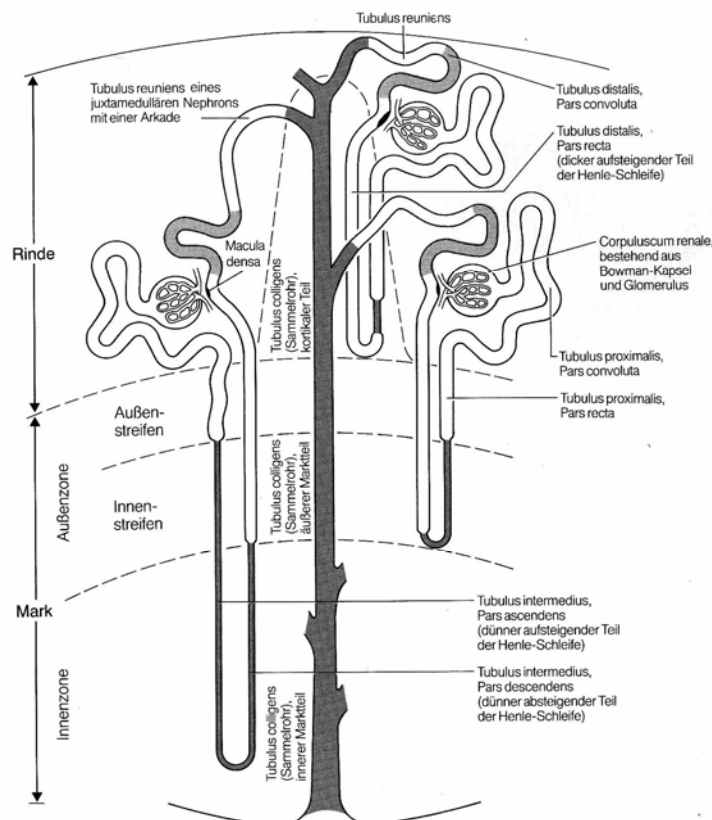


**Fig. 1.1** – Localisation of proximal tubular cells in the kidney. Adopted from [1].

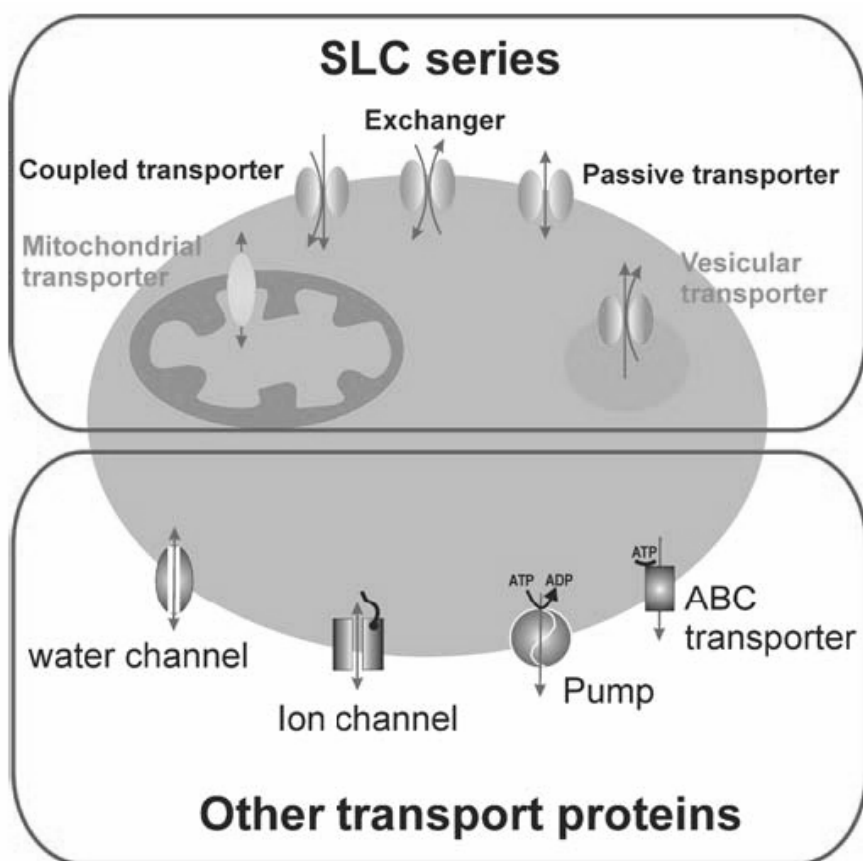


**Fig. 1.2** – Expression of SLC and ABC transporter in the membrane or in intracellular compartments. Non SLC transporters can also be localised intracellular. Adopted from [2].

## 1.2. Transporters

Cellular drug transporters are integral membrane proteins acting as gatekeepers for cells and organelles. They control uptake of important nutrients such as sugar, amino acids and nucleotides into cells and efflux of xenobiotics out of the cells. Typically these membrane proteins have 12 transmembrane domains. Two most important groups of transporters exist: ATP-binding cassette (**ABC**) and solute carrier (**SLC**)

transporters (Fig. 1.2). The ABC family transporters consist of 1200-1500 amino acids with a molecular weight of 140-180kDa, while the SLC family includes 300-800 amino acids with 40-90kDa [11].

In contrast to passive transporters facilitating the passage of e.g. nutrients down their electrochemical gradients, ABC proteins are directly dependent on ATP in order to transport solutes actively against their concentration gradient.

They are also called primary active transporters, as secondary active transporters (e.g. some SLC transporters) use ion gradients, previously established by ion pumps, in order to transport their substrates against their gradient [2].

One of the two ATP binding domains of the ABC protein, also called nucleotide-binding fold/domain (NBF), possesses characteristic Walker A and B motifs [12]. In between those two conserved NBFs, located in the cytoplasm, ATP is trapped like a sandwich. A functional ABC protein, a full transporter, typically contains two NBFs and two transmembrane domains (TM) [13]. Half transporters must dimerise in order to gain



functionality. These TMs, containing 6-11 membrane spanning  $\alpha$ -helices, determine substrate specificity.

**ABC transporters** are divided into seven subfamilies **ABCA-ABCG**, depending on gene similarity, sequence homology in the TM and NBF domains, the order of the domains. In the following, a short overview is given for those subfamilies which are not mentioned in 1.2.1.-1.2.3. [13, 14]:

#### ABCA

This subfamily covers 12 full transporters of which 5 are localised on the chromosome 17q24 (ABCA5, 6, 8-10) and expressed in skeletal muscle, heart, ovary and in the liver. ABCA1 protein manages cholesterol transport and influences membrane plasticity and fluidity. ABCA4, found in photoreceptor cells, transports Vitamin A derivatives and influences therefore vision.

#### ABCD

Four genes belong to the ABCD subfamily, often associated with ALD (adrenoleukodystrophy). These half transporters are only expressed in the peroxisomes which have to homo- or heterodimerise. These substrates are transport long chain fatty acids. Namely ABCD1 seem to be responsible for the X-linked form of ALD, as patients accumulate unbranched saturated fatty acids in their cells.

#### ABCE & ABCF

The ATP-binding domains of these two subfamilies derive from ABC transporters, however they do not possess a TM domain. To date ABCE and ABCF are not known to be involved in membrane transport functions. The oligo-adenylate-binding protein, OABP, the only member of ABCE, recognises oligo adenylate produced by some viruses indicating a probable involvement in immune answers. Each ABCF gene has a pair of NBFs. The best characterised gene is GCN20, found in *S. cerevisiae*, mediating the activation of eIF-2 $\alpha$  kinase, a translation initiation factor. ABCF1, a human analogue, seems to exert similar effects.

The **SLC family** includes passive transporters, ion coupled transporters and exchangers. Some of these transporters are also located intracellular (see Fig. 1.2). If a transporter has <20-25% amino acid sequence homology to other transporters in the SLC family, it is assigned to this family. A overview of different members of the SLC-family is given in table 1.1. SLC members which were found in porcine proximal tubular cells are mentioned below (see 1.2.4-1.2.9).

### 1.2.1. ABCB1 (*MDR 1* alias *P-gp*) and members of ABCB

To date, four full and seven half transporters compose the ABCB family, of which ABCB1 was first discovered and characterised in drug resistant tumour cell lines. ABCB was found to extrude cytostatic drugs out of the cells [14].

ABCB1 consists of two similar regions, each containing six putative transmembrane segments and an intracellular ATP binding site [15]. Later,

functional activity of ABCB1 was found in several tissues such as blood-brain barrier, liver, kidney and intestine [13]. In the kidney, expression was localised in the apical membrane of proximal tubular cells [7]. Therefore, ABCB1 protects the body from xenobiotics by either reducing absorption at the intestine as it pumps out already absorbed substances back into the gut or by enforcing renal secretion into urine.

**Table 1.1** - Overview of the SLC family adopted from [2].

The HUGO Solute Carrier Family Series		Total
SLC1	The high-affinity glutamate and neutral amino acid transporter family	7
SLC2	The facilitative GLUT transporter family	14
SLC3	The heavy subunits of the heteromeric amino acid transporters	2
SLC4	The bicarbonate transporter family	10
SLC5	The sodium glucose cotransporter family	8
SLC6	The sodium- and chloride-dependent neurotransmitter transporter family	16
SLC7	The cationic amino acid transporter/glyco-protein-associated amino-acid transporter family	14
SLC8	The Na <sup>+</sup> /Ca <sup>2+</sup> exchanger family	3
SLC9	The Na <sup>+</sup> /H <sup>+</sup> exchanger family	8
SLC10	The sodium bile salt cotransport family	6
SLC11	The proton coupled metal ion transporter family	2
SLC12	The electroneutral cation-Cl cotransporter family	9
SLC13	The human Na <sup>+</sup> -sulfate/carboxylate cotransporter family	5
SLC14	The urea transporter family	2
SLC15	The proton oligopeptide cotransporter family	4
SLC16	The monocarboxylate transporter family	14
SLC17	The vesicular glutamate transporter family	8
SLC18	The vesicular amine transporter family	3
SLC19	The folate/thiamine transporter family	3
SLC20	The type-III Na <sup>+</sup> -phosphate cotransporter family	2
SLC21/ SLCO	The organic anion transporting family	11
SLC22	The organic cation/anion/zwitterion transporter family	18
SLC23	The Na <sup>+</sup> -dependent ascorbic acid transporter family	4
SLC24	The Na <sup>+</sup> /(Ca <sup>2+</sup> -K <sup>+</sup> ) exchanger family	5
SLC25	The mitochondrial carrier family	27
SLC26	The multifunctional anion exchanger family	10
SLC27	The fatty acid transport protein family	6
SLC28	The Na <sup>+</sup> -coupled nucleoside transport family	3
SLC29	The facilitative nucleoside transporter family	4
SLC30	The zinc efflux family	9
SLC31	The copper transporter family	2
SLC32	The vesicular inhibitory amino acid transporter family	1
SLC33	The acetyl-CoA transporter family	1
SLC34	The type-II Na <sup>+</sup> -phosphate cotransporter family	3
SLC35	The nucleoside-sugar transporter family	17
SLC36	The proton-coupled amino acid transporter family	4
SLC37	The sugar-phosphate/phosphate exchanger family	4
SLC38	The System A and N, sodium-coupled neutral amino acid transporter family	6
SLC39	The metal ion transporter family	14
SLC40	The basolateral iron transporter family	1
SLC41	The MgtE-like magnesium transporter family	3
SLC42	The Rh ammonium transporter family (pending)	3
SLC43	The Na <sup>+</sup> -independent, system-L-like amino acid transporter family	2
Total		298

A broad diversity of hydrophobic compounds are actively secreted by ABCB1, e.g. vinca alkaloids, digoxin, anthracyclines, steroids, cyclosporines, tacrolimus, HIV-1 protease inhibitors and organic cations [7, 14] which explains the importance of this transporter in drug-drug interactions and reduced bioavailability. A remarkable example is a small clinical cross over study with 12 healthy male receiving ritonavir for 11 days, digoxin was given on day 3 [16]: Ritonavir increased digoxin AUC (area under the plasma concentration-time curve) by over 80%, decreased the renal digoxin clearance by 35% and thus increased half-life by 156%. Another possibility for an unwanted increased AUC of digoxin is the most prevalent SNP (single nucleotide polymorphism) C3435T in ABCB1, which resulted in lower expression of this protein and higher digoxin plasma levels [17].

Further essential ABCB transporters are 4 and 11 located in the liver and responsible for the secretion of phosphatidylcholine and bile salts, as mutations result in numerous forms of progressive familial intrahepatic cholestasis [14]. ABCB2 and 3 form heterodimers translocating foreign proteins into the endoplasmatic reticulum, where these antigens form complexes with class I histocompatibility proteins in order to present them on cell surfaces [14]. As one can imagine, defects in these areas result in a suppressed immune system.

The remaining ABCB transporters, except for ABCB5, whose function has not been described to date and is expressed in all cells, are found in the lysosome (ABCB9) and in the mitochondria (ABCB6-8, 10) [14]. Their functions are partly unknown, though ABCB6 and 7 are closely related and responsible for the transport of a precursor of the Fe/S cluster from mitochondria to the cytosol [13]. Gene mutations in the ABCB7 are found in X-linked sideroblastic anemia and ataxia patients [14].

### 1.2.2. *ABCC1-6 (MRP 1-6) and members of ABCC*

The ABCC family includes 12 full transporters managing ion transport, cell-surface mediated processes and toxin secretion [13]. Nine of them are MRP (multidrug resistance protein) related genes, of which ABCC1-3 transport glutathione conjugates and organic anions. The isoforms 4, 5, 11 and 12 are smaller than the other MRP transporters without a N-terminal domain, that is not required for transport function [13]. ABCC4 and 5 translocate nucleosides. Cystic fibrosis is caused by a mutation of the ABCC7 alias CFTR protein, which is a chloride ion channel and responsible for the exocrine secretion [14]. ABCC8 is a high affinity receptor for the drug sulfonylurea, an oral anti-diabetic drug. After binding of sulfonylurea an associated potassium channel is inhibited, that modulates

insulin secretion [13, 14]. Sulfonylurea binds with low affinity to the closely related ABCC9 protein, regulating potassium channels in muscle [13].

The authors in [6] give an excellent overview of substrates for MRP1-6 and their inhibitors: In general, these transporters translocate different substances such as leucotriene C4 and D4, MTX, PAH, anti-HIV drugs, vinca alkaloids, indomethacin and estradiol-17 $\beta$ -D-glucuronide. Typical inhibitors are probenecid, indomethacin and MK571.

Interestingly, ABCB1 (MDR1) and ABCC1 (MRP1) share overlapping substrate specificity, e.g. anthracyclines, vinca and colchicine alkaloids, with the difference, that ABCC1 is able to translocate glutathione conjugated drugs [13]. ABCB1 prefers large uncharged hydrophobic or slightly positively charged substances, whereas the MRP family prefers hydrophobic anions [18]. Furthermore, ABCC1 mediates inflammatory responses as it is capable of transporting leukotrienes. This transporter was found in various tissues, especially in liver, lung and kidney [7].

ABCC2 is expressed in canalicular cells in the liver, often referred as cMOAT (canalicular multispecific organic anion transporter), in the kidney at the apical side of proximal tubular cells as well as in the intestine [19]. In the liver, it contributes to a great part to extrusion of organic anions e.g. bilirubin into the bile. The TR rat, which suffers under chronic hyperbilirubinemia, has a mutation in its *abcc2* transporter [20]. The correlation of an ABCC2 mutation with Dubin-Johnson syndrome, a form of hyperbilirubinemia, was shown in human patients, too [21].

ABCC3 was found in liver, colon, pancreas and to a lesser extent in the kidney [7], while ABCC4 was detected in several tissues, in the kidney at the apical side of proximal tubular cells [22]. Interestingly, both apically localised ABCC2 and 4 transport PAH, a prototypical substrate for renal organic anion transporters, with  $K_M$  of 2mM respectively 160 $\mu$ M [23]. However, ABCCs seem to play a minor role in this regard, as  $K_M$  values of PAH in SLC22A6 and A8 are significantly lower (see 2.6.6). More clinical relevant is the fact, that ABCC2, 4 and 5 are responsible for the renal elimination of antiviral drugs in the kidney, playing an important role in drug-drug interactions, (nephro) toxicity and resistance to nucleoside analogues (e.g. AZT) [6, 13].

ABCC5 is ubiquitously expressed in tissues, including kidney, and translocates the antiviral agent adefovir, cAMP and cGMP [6]. Interestingly, ABCC5 and phosphodiesterase 5 (PDE5) are co-expressed in smooth muscle cells of the corpus cavernosum, indicating a second catabolic pathway of cGMP besides the PDE5 [24]: For a penile erection the increase of intracellular cGMP is mandatory. Sildenafil (Viagra) reduces

the degradation of cGMP by PDE5 thus inducing and prolonging erection. As sildenafil is translocated by ABCC5 [6] which also exports cGMP out of cells, a secondary mechanism of sildenafil action might be postulated: The inhibition of cGMP transport out of the cell and thus increasing intracellular cGMP.

ABCC6 was mainly found in kidney and liver and translocates BQ123 (endothelin receptor blocker), so far this is its only known substrate besides LTC<sub>4</sub> [6]. Unfortunately, a mutation (R1141X) in ABCC6 is related with a connective tissue disorder, called pseudoxanthoma elasticum (PXE), characterised by calcification of connective fibres in skin, arteries and retina leading to loss of elasticity, cardiovascular disease and ocular bleeding [25]. Another mutation, R1268Q, has been correlated with high plasma triglyceride and HDL levels [26].

### 1.2.3. ABCG2 (BCRP) and members of ABCG

The ABCG family consists of six “reverse” half transporters, as the NBF is at the N terminus and the TM domains at the C terminus, an orientation which is contrary in other eukaryotic ABC proteins [14].

The authors in [13, 14] provide a good overview of this family:

ABCG1 is the human homologue to *Drosophila* white gene, with an amino acid identity of 31%. The latter is the first gene found in this family. Therefore the ABCG family is often named as white half transporter family. The *Drosophila* white gene is a transporter for eye pigment precursors. ABCG1 is involved in cholesterol transport, similar to ABCG5 and 8 (expressed in intestine and liver), genes which are mutated in patients with sitosterolemia (defective transport of dietary sterols such as sitosterol, stigmasterol, campesterol, etc...). To date ABCG3 has been exclusively found in rodents, ABCG4 is mainly expressed in brain [27]. For both transporter, their function is still unknown.

ABCG2 was discovered as a multidrug resistance gene and is to date eagerly under investigation. ABCG2 has been made responsible for resistance to anthracycline drugs (doxorubicin and daunorubicin), mitoxantrone and camptothecin derivatives (topoisomerase I inhibitors e.g. topotecan and irinotecan) [28]. Interestingly, ABCG2 transports also estrone-3-sulfate (known as SLC22A8 substrate), methotrexate (a classical ABCG1-3 substrate) and 17 $\beta$ -estradiol 17- $\beta$ -D-glucuronide (free estradiol: ABCG2-4 and ABCB1 substrate) [29].

At protein level, ABCG2 expression was found not only in carcinogenic cell types, but also in normal human tissues e.g. lung, bladder, prostate, uterus, intestine, pancreas, kidney and liver [30]. In kidney, the authors in [30] could sub-localise ABCG2 to cortical tubules,

while in mouse kidney it was found at the apical side of proximal tubular cells [31]. Furthermore its expression was detected in the placenta, suggesting a protective function for the foetus [14].

As all ABCG transporters are half transporters, they have to form either homo- or heterodimers in order to gain functionality. ABCG2 is supposed to build a homodimer [32]. Interestingly, *abcg2* knock out mice developed symptoms similar to protoporphyria, as a degradation product of chlorophyll, called pheophorbide induced severe dermal phototoxic lesions after light exposure [33]. Therefore ABCG2 seems to be responsible for reducing uptake of pheophorbide, found in numerous plant-derived foods and food supplements, after meal ingestion. In addition, *abcg2* knock out mice had a threefold higher AUC after oral intake of the food carcinogen PhIP (2-amino-1-methyl-6-phenylimidazo[4,5-b]pyridine), demonstrating ABCG2's role in protecting the body from toxic compounds [34]. Its role could be even more crucial as that of ABCB1, since in human jejunum the mRNA level of ABCG2 was higher compared to ABCB1 [35]. Analyses of human sequences revealed numerous (over 80) different variations, of which two can be called as polymorphic forms (V12M and Q141K) of ABCG2 in several populations [32]. Though many investigations have been performed regarding expression, localisation and function, the results are contradictory and to date it is not possible to pose a clear statement [32].

#### 1.2.4. *SLC4A4 (NBCe1)*

In the SLC4A family are to date 11 members known, which can be divided, dependent on their function, into three groups, [36]: 1.  $\text{Cl}^-/\text{HCO}_3^-$  exchangers; 2.  $\text{Na}^+/\text{HCO}_3^-$  cotransporters (NBCs); and 3.  $\text{Na}^+$  dependent  $\text{Cl}^-/\text{Na}^+\text{HCO}_3^-$  exchangers (NDCBEs). SLC4A11 (alias BTR1 or NaBC1) represents an exception, as it translocates borate  $\text{Na}^+$ -dependently and can't be classified in one of the three groups. It was included in the SLC4 family due to its homology with other members of this family.

The second group,  $\text{Na}^+/\text{HCO}_3^-$  cotransporters (NBCs), can be divided further into an electroneutral group with a  $\text{HCO}_3^-$  (or  $\text{CO}_3^{2-}$ ) :  $\text{Na}^+$  stoichiometry of 1:1, while the electrogenic cotransporters translocate with a stoichiometry of 2:1 or 3:1. A stoichiometry of 3:1 favours energetically extrusion of bicarbonate from cells while 2:1 stoichiometry favours cellular uptake [37]. Interestingly, rat kidney NBCe1 expressed in *Xenopus laevis* oocytes could change its stoichiometry from 2:1 to 3:1 after an calcium increase [38]. In murine proximal tubular cells the stoichiometry of NBCe1 shifted from 3:1 to 2:1 after

phosphorylation at position Ser982 [39]. Thus this transporters has the ability to shift between influx and efflux of bicarbonate.

In humans, two splice variants have been found [36]: kNBC1, which is highly expressed on the basolateral membrane of proximal tubular cells, and pNBC1 highly expressed in pancreas and at lower level in various other tissues, e.g. kidney, brain, liver, prostate, colon, stomach, thyroid, and spinal chord [40]. Intriguingly, more than 85% of the filtered load of  $\text{HCO}_3^-$  is re-absorbed in proximal tubular cells, accomplished by an apical  $\text{Na}^+/\text{H}^+$  exchanger and the basolateral SLC4A4 [41].

As SLC4A4 is crucial for the acid-base regulation, mutations in the human gene resulted in metabolic acidosis [41]. Furthermore, mental retardation, short stature and ocular abnormalities have been described with mutations in this gene [37].

The other family members of SLC4, such as SLC4A1-3 (AE1-3), SLC4A5 (NBC4 or NBCe2), SLC4A7 (NBC3 or NBCn1), SLC4A8 (NDCBE), SLC4A9 (AE4), SLC4A10 (NCBE) and SLC4A11 (NaBC1) were partly found in kidney but have to date not been localised in proximal tubules [36, 37].

#### 1.2.5. SLC5A1/2 (SGLT 1/2)

The SLC5A family consists amongst others of six sodium-dependent glucose transporters, which are secondary active transporters translocating glucose (and other monosaccharides) against its concentration gradient into cell. The driving force here is, similar to the SLC9A family, the inwardly directed  $\text{Na}^+$  gradient established by the  $\text{Na}^+/\text{K}^+$  ATPases [42].

The high affinity, low capacity transporter SLC5A1 (SGLT1) has been found in intestine and in renal proximal tubules (S3 cells) with a  $\text{Na}^+$  to glucose coupling ratio of 2:1 [43]. In this part of the renal tubules (S3) SLC5A1 is expected to re-absorb remaining glucose, which has not been re-absorbed completely by the high capacity, low affinity transporter SLC5A2 (SGLT2), mainly located at the apical side of proximal tubules (S1 and S2 cells) and mediating  $\text{Na}^+$  to glucose with a ratio of 1:1 [44]. The third renal transporter SLC5A4 (SGLT3), probably located at an earlier segment of proximal tubules, is a high capacity transporter similar to SGLT2 but with the same  $\text{Na}^+$ /glucose stoichiometry as SGLT1 of 2:1 [45]. Recently, SLC5A9 (SGLT4) has been found to some extent in human kidney (with a higher mRNA than SGLT1), however its exact localisation has to be elucidated [46]. SLC5A10 (SGLT5) has been found in bovine kidney [47]. The sodium-dependent glucose

transporter SLC5A11 (SGLT6 alias KST1 or SMIT2) seems to be expressed in various tissues [48].

Mutations of human SLC5A1 (SGLT1) led to a glucose / galactose malabsorption resulting in severe diarrhoea and dehydration [49], indicating, that in the intestine, SGLT1 seems to be the major glucose absorbing transporter. However, SLC5A4 (SGLT3 former SAAT1) has been also detected in pig intestine (at mRNA level) [50]. As one would expect, mutations in the SLC5A2 gene result in renal glucosuria [51]. Other mutations in sodium-dependent glucose transporters are to date not known.

The facilitative Na<sup>+</sup>-independent sugar transporters GLUT 2, 5, 9 belonging to the SLC2A family are also present in kidney [42]. GLUT2 and 5 are fructose transporter. The latter has been localised at the brush border membrane of the S3 proximal tubules in rats [52]. However, GLUT2 is found at the basolateral side of proximal tubules and is also transporting glucose with low affinity [42]. Recently, GLUT1 and 12 has been found in kidney: in rat GLUT1 was located basolateral throughout the nephron, whereas GLUT12 was found at the apical side in human and rat distal tubules and collecting ducts [53]. Their main function is to facilitate transport of glucose and other sugars (e.g. fructose) along their concentration gradient.

#### 1.2.6. SLC9A3 (NHE 3)

To date, nine members of the SLC9A family (Na<sup>+</sup>/H<sup>+</sup> exchange respectively NHE family) are known [54-56]. However, at [www.gene.ucl.ac.uk/cgi-bin/nomenclature/searchgenes.pl](http://www.gene.ucl.ac.uk/cgi-bin/nomenclature/searchgenes.pl) eleven members are described. These secondary active transporters regulate intracellular pH, cell volume, systemic electrolyte, acid-base and fluid volume homeostasis by exchanging Na<sup>+</sup> into cell with H<sup>+</sup> out of cell. Their driving force is accomplished by Na<sup>+</sup>/K<sup>+</sup> ATPase pumps which establish the inward Na<sup>+</sup> gradient. The SLC9A family can be divided into five isoforms SLC9A1-5 located at the plasma membrane and the intracellular organellar forms SLC9A6-9 [57]. Interestingly, SLC9A3 and SLC9A5 cycle between endosomes and plasma membrane while the other three NHE1, 2 and 4 stay stationary.

SLC9A1, 6-8 are ubiquitously expressed, whereas other SLC9A members are expressed in various tissues such as stomach, intestine, skeletal muscle and brain [56]. SLC9A1-4 and 8 have been found in kidney [58]. NHE3 is located predominantly in kidney proximal tubule, at the luminal/apical side [58]. There, NHE3 is crucial for Na<sup>+</sup> and water re-absorption [59]. The associated secretion of H<sup>+</sup> contributes to a major part (approx. 66%) of renal HCO<sub>3</sub><sup>-</sup> re-absorption [60]. Interestingly, NHE3 forms complexes with other



proteins, such as CHP1/2, megalin, dipeptidylpeptidase IV (DPPIV) and PDZ-proteins (post synaptic density protein, *Drosophila* disc large tumour suppressor, and zo-1 protein). CHP are calcineurin B homologous proteins which are vital for the activity of NHE3 [61, 62]. NHE3 exists in two forms: either active in microvilli or inactive, when megalin associated, in intermicrovillar microdomains of the apical plasma membrane [63]. DPPIV inhibitors such as P32/98 reduce NHE3 activity significantly, although the mechanisms behind this action remains unclear [58]. The PDZ proteins NHE-RF1 / 2 inhibit NHE3 in a cAMP dependent way [64, 65].

Loss of NHE3 function has been associated with diarrhea characterised with Na<sup>+</sup> enriched alkaline stools, hyponatremia and metabolic acidosis [66]. This finding correlates with NHE3 knock out mice [67, 68]. Furthermore these results demonstrate the significance of SLC9A3 in the intestine and kidney regarding systemic homeostasis of electrolytes, acids and bases as well as blood pressure.

#### 1.2.7. *SLC15A1/2 (PEPT 1/2)*

The SLC15A family consists of four peptide transporters: PEPT1 (SLC15A1), PEPT2 (SLC15A2), PHT1 (SLC15A4) and PHT2 (SLC15A3) [3]. They all transport di- and tripeptides into intestinal and renal epithelial cells, whereas only PHT1 and 2 are capable of translocating free histidine. PEPT1 is mainly expressed in the small intestine, in the S1 segment of proximal tubules and in bile duct epithelial cells and has been characterised as high-capacity, low-affinity peptide transporter [69-71], whereas PEPT2 has its predominant expression in the S2 and S3 segment of proximal tubules as a low-capacity, high-affinity transporter [72]. Interestingly, this topographic arrangement of first, a high-capacity, then a low-capacity but high affinity peptide transporter in the proximal tubules is similar to the glucose dependent SGLT1/2 transporters (see 1.2.5.). PEPT2 was also found in brain astrocytes, mammary lands and in the lung [73-75]. The histidine/peptide transporter PHT1 was found in rat brain and human placenta, whereas PHT2 was found in various rat tissues, such as lymphatic system, spleen, lung and thymus [76].

The driving force for the re-absorption of di- and tripeptides in proximal tubular cells is the inwardly directed H<sup>+</sup> gradient, established by the prior mentioned sodium-proton exchanger NHE3 (SLC9A3) [3]. The influx of sodium is compensated by the Na<sup>+</sup>/K<sup>+</sup>-ATPases at the basolateral side, pumping 3 Na<sup>+</sup> out of the cell in return of 2 K<sup>+</sup> into cell, the latter leaving the cell by potassium channels. The re-absorbed peptides, respectively amino-acids, as the peptides are rapidly degraded by intracellular peptidases, are then

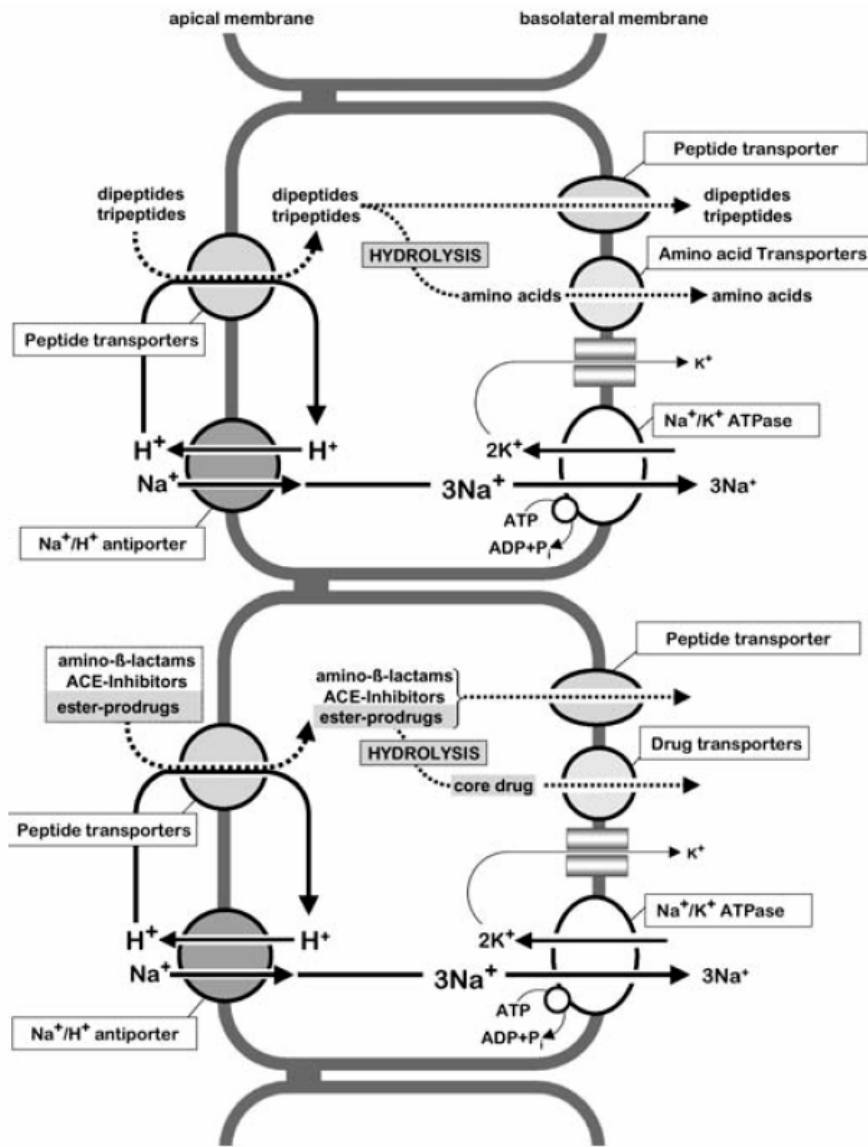


**Fig. 1.3** – Uptake of di- and tripeptides (upper compartment) and of peptidomimetics into cell. Adopted from [3].

transported out of the cell at the basolateral side by a not yet defined peptide transporter (Fig. 1.3).

For PEPT1, the coupling ratio of protons with neutral and cationic peptides is 1:1 and for anionic peptides 2:1 [77, 78]. PEPT2 transports neutral peptides together with 2 protons, anionic peptides together with 3 protons and cationic peptides are transported together with a variable numbers of protons [79].

PEPT 1/2 transport also various beta-lactam antibiotics [80-82], oral antidiabetics, such as glibenclamide [9], ACE inhibitors, the anticancer drug bestatin and other peptidomimetics such as valacyclovir [7]. It is quite obvious that concomitant use of the above mentioned drugs results in 1. reduced absorption of the drug in the intestine and 2. influences the

pharmacokinetics as renal clearance might be enhanced due to reduced re-absorption in proximal tubular cells.

To date, neither pathology associated with malfunction of these transporters nor polymorphism are known in humans [3]. However, PEPT1 is expressed in inflamed colonic tissues and is capable to transport the known neutrophile attractant peptide formyl-Met-Leu-Phe derived from certain bacterial species [83, 84].

#### 1.2.8. *SLC21A (SLCO alias OATP)*

In order to cope with the rapid growth of the SLC21A family, a new species independent classification and naming system has been introduced: In the OATP / organic anion transporting protein family, 21A has been replaced by O (letter) [2]. In the following, both nomenclatures inclusive aliases are used.

To date, 14 rat and 11 human Oatps/OATPs have been identified [85]. Although some OATPs are restricted to liver only, e.g. SLCO1B1 (SLC21A6 alias OATP-C) and SLCO1B3 (SLC21A8 alias OATP8) managing uptake of bulky and relative hydrophobic organic anions, most OATPs are expressed in various tissues such as kidney, brain, heart, lung, placenta and testes [86].

Typical OATP substrates are mainly amphipathic molecules with a high molecular weight (>450kDa), e.g. bile salts, steroid hormones and their conjugates, substances which are often bound to albumin [86]. In humans, only SLCO4C1 (SLC21A20 alias OATP4C1) is expressed in the kidney. This transporter is located at the basolateral side of the proximal tubules where it translocates digoxin, ouabain and T3 (triiodothyronine) from blood into the proximal cells [85, 87].

OAT-K1/K2 are transporters found specifically in rat kidney, while human orthologs are to date not existent [85]. These two transporters are located at the apical side with a narrow substrate specificity such as MTX (methotrexat), AZT (azidothymidine), folate and digoxin [6].

The first characterised human OATP was SLCO1A2 (SLC21A3 alias OATP-A) and was found at mRNA level in the brain, liver and kidney [6]. This transporter translocates various compounds such as bile salts, hormones and their conjugates, prostaglandine E2, peptides (endothelin receptor antagonist BQ-123, thrombin inhibitor CRC-220, opioid receptor agonist d-penicillamine 2, 5-enkephalin), fexofenadine, N-methylquinine and N-methylquinidine [86].

All OATPs transport the above mentioned substances sodium independently [86]. In addition, there is evidence for an anion exchange mechanism between organic anions and GSH (glutathion) functioning as driving force, although this has only been shown for the mouse/rat Oatp1 and Oatp2 [86].

#### 1.2.9. Overview of the SLC22A family

The SLC22 family (to date A1-A18) includes not only the organic cation / anion transporters but also organic carnitine transporters OCTN 1/2, CT2 (SLC22A4/5, A16) and URAT1 (SLC22A12), responsible for urate transport in the kidney [88]. Further SLC22 members are FLIPT 1/2, BOCT and ORCTL2-4, all organic cation transporters. Most of the previously mentioned transporters are expressed in kidney, especially in proximal tubular cells [5, 8, 11, 85].

Small (<500kDa) and hydrophilic organic anions are mainly excreted via the kidneys, whilst large (>500kDa) and hydrophobic anions favour the excretion pathway by the liver [85].

In order to excrete organic anions / cations from blood into urine, it is mandatory to enable the entrance of organic anions / cations at the basolateral (blood) side of e.g. proximal tubular cells and the excretion at the apical (urine) side. Therefore, organic anion / cation transporters are located on both cellular sides. In figure 2.1, the localisation of the transporters in proximal tubular cells is given: SLC22A6-8 and SLC22A1-3 are located basolaterally (blood side), whereas SLC22A10-11 and SLC22A2, too, are located apically (urine side). Following example illustrates that the SLC22 family members do not only function as eliminators of organic anions / cations but also withhold important substances: Carnitine, a vital co-factor of mitochondrial  $\beta$ -oxidation [89], is an amine which is re-absorbed by SLC22A4/5. Both transporters are located at the apical side and directed inwardly [90].

##### 1.2.9.1. SLC22A1-3 (OCT 1-3)

Interestingly, SLC22A1-3 has to be regarded as a facilitative diffusion system that can transport cations in both directions. Transport direction is driven by its concentration gradients, dependent on the membrane potential and independent of sodium [8]. SLC22A1 has been studied in different species (rat, mouse, rabbit and human) where it was mainly expressed in the liver. However in rodents, high expression of SLC22A1 was also found in kidney [91]. In contrast, SLC22A2 is mainly expressed in kidney, whereas SLC22A3 is

expressed in different tissues e.g. skeletal muscle, liver, placenta, kidney and heart [91]. SLC22A1-3 have a broad substrate specificity [91]. All three transporters translocate to a certain extent the following substances:  $\beta$ -estradiol, progesterone, cimetidine, clonidine, desipramine, prazosin, quinine, verapamil, MPP<sup>+</sup> (1-Methyl-4-phenylpyridinium) and TEA (tetraethylammonium) [92]. The last two mentioned substances MPP<sup>+</sup> and TEA are not used therapeutically but as model substances for SLC22A1-3 transport studies.

Single nucleotide polymorphisms (SNPs) have been investigated and found in SLC22A1 & 2 [92]: In 57 Caucasians, the most frequent polymorphism with 16% frequency (Arg61Cys, located at the large extracellular loop) resulted in a reduction of MPP<sup>+</sup> uptake by half. More extreme, although less frequent, the mutation Cys88Arg (1.2%) and Gly401Ser (6.7%) demonstrated a MPP<sup>+</sup> uptake of 2% of wild type SLC22A1. This fact is of clinical importance, as the uptake of cationic drugs and xenobiotics in liver is mediated by SLC22A1. A reduced activity of this transporter can be beneficial or devastating: beneficial, if the substance is toxic to the liver and is eliminated by other means (e.g. kidney) or devastating, if the substance is toxic for the body and can't be eliminated/excreted fast enough, as the uptake into liver is reduced. Sixteen SNPs in the coding region of SLC22A2 were found, of which eight caused single amino acid substitutions and one resulted in a premature termination of the protein. Interestingly, Met165Ile and Arg400Cys led to an two – threefold higher uptake of MPP<sup>+</sup> than wild type SLC22A2, which again can be beneficial in the kidney in order to excrete toxic xenobiotics faster or can be disadvantageous if a drug should stay in body.

Anyhow, to date no specific disease or adverse drug reaction can be attributed to malfunction of SLC22A1-3, as substrate specificities and expression patterns are overlapping within these transporters and with other transporters [92], e.g. SLC22A8 translocating cimetidine or ABCB1 mediating quinidine and verapamil [93-95].

#### 1.2.9.2. SLC22A6-8, 11, 10 (OAT 1-5)

Many clinical important anions like  $\beta$ -lactam antibiotics, diuretics, NSAIDs (non-steroidal anti-inflammatory drugs), virostatics, anticancer agents and ACE (angiotensin-converting enzyme) inhibitors are substrates of the organic anion transporters (OAT 1-5) [5]. This demonstrates a broad substrate specificity for these SLC members. Translocation of various drugs/substrates are overlapping between different isoforms of organic anion transporters [4, 6, 85]. In general, renal tubular cells are negatively charged, therefore basolateral uptake of organic anions has to be accomplished against their electrochemical

gradient [6]. In order to achieve this aim,  $\text{Na}^+/\text{K}^+$  - ATPase pumps  $\text{Na}^+$  out of the cell establishing a gradient, which is used to co-transport  $\text{Na}^+$  with  $\alpha$ -ketoglutarate through SLC13A3 alias SDCT (sodium/dicarboxylate cotransporter) into cell. Finally  $\alpha$ -ketoglutarate is exchanged by an organic anion and, therefore, the organic anion enters into the proximal tubular cells [5]. As the mechanism of the exit of organic anions at the apical side is not yet completely solved, different mechanisms are postulated, like involvement of the PAH (para-aminohippuric acid)/dicarboxylate or PAH/anion exchanger or a membrane potential dependent mechanism [5].

The first discovered organic anion transporter was SLC22A6 in rat kidney [96, 97]. Functional activity was tested with the prototypic organic anion PAH, explaining why SLC22A6 is often referred as PAH transporter [85]. Expression of the human ortholog hOAT1 was also shown in skeletal muscle, placenta and brain [91].

SLC22A7 (OAT2) was originally found in rat liver and was first named NLT (novel liver-specific transporter) [7]. Rat OAT2 is highly expressed in liver but low expression was found in kidney [6]. Interestingly, SLC22A7 is not driven by the outwardly directed  $\alpha$ -ketoglutarate gradient [98]. The intrarenal distribution of OAT is not clearly solved yet, as rat OAT2 was localised to the apical side of renal tubular cells while human OAT2 was localised at the basolateral side of proximal tubular cells [6, 85].

SLC22A8 was discovered in rat and human, in rat mRNA expression was found in liver, brain and kidney while in humans high levels of mRNA were detected only in kidney [6]. According to the authors in [91] hOAT3 is also expressed in brain and skeletal muscle and interestingly not in liver.

SLC22A11 is abundantly expressed in kidney and placenta [85], whereas SLC22A10 (hOAT5) mRNA was exclusively found in liver and rOAT5 was exclusively expressed in kidney [91]. Due to its low amino acid identity of 55% between hOAT5 and rOAT5 it is questionable if these two transporters are homologues [91].

Drug-drug interactions involving OAT transporters are very likely, due to their broad substrate specificity. For example, intake of MTX (methotrexate), a cytostatic drug, with anionic drugs such as NSAIDs or  $\beta$ -lactam antibiotics, resulted in severe suppression of bone marrow as a result of reduced renal clearance of MTX [5].

Paradoxically, organic anion transporters, which detoxify our body from xenobiotics, can enforce nephrotoxicity of drugs, e.g. cephaloridine or oxytocin A, due to accumulation in proximal tubular cells [5]. Co-medication of substrates or inhibitors of the involved OAT

can decrease nephrotoxicity by a reduced renal excretion of the given drug leading to increased efficacy but also to increased adverse events [91].

SLC22A11 (OAT4) secretes not only anions at the apical side of proximal tubular cells but also re-absorbs filtered prostaglandins [91]. Furthermore, OAT4 seems to excrete toxic anions from fetal into maternal circulation. Thus, an impairment of OAT4 can lead to a loss of prostaglandins and fetal intoxication.

### **1.3. Proximal tubular cells – which species?**

It is clear that obtaining healthy human kidney is difficult and self-limiting. To date, little is known about species differences between e.g. human, rat, mouse, dog, rabbit, monkey and pig regarding renal drug transport. Monkey seems to be a good predictor model for renal drug-drug interactions in humans [99-101], whereas the dog remains a questionable alternative [102]. The authors in [10] emphasise that humans are physiologically more closely related to pig than to rat, rabbit or mouse. Taken this into consideration and the fact that porcine kidney is easily available, a validation of primary porcine proximal tubular cells seem to be an interesting alternative as an in vitro model for drug transport in human kidney.

## 2. Primary porcine proximal tubular cells as a model for transepithelial drug transport in human kidney

Schlatter Philipp, Gutmann Heike, Drewe Juergen

Department of Clinical Pharmacology and Toxicology University Hospital, Basel, Switzerland.

**European Journal of Pharmaceutical Sciences**

**2006 May;28(1-2):141-54.**



## 2.1. Abstract

*Background:* Kidney proximal tubular cells play a major role in the transport of endogenous and exogenous compounds. A multitude of different transporters are expressed starting with multidrug ABC transporters (e.g. abcb1, abcc1-6), slc22a6-8 (organic anion transporters) and slc22a1-3 (organic cation transporters). For transport studies of renal drug transport, cell lines like MDCK and LLC-PK1 are often used to overexpress and study one or two transporters, such as abcb1 or abcc1-6. However, the use is limited since under physiological conditions xenobiotics are transported through different transporters at the same time. Therefore, a primary in vitro model expressing functionally different transporters simultaneously, as it is the case in vivo, would be of great benefit.

*Methods:* Primary proximal tubular cells were isolated from porcine kidney. Cells were cultured under selective culturing conditions leading to specific growth of primary proximal tubular cells. Expression of important proximal transporters was checked at mRNA level with RT-PCR, at protein level with immunocytochemistry and functionally by transport and uptake assays.

*Results:* A model of primary proximal tubular cells was established expressing the most important transporters: abcb1, abcc1, abcc2, slc22a8, slco1a2, slc15a1, slc5a2 and slc4a4. In freshly isolated cells, slc22a1 and slc22a6 were expressed, but were down-regulated in culture. Abcb1, abcc1, abcc2 and slc4a4 were detected at protein level with immunostaining. Functional activity was confirmed for abcb1, abcc1/2, slc22a8, slc15a1/2 and slc5a1/2. The tightness of the monolayers of this model was better than in previously established in vitro models.

*Conclusion:* This primary cell culture model might be an interesting tool to investigate proximal tubular transport and to predict toxicity and drug interactions since it expresses functionally several transporters simultaneously.

## 2.2. Introduction

Renal elimination of drugs and toxins is necessary for the survival of mammalian species. Regarding physiology of different species, humans are more closely related to pig, than to rat, rabbit or mouse [10]. Thus a porcine *in vitro* model might be more suitable for prediction of transepithelial drug transport, than other non-human species. The existing cell lines e.g. HK2 and HKC (human proximal tubular cells), HEK293 (human embryonic kidney), LLC-PK1 (proximal tubular cells from pig) and MDCK I/II (distal tubular cells from dog) would provide enough possible models to study renal elimination. However, these cell

lines are immortalised. The advantage of having a cell line for many passages available is diminished by the fact, that transporter or enzyme activities may have been changed. For example, in rabbit kidney proximal tubule, the activities of sodium-glucose co-transport system, gamma-glutamyl transpeptidase and alkaline phosphatase were reduced after few passages [103]. Also, signal transduction pathways seem to be more intact in primary cultures than in immortalised cell lines [104]. Many transport studies were performed in each of the above mentioned immortalised cell lines, which were transfected with transporters and thus altering the system [105-110]. As many different transporters are involved in the elimination of xenobiotics (Fig. 2.1), a transfection and thus over-expression of one or more drug transporters ignores possible influences of other transporters. Using the parental cell line as reference, where transporters might be already partially down regulated in their function, is questionable. Therefore a primary cell culture

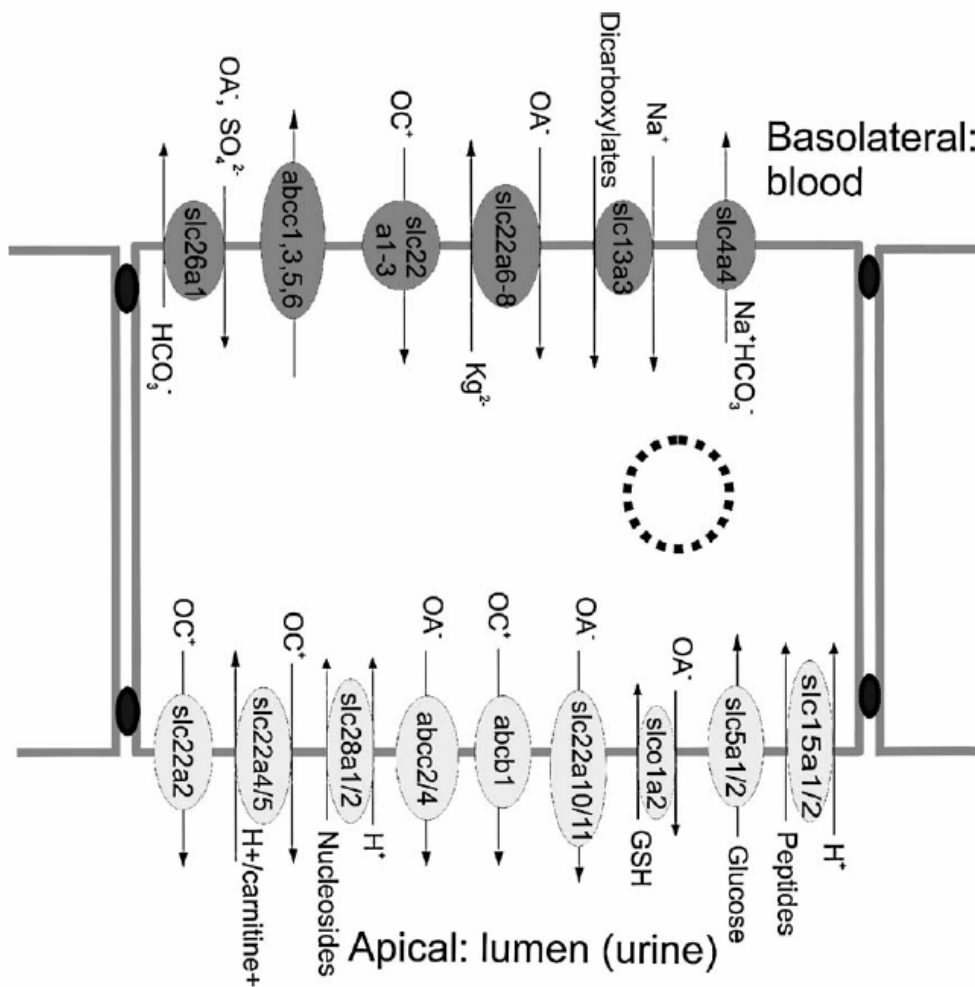


Figure 2.1 - Different transporters in the proximal tubular cells as described in the literature [4-9].

model expressing different drug transporters simultaneously like in the *in vivo* situation would be of great interest.

In the following, an overview of different drug transporters in the kidney is given.

In order to excrete large (amphophilic) drugs, transporters are needed to overcome the transepithelial barrier [6]. The expression of slc15a1/2 (peptide transporter PEPT1/2) [9, 81] and slc5a1/2 (sodium-dependent glucose transporter SGLT1/2) [111] for the re-absorption of important nutrients like amino acids, peptides and glucose from the urine is mandatory. The kidney is, together with the liver, the most important detoxifying organ [7]. In drug discovery and development, an *in vitro* model expressing the most important transporters concurrently would be an important tool in order to predict elimination, toxicity and drug interactions at a functional level. From all renal segments, the proximal tubular cells have the highest transport activity and are exposed to highest concentrations of xenobiotics [6, 10].

Multidrug-resistance transporters (such as abcb1, respectively P-gp or abcc1-6, respectively MRP1-6) are important for proximal tubular secretion of many drugs. Abcb1 interacts mainly with neutral and cationic xenobiotics (e.g. digoxin, cyclosporine A, vinblastin, antiviral drugs) [112]. Abcc1-6 have like abcb1 a broad substrate specificity [113]. Although abcc1-6 prefer anionic molecules many substrates are transported by both, abcb1 and abcc1-6 (especially neutral molecules and some polypeptides) [114]. Slc22a6-8 (organic anion transporters: OAT1-3) are transporting a broad spectrum of xenobiotics such as  $\beta$ -lactam antibiotics, antiviral drugs, diuretics, NSAIDs, PAH, estrone sulfate, fluorescein but also MTX (methotrexate), pravastatin and cimetidine [6, 115-120].

The Slc21 family (organic anion transporting polypeptides: OATPs) interacts with bile acids, steroids, fexofenadine, estrone sulfate, pravastatin and antiviral drugs [5-7, 86].

Slc22a1-3 (organic cation transporters: OCT1-3) are translocating a variety of cationic drugs such as procainamide, desipramine, clonidine, araC, cimetidine, nicotine, quinidine, verapamil, corticosterone, dopamine, epinephrine, 5-hydroxytryptamin, and amantadine [6, 8, 121].

Slc15a1/2 (peptide transporters: PEPT1/2) are important for re-absorption of amino acids and oligopeptides [6]. Furthermore valacyclovir, glycylsarcosine,  $\beta$ -lactam antibiotics, ACE-inhibitors, glibenclamide and dipeptide-like anticancer drug bestatin are substrates of these transporters [6, 9, 81, 82, 122]. Glycylsarcosine is used as a model substrate for slc15a1/2 [80]. Re-absorption of glucose and its derivatives are managed through sodium-dependent glucose transporters, which are classified in a high affinity  $\text{Na}^+$ /Glucose co-

transporter slc5a1 (SGLT1) und low affinity Na<sup>+</sup>/Glucose co-transporter slc5a2 (SGLT2) [111]. Both transporters can be inhibited by phlorizin. The facilitated-diffusion glucose transporter family (SLC2 respectively GLUT) is also expressed with different subtypes (1-5) located on both sides of the proximal tubular cells (apical and basolateral) [123, 124]. The electrogenic Na<sup>+</sup>-HCO<sub>3</sub><sup>-</sup> co-transporter slc4a4 (NBC1) located at the basolateral side of proximal tubular cells in the kidney is responsible for the re-absorption of NaHCO<sub>3</sub> (80% through slc4a4) and regulation for acid base status [37, 125].

All these, and some other not mentioned transporters, contribute to the renal transport function to detoxify the body from xenobiotics or endogenous waste products.

To study isolated transport of one transport protein, tumour cells derived cell lines are often utilised, which over-express e.g. either abcb1 and/or abcc1-6 [126]. However, to predict proximal tubular elimination, a more realistic model would be desirable. Therefore, it was our aim, to characterise functional expression of a primary cell culture based model of porcine proximal tubular cells expressing important transporters simultaneously.

## 2.3. Materials

[<sup>3</sup>H]glucose (573.5GBq/mmol) was purchased from DuPont NEN Research (Boston, USA), [<sup>3</sup>H]digoxin (865.8GBq/mmol) from Perkin Elmer Life Science (Boston, USA), [<sup>3</sup>H]MTX (1239.5GBq/mmol) and [<sup>14</sup>C]glycylsarcosine (4.07GBq/mmol) from Moravek Biochemicals (Brea, USA), [<sup>14</sup>C]PEG4000 (496MBq/g) from Amersham Bioscience (Buckinghamshire, England), MK571 from Biomol Research Labs (Plymouth Meeting, USA), Nycodenz from Axon Lab (Baden-Dättwil, Switzerland), MEM Eagle D-Valine w/L-glutamine from Lucerna Chem AG (Luzern, Switzerland), Dulbecco's MEM / Nut Mix F-12 (DMEM/F12), Fetal calf serum (FCS) and penicillin/streptomycin from Gibco (Gibco Life Sciences, Basel, Switzerland), Insta-Gel Plus from Perkin Elmer (Boston, USA), cell flask 75cm<sup>2</sup> from BD (Franklin Lakes, USA). All other substances were purchased from Sigma/Fluka in highest quality.

## 2.4. Functional characterisation of transporters

### 2.4.1. Cell Culture

Porcine proximal tubular cells were isolated and seeded as described previously [127]. In brief, fresh pig kidneys with the capsule were retrieved in the slaughterhouse and put into ice-cold Eurocollins, pH 7.4 and 2mM glycine. The cortex was removed, minced and

washed with  $\text{Ca}^{2+}$  and  $\text{Mg}^{2+}$  free Hanks' buffer, containing 25mM HEPES and 2mM Glycine (Buffer A). The washed cortex was then digested with collagenase (0.07%w/V) in buffer A with 1mM desferal and 4mM  $\text{Ca}^{2+}$  at 37°C for one hour. For 30g cortex 25ml of this buffer was used. The incubation was terminated with ice-cold buffer A including 4mM  $\text{Ca}^{2+}$  and 1.5% (w/V) bovine serum albumin (buffer C). All buffers contained 100U/ml respectively 100 $\mu\text{g/ml}$  penicillin/streptomycin. After filtration through an 80 $\mu\text{m}$  nylon gauze, washing, centrifugation (80g, 5min, 4°C) the cells were diluted in a Nycodenz solution with 11.3% Nycodenz. Establishing a gradient of Nycodenz solutions with layers of 17%, 11.3% (containing cortex cells) and 8.5%, all of them containing 6.7mM KCl, 1.22mM  $\text{CaCl}_2$  and 10mM HEPES, the mixture was centrifuged (2300g, 6min, 4°C). The cells at the interface between the upper two layers were harvested, washed (80g, 6min, 4°C) with buffer C. Viability was determined by trypan blue exclusion. One ml cell suspension with  $1.5 \cdot 10^6$  cells was cryoconserved in cell culture medium 1 (see below) with 10% DMSO. Cells were seeded ( $1.5 \cdot 10^6$  cells in 75cm<sup>2</sup> flask) in 50ml of 9.6g/1000ml MEM D-Val, 10% FCS and 100U/ml penicillin/streptomycin (medium 1) and cultured for 5 days (after the first 48h medium was changed every day). As in medium 1 proximal tubular cells can use D-valine and fibroblasts do not, fibroblast growth was suppressed. Then culturing was continued with DMEM/F12 (containing L-Valine) with 10% FCS and 100U/ml penicillin/streptomycin (medium 2) until confluence was reached (about 3 days, medium 2 was changed on the second day). For both medium conditions the cells were incubated at 37°C in 95% air and 5%  $\text{CO}_2$ . For passaging the monolayer was trypsinised with 10ml (trypsin EDTA from Gibco) for 15min. Then 10ml of medium 2 was added and centrifuged. After removing supernatant the cell pellet was diluted in medium 2. For transport studies cells were transferred onto uncoated Transwell filter cell culture systems. On Transwell filters tightness was reached after 3-4 days in medium 2, so that primary cells were cultured in total for 11-12 days. After this period the cells were discarded.

#### 2.4.2. Transepithelial electrical resistance (TEER) measurement

TEER was measured with Millipore Millicell ERS (Volketsville, Switzerland). Measurements were carried out as described in the manufacturer's description. The electrode was at least 24 hours in the same culture medium as the cells. The transepithelial electrical resistance (TEER) of blank filters in culture medium 2 was  $146 \pm 4.7 \Omega \cdot \text{cm}^2$ . There was a correlation between low FITC-dextran or [<sup>14</sup>C] PEG4000 transport and high TEER values and *vice versa*. In blank filters,  $14.8\% \pm 2.1\%$  (SEM) FITC-dextran

diffused after 75min apical-to-basolateral. Monolayers with the value  $\Delta\text{TEER} > 900 \Omega\cdot\text{cm}^2$  were defined as confluent, as the FITC-dextran or [ $^{14}\text{C}$ ] PEG4000 transport after two hours was below 2% respectively 0.15% (data not shown).

After three days, cells formed a confluent monolayer on the membranes, where  $\Delta\text{TEER}$  values of  $900\text{-}3200 \Omega\cdot\text{cm}^2$  were achieved. After 7 days, cells were still confluent. When the values dropped down to  $290 \Omega\cdot\text{cm}^2$ , FITC-dextran was transported up to  $11.1\% \pm 1.14\%$  (SEM) after 120min from apical-to-basolateral (data not shown). Literature data have shown, that monolayers with  $\Delta\text{TEER}$  values of  $100 \Omega\cdot\text{cm}^2$  for HK-2 cell lines and  $350 \Omega\cdot\text{cm}^2$  for MDCK cell lines offer already sufficient tightness [128]. Time course of cell growth on transwell filters showed, that tightness of cells changes rapidly ( $300 \Omega\cdot\text{cm}^2$  versus  $1100 \Omega\cdot\text{cm}^2$  one day later).

So far  $900 \Omega\cdot\text{cm}^2$  was the lowest value where monolayers of porcine proximal cells were still tight. Thus, the limit of tightness was deliberately set to  $900 \Omega\cdot\text{cm}^2$  and to ensure absolute tightness, cells with  $\Delta\text{TEER}$  values below  $900 \Omega\cdot\text{cm}^2$ , were not used in further experiments.

#### 2.4.3. Functional assays

For functional assays the Transwell Costar 3460 system was used (Corning Incorporation, NY, USA). Cells were preincubated with the inhibitors for twenty minutes. Both sides of the diffusion cells were filled with pre-warmed transport buffer (see below). The whole system was kept at constant temperature ( $37^\circ\text{C}$ ). At time  $t = 0$ , the substrate with or without inhibitor was added to the donor chamber. At defined time intervals, samples were drawn from the acceptor chamber and analysed. Uptake/transport assays were carried out in HBSS (Gibco) with 1mM MEM sodium pyruvate (Gibco), pH 7.4. Except for the dose-dependent assays, radioactive substances were used at a concentration of 11100Bq per well (0.5ml in the apical and 1.5ml in the basolateral compartment). FITC-dextran ( $250\mu\text{g/ml}$ ) or [ $^{14}\text{C}$ ] PEG4000 (11000Bq/well) was used for monitoring the monolayer integrity.

For detection of radioactive substances, Packard 1900TR liquid scintillation counter was used. The samples were diluted in 3ml Insta-Gel Plus (Perkin-Elmer, Schwerzenbach, Switzerland). Detection of FITC-dextran and fluorescein was carried out with Perkin-Elmer HTS 7000 Bio Assay Reader with the following parameters: excitation at 485nm, emission 535nm.

**Table 2.1** – Primers designed for qualitative PCR, and primers/probes designed for quantitative PCR (Taqman® assay)

Gene	Accession no.	Forward primer/reverse primer
<b>RT-PCR Primers</b>		
GAPDH	AF017079	5'-AGATCATCAGCAATGCCTCCTG-3'/5'-GAGCTTGACAAAGTGGTCGTTG-3'
slc5a2 (pSGLT2)	L02900	5'-CAAGATTAGGAAGCAGGCATCAG-3'/5'-TCTGCATCTAAATCAATTCGTTCTTC-3'
slc22a1 (pOCT1)	AY238476	5'-TGCAGACAGGTTGGTCGGA-3'/5'-TCCTCTTCGAGGGACAGCAT-3'
slc22a6 (pOAT1)	AJ308234/AJ308235	5'-ACAACACCCTGCAGAACTTCAC-3'/5'-GAATATCATGGCTCCGAGAAGC-3'
slc22a8 (pOAT3)	NM_214455	5'-ACCCGGTTTCGAGCCATC-3'/5'-GTATAACTCGCTCGTGTAGAGGAAGA-3'
slco1a2 (pOATPA)	AF403248	5'-CCATGCTCACACAAATAGAGAGAC-3'/5'-ACTTCCTTCACACACTCTGATGGA-3'
slc15a1 (pPEPT1)	AY180903	5'-CACTGCAAGCAACGACCATG-3'/5'-GCTGGCGTTGTGACTGGTG-3'
slc4a4 (pNBC1)	AY253302	5'-TCCCATCTTGAAGTTTATTCCTCA-3'/5'-TGATAGCAGCCACAGTTGACTTG-3'
Gene	Accession no.	Forward primer/reverse primer/probe
<b>Taqman primers and probes</b>		
GAPDH	AF017079	5'-GTTGAAGGTCGGAGTGAACG-3'/5'-CGACAATGTCCACTTTGCCA-3'/5'-CGCCTGGTCACCAGGGCTGC-3'
abcb1 (pMDR1)	U27704	5'-ATGGCACACACCAGCAGCTAC-3'/5'-CAGTTGATGAGCGCTTTGCTC-3'/5'-AGGCATCTATTTCTCCATGGTCAGCGTCC-3'
abcc1 (pMRP1)	AF403246	5'-GATGTGGAATTGCCGGGA-3'/5'-GTGCTTGAGAACCAGGTCCAG-3'/5'-ACGGCATTGCGTTACCGAGACGA-3'
abcc2 (pMRP2)	AF403247	5'-TGTTGGGCTTTGTCTGTCCA-3'/5'-CAGCCACAATGTTGGTCTCG-3'/5'-CTCAATATCACACAAACCCTGAAGTGGCTG-3'

Primers were designed for qualitative PCR, and primers/probes designed for quantitative PCR (Taqman® assay) according to the guidelines of Applied Biosystems with help of the Primer Express 2.0 software. Qualitative PCR was performed with Mastercycler personal (Eppendorf AG, Hamburg, Germany) using the following program: (1) step: 95 °C 10 min, (2) step: 95 °C 30 s, (3) step: annealing temperature: 60 °C for GAPDH (glyceraldehyde 3-phosphate dehydrogenase), slc4a4, slco1a2, the annealing temperature for the other genes were 55 °C for 1 min, (4) step: 72 °C 1 min, (5) step: 72 °C 10 min, (6) step: cooling at 4 °C. Steps (2–4) were repeated 39 times. Gene amplification was performed in 25 µl reaction unit using AmpliTaq Gold DNA polymerase 1.25 U (Applied Biosystems, Foster City, USA), dNTPs 200 mM (Promega, Catalys AG, Wallisellen, Switzerland), 35 ng cDNA (or DNA digested RNA for negative control), forward and reverse primers 0.4 µM. Mg<sup>2+</sup> concentrations were 3 mM for slc5a2 and slc15a1, 2 mM for slc22a1 and slc22a6, 2.5 mM for slc22a8 and 1.75 mM for slc4a4 and slco1a2. Quantitative PCR (Taqman® Assay) conditions were 10 min 95 °C followed by 40 cycles of 15 s 95 °C and 1 min 60 °C. Each TaqMan reaction contained 25 ng of cDNA in a total volume of 25 µl. TaqMan Universal PCR Master Mix from Applied Biosystems was used. The concentrations of primers and probes were 900 and 225 nM, respectively.

Data were analysed using apparent permeability coefficient  $P_{app} = \Delta Q / \Delta t \cdot 1 / (60 \cdot A \cdot C_0)$  with the unit cm/s [129].  $\Delta Q / \Delta t$  is the permeability rate (mol/min), A the surface area of the membrane (cm<sup>2</sup>) and C<sub>0</sub> is the initial concentration (mol/ml). Reading points were 5, 10, 15, 20, 30, 60, 90 and 120 minutes.

#### 2.4.4. PCR

Total RNA was isolated from confluent monolayers using the RNeasy Mini Kit (Qiagen, Hilden, Germany). RNA was quantified with a GeneQuant photometer (Pharmacia, Uppsala, Sweden). The purity of the RNA preparations was high, as demonstrated by the 260 nm/280 nm ratio (range, 1.8-2.0). Its integrity was checked by ethidium bromide agarose gel electrophoresis. After DNase I digestion (Invitrogen, Basel, Switzerland), 2 µg of total RNA was reverse transcribed by SuperScript II RT-Kit (Gibco) according to the manufacturer's protocol using random hexamers (Perkin-Elmer) as primers. The primer sequences and conditions for PCR are displayed in Table 2.1. Primers were synthesised by Invitrogen (Basel, Switzerland), probes by Eurogentec (Seraing, Belgium). PCR products were detected with agarose-gel electrophoresis using an agarose concentration

of 1.5% (w/V) (Invitrogen) and 0.5 $\mu$ g/ml ethidium bromide. The gel was run at 120V for 50min.

TaqMan analysis (quantitative RT-PCR) was carried out on a Gene Amp 5700 Sequence Detection System (Applied Biosystems, Rotkreuz, Switzerland). All samples were run in triplicates. A relative standard curve was generated by serial dilutions of cDNA. The dilution of the latter cDNA was expressed by the respective dilution value. Ct values of standards were plotted against the log of the respective dilution factors. Slope and y-intercept of the standard curve line were then calculated by linear regression and used to calculate the input amount for unknown samples for respective genes. To standardise the amount of sample cDNA added to reaction the calculated amount of the gene of interest was divided by the calculated amount of the constitutively expressed glyceraldehydes-3-phosphate dehydrogenase (GAPDH) gene in the sample. These normalised amounts were then used to compare the relative amount of target in different samples.

#### *2.4.5. Sequencing of *slc15a1* (PEPT1) and *slc22a8* (OAT3) PCR products*

PCR products were, after isolation with the Qiaquick Gel extraction kit (Qiagen, Hilden, Germany) according to the manufacturer's description and after quantification of DNA with Quant-iT™ Picogreen dsDNA Assay Kit (Molecular Probes, Leiden, The Netherlands), sent to Microsynth AG (Balgach, Switzerland) for sequencing. The received sequences were checked for homology with nucleotide-nucleotide blast at [www.ncbi.nlm.nih.gov/BLAST/](http://www.ncbi.nlm.nih.gov/BLAST/).

#### *2.4.6. Confocal microscopy*

For immunostaining, cells grown in Chamberslides® (Nalge Nunc International, Rochester, NY, USA) were used. Cells were washed 3 times with PBS and fixed for 20 minutes with 4% (w/v) paraformaldehyde in PBS. After washing 3 times with PBS, tissues were permeabilised for 5 minutes with 0.5% (v/v) Triton X-100 in PBS. For immunostaining, cells were incubated for one hour at 37°C in a humid chamber with the primary antibody dissolved in PBS supplemented with 3% (w/v) BSA (bovine serum albumin). After washing twice with PBS, the fluorochrome conjugated secondary antibody dissolved in PBS supplemented with 3% (w/v) BSA was added for one hour at room temperature, in a dark chamber. Stained cells were then washed twice with PBS and mounted with FluorSave® (Calbiochem, San Diego, CA). Fluorescence stained cells were examined on a confocal Zeiss LSM 150 inverted laser scanning microscope (Carl Zeiss, Oberkochen, Germany). For fluorescein uptake, temperature control was used at 37°C, software: Carl Zeiss



LSM510 V3.2. All pictures except uptake of fluorescein are 400x magnified, excitation at the wavelength 488nm, fluorescein uptake: 100x magnification. The intensity of fluorescence was quantitatively determined with ImageJ 1.33u (National Institutes of Health, USA, <http://rsb.info.nih.gov/ij/>) by selecting 20 different spots in each image. Mean gray values were measured and analysed as described under statistical analysis.

Primary antibodies used for these experiments were purchased at Alexis Biochemicals and used for ABCB1, ABCC1-5 staining: monoclonal antibody (Mab) to ABCB1 (human, JSB-1); mouse IgG1 Mab to ABCC1 (human; MRPm6); mouse IgG1 Mab to ABCC2 (human; M<sub>2</sub>l-4), mouse IgG1 Mab to ABCC3 (human; M<sub>3</sub>ll-9), rat IgG2a Mab to ABCC5 (human; M<sub>5</sub>l-1). The primary antibodies for ABCB1, ABCC1, ABCC2 and ABCC3 were each diluted at a ratio of 1:50 and ABCC5 at a ratio of 1:25 with PBS and 3% FCS. For the staining of slc4a4 a polyclonal antibody was used from guinea pig serum (Chemicon International, Temecula, USA). The dilution rate used was 1:100.

The following secondary fluorescent antibodies were used (Jackson Immuno Research): for ABCB1 and ABCC1-3 Cy2 AffiniPure rabbit Anti-Rat IgG (H+L), for ABCC5: Cy2 AffiniPure Goat Anti Mouse IgG (H+L), for slc4a4 Cy2: AffiniPure Goat Anti Guinea Pig IgG (H+L), for double staining of ABCB1 and slc4a4 Cy3: AffiniPure Goat Anti Mouse IgG (H+L), and for slc4a4 the same secondary antibody as described above.

#### *2.4.7. Statistical analysis*

Statistical significance was investigated with t-test (two-tailed distribution with unequal variances). A probability of  $p < 0.05$  was defined as statistically significant. All transport and uptake studies were performed with primary cells obtained from two different isolations (exception: uptake with MTX and probenecid, see Table 2.2). Each isolation originated from at least two different pigs, as three or more pig kidneys have been used for one isolation procedure. Each transport or uptake assay was performed in triplicate. Results are expressed as the mean  $\pm$  SEM.

## **2.5. Results**

### *2.5.1. Expression of transporters at mRNA level*

With RT-PCR (qualitative PCR), mRNA expression of *slc5a2* (SGLT2), *slc15a1* (PEPT1), *slc22a8* (OAT3), *slc4a4* (NBC1), *slco1a2* (OATP-A) was shown, while *slc22a1* (OCT1) and *slc22a6* (OAT1) were only detected in freshly isolated proximal tubular cells (Fig. 2.2). Porcine GAPDH, *slc5a2* and *slc15a1* mRNA expression served as positive controls. Fig. 2.2B shows that *slc5a2* is expressed. With quantitative RT-PCR (Taqman<sup>®</sup> assay), *abcc1* (MRP1), *abcc2* (MRP2) and *abcb1* (P-gp) mRNA expression was revealed (Figure 2.3). Generally, an up-regulation of *abcc1* and a down regulation of *abcc2* during culture were noticed, while the level of *abcb1* mRNA expression seems to remain constant.

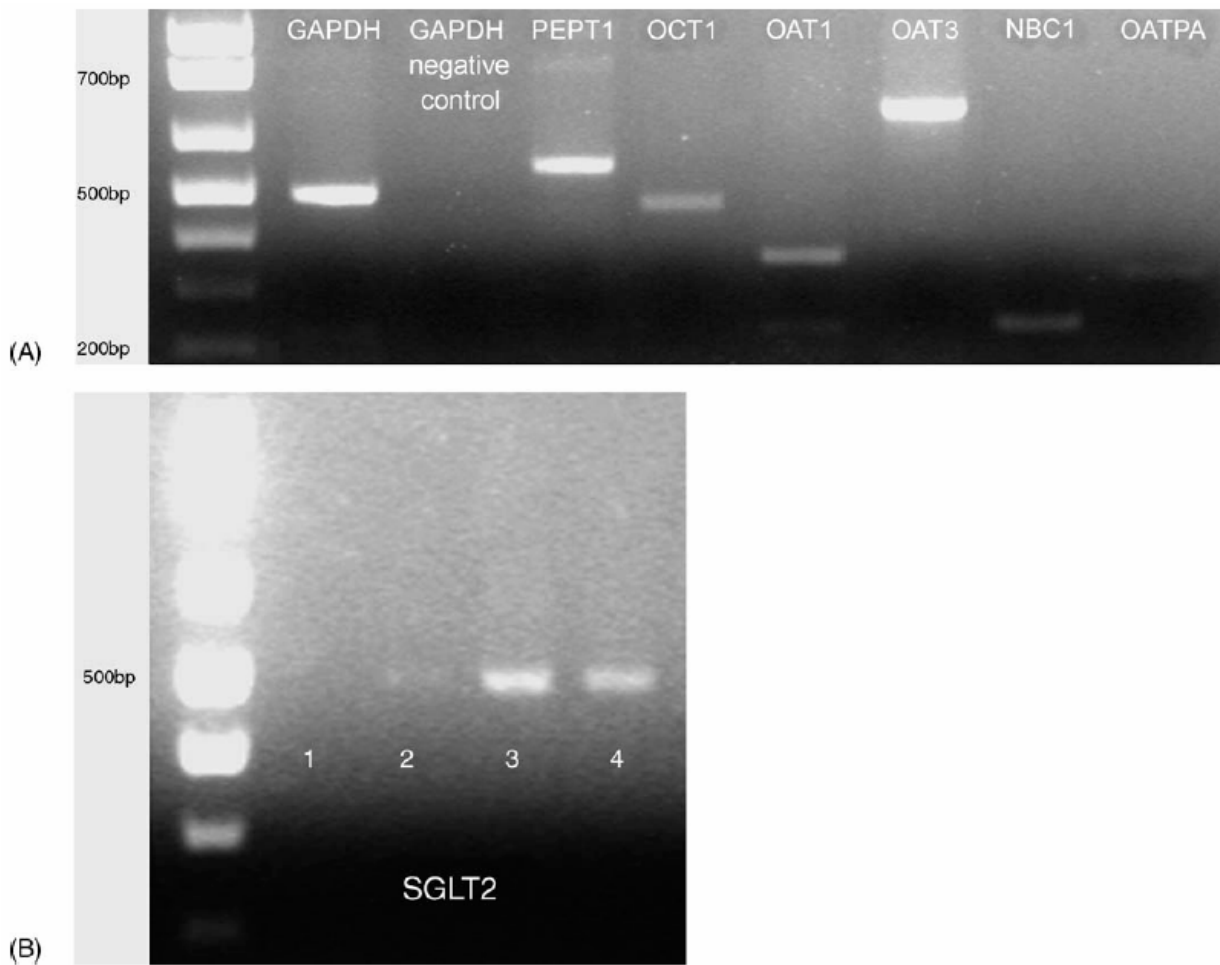


**Figure 2.2** – (A): PCR of different transporters from freshly isolated primary proximal tubular cells: GAPDH (496bp), *slc15a1* / PEPT1 (634bp), *slc22a1* / OCT1 (464bp), *slc22a6* / OAT1 (355bp), *slc22a8* / OAT3 (701bp), *slc4a4* / NBC1 (241bp) and *slco1a2* / OATPA (333bp). (B): PCR of *slc5a2* / SGLT2 (494bp). The probes 1 and 2 are from pig kidney cortex while probes 3 and 4 are derived from isolated primary pig proximal tubular cells.

### 2.5.2. Sequencing

Sequencing of *slc15a1* (pPEPT1) band gave a 99% homology with the *sus scrofa* peptide transporter 1 (accession number: [NM\\_214347](#) respectively [AY180903](#)).

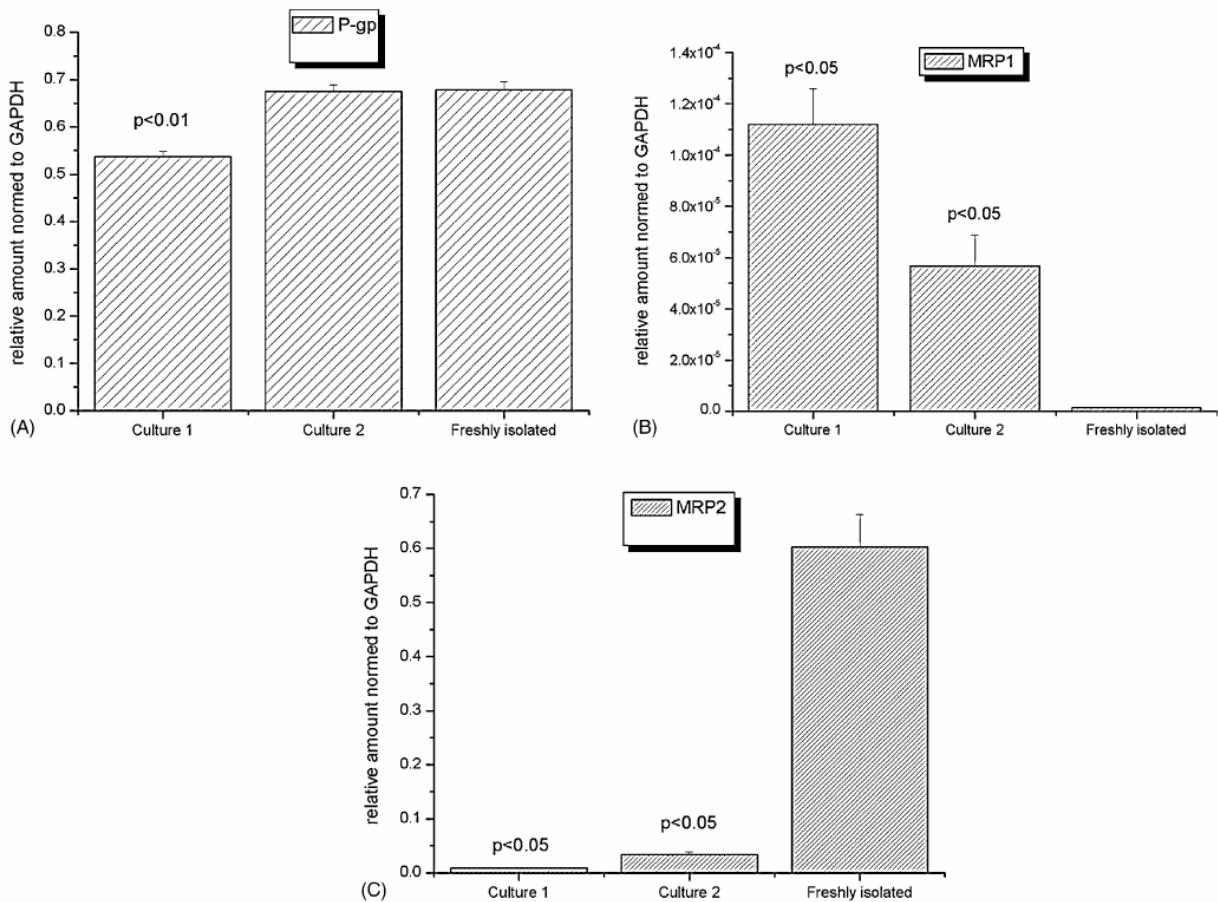


**Figure 2.3** - Quantitative expression of *abcb1* / P-gp (A), *abcc1* / MRP1 (B) and *abcc2* / MRP2 (C) normed to GAPDH. Culture 1 and 2 derived from two different isolations of different pigs. They were cultured as described in methods for 10-11 days. “Freshly isolated” means the proximal tubular cells were directly processed for RNA-isolation, DNA digestion and reverse transcription after isolation from pig kidneys.

Slc22a8 (pOAT3) sequence gave a match of 99% with pOAT3 (accession Number: **AJ587003** and **NM\_214455**) (sequence data not shown).

### 2.5.3. Functional assay

The polar orientation of the cells growing on a surface was checked with confocal microscopy by double staining. The basolateral side of the cells was attached to the microscope slide. *Abcb1* was shown to be predominantly expressed on the apical side of the cells (Fig. 2.4). The basolateral-to-apical *abcb1* mediated transport and uptake of digoxin were inhibited by verapamil (Fig. 2.5A - B). Verapamil inhibited digoxin transport from basolateral-to-apical in a dose-dependent manner, whereas from apical-to-basolateral transport of digoxin was enhanced with verapamil (not significant, data not shown).

Uptake and transport of MTX seems to be complex as it is transported through different

**Table 2.2** - Uptake data after 2h. MTX (methotrexate) is used as model substrate for abcc1-6 (MRP1-6), whereas glycylsarcosine serves as a substrate for slc15a1/2 (PEPT1/2) and glucose for slc5a1/2 (SGLT1/2).

Basolateral → apical	Percent of dose ± S.E.M. [%]
<sup>3</sup> H-MTX 23.6 nM	0.053 ± 0.001
with probenecid 20 μM	0.043 ± 0.002 <sup>*</sup>
<sup>3</sup> H-MTX 24.1 nM + MTX 10 μM	0.033 ± 0.002
With MK571 20 μM	0.048 ± 0.003 <sup>*</sup>
<sup>3</sup> H-MTX 6.0 nM + MTX 1 μM	0.017 ± 0.001
With MK571 50 μM	0.031 ± 0.001 <sup>**</sup>
With indomethacin 50 μM	0.025 ± 0.001 <sup>*</sup>
Apical → basolateral	Percent of dose ± S.E.M. [%]
<sup>3</sup> H-MTX 24.1 nM + MTX 10 μM	0.051 ± 0.009
With 20 μM MK571	0.096 ± 0.016
<sup>3</sup> H-MTX 18.2 nM + MTX 1 μM	0.035 ± 0.002
With MK571 10 μM	0.052 ± 0.002 <sup>**</sup>
With indomethacin 50 μM	0.029 ± 0.005
<sup>14</sup> C-glycylsarcosine 5.5 μM	0.197 ± 0.014
With penicillin G 10 mM	0.102 ± 0.018 <sup>*</sup>
<sup>3</sup> H-glucose 0.5 μM	0.12 ± 0.008
With phlorizin 20 μM	0.081 ± 0.005 <sup>*</sup>

Bold: control.  
<sup>\*</sup> p < 0.05. Data represents means (±S.E.M.) of three experiments.  
<sup>\*\*</sup> p < 0.01. Data represents means (±S.E.M.) of three experiments.

**Table 2.3** - P<sub>app</sub> values after 1h. Fluorescein is a model substrate for slc22a6-8 (OAT1-3), MTX (methotrexate) for abcc1-6 (MRP1-6) and glycylsarcosine for slc15a1/2 (PEPT1/2).

Basolateral → Apical	P <sub>app</sub> ± S.E.M. [cm/s]
Fluorescein 5 μM	1.79 × 10 <sup>-6</sup> ± 6.19 × 10 <sup>-8</sup>
With probenecid 200 μM	1.37 × 10 <sup>-6</sup> ± 1.63 × 10 <sup>-7</sup>
With estrone sulfate 200 μM	1.04 × 10 <sup>-4</sup> ± 1.06 × 10 <sup>-7<sup>*</sup></sup>
With PAH 200 μM	1.79 × 10 <sup>-6</sup> ± 9.75 × 10 <sup>-8</sup>
<sup>14</sup> C-glycylsarcosine 5.5 μM	1.96 × 10 <sup>-6</sup> ± 3.39 × 10 <sup>-7</sup>
With benzylpenicillin 10 mM	2.87 × 10 <sup>-6</sup> ± 6.54 × 10 <sup>-7</sup>
Apical → Basolateral	P <sub>app</sub> ± S.E.M. [cm/s]
<sup>3</sup> H-MTX 17.9 nM & MTX 1 μM	8.31 × 10 <sup>-4</sup> ± 5.43 × 10 <sup>-5</sup>
With indomethacin 50 μM	6.90 × 10 <sup>-4</sup> ± 3.81 × 10 <sup>-5</sup>
<sup>14</sup> C-glycylsarcosine 5.5 μM	1.36 × 10 <sup>-6</sup> ± 7.91 × 10 <sup>-8</sup>
With benzylpenicillin 10 mM	7.88 × 10 <sup>-7</sup> ± 5.33 × 10 <sup>-8<sup>*</sup></sup>

Fluorescein is a model substrate for slc22a6-8 (OAT1-3), MTX (methotrexate) for abcc1-6 (MRP1-6) and glycylsarcosine for slc15a1/2 (PEPT1/2). Bold: control.  
<sup>\*</sup> p < 0.05. Data represent means (±S.E.M.) of three experiments.

subtypes of abcc1-6 (MRP1-6). All subtypes pump xenobiotics out of the cells, those at the basolateral side (abcc1, 3, 5, 6) are directed

into blood while those at the apical side (abcc2, 4) pump into urine. At the apical side (Fig. 2.6) the dose-dependent uptake of MTX, an abcc1-6 substrate, was enhanced by the specific abcc1-6 inhibitor MK571. Basolateral inhibition of abcc1 by MK571 resulted also in an increased MTX uptake (Table 2.2). These findings show a translocation of MTX both by abcc1 and abcc2. Indomethacin, a known abcc1 inhibitor, inhibited significantly MRP activity only at the basolateral side, where abcc1 is located (Table 2.2). Indomethacin tends to inhibit transport of MTX from apical-to-basolateral (Table 2.3) which also can be explained by selective inhibition of abcc1 at the basolateral

side. This model, therefore, may allow a functional discrimination of the two subtypes abcc1, 2. MTX uptake in the cells was also inhibited by probenecid (Table 2.2). Fluorescein was used as model substrate for slc22a6-8 located at the basolateral side, transporting fluorescein from the blood into the cells. An inhibition of slc22a6-8 at the basolateral side means a reduced uptake and transport of organic anions.

Transport of fluorescein from basolateral-to-apical was inhibited by estrone sulfate, while PAH didn't show any inhibitory effect. Probenecid showed a small and not significant inhibition (Table 2.3).

Slc15a1/2 (PEPT1/2) is located at the apical side of renal proximal tubular cells and is

responsible for re-absorption of amino acids and oligopeptides. As a model compound, glycylsarcosine was used to demonstrate functional expression in our cells. Penicillin G (benzylpenicillin) was used as an inhibitor. Transport and uptake of glycylsarcosine could be demonstrated in our cells and it was inhibited by penicillin (Table 2.3).

Glucose is re-absorbed by slc5a1/2 (SGLT1/2) at the apical side of the proximal tubular cells. In our cells glucose uptake could be inhibited by phlorizin (Table 2.2).

#### *2.5.4. Uptake of fluorescein in viable cells*

With confocal microscopy it was possible to visualise the uptake of fluorescein into viable cells. In Fig. 2.7 the intensities are quantitatively plotted. The uptake was strongly reduced by addition of 200 $\mu$ M probenecid, 200 $\mu$ M estrone sulfate and 10mM penicillin (Fig. 2.7). With 100 $\mu$ M MTX and 200 $\mu$ M p-aminohippurate (PAH) the uptake of fluorescein was also inhibited (Fig. 2.7). However, the effect is not as strong as with probenecid. PAH was used as a slc22a6 (OAT1) inhibitor. An explanation for the lower inhibitory effect of PAH could be that slc22a8 (OAT3) expression was possibly higher than slc22a6 expression.

#### *2.5.5. Immunostaining*

In figure 2.8, staining of cells for slc4a4 (NBC1), abcb1 (P-gp), abcc (MRP) 1-3, 5 is shown. The presence of slc4a4, abcb1, abcc1 and abcc2 at protein level was shown by immunocytochemistry. Abcc3 and 5 protein expression could not be shown by immunostaining.

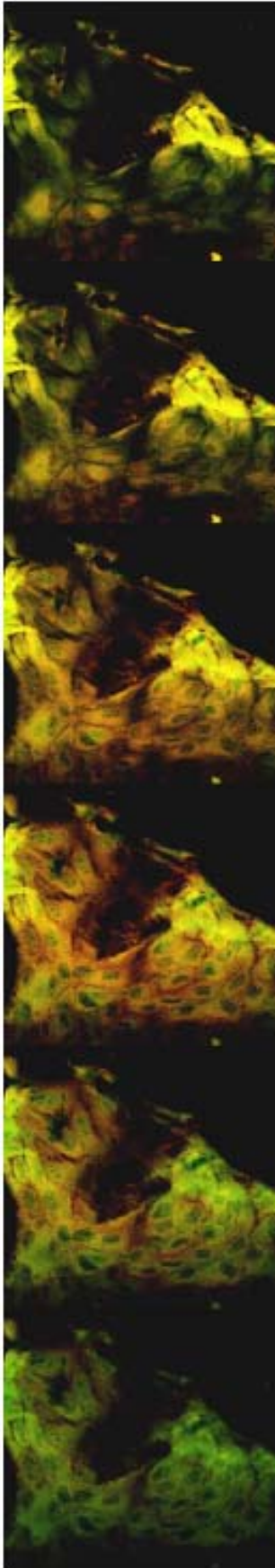


**Figure 2.4** - Z-Stack of primary proximal tubular cells stained with ABCB1 and SLC4A4 starting from the apical side down to the basolateral side. CY3 staining (red) represents ABCB1 and CY2 staining (green) SLC4A4.

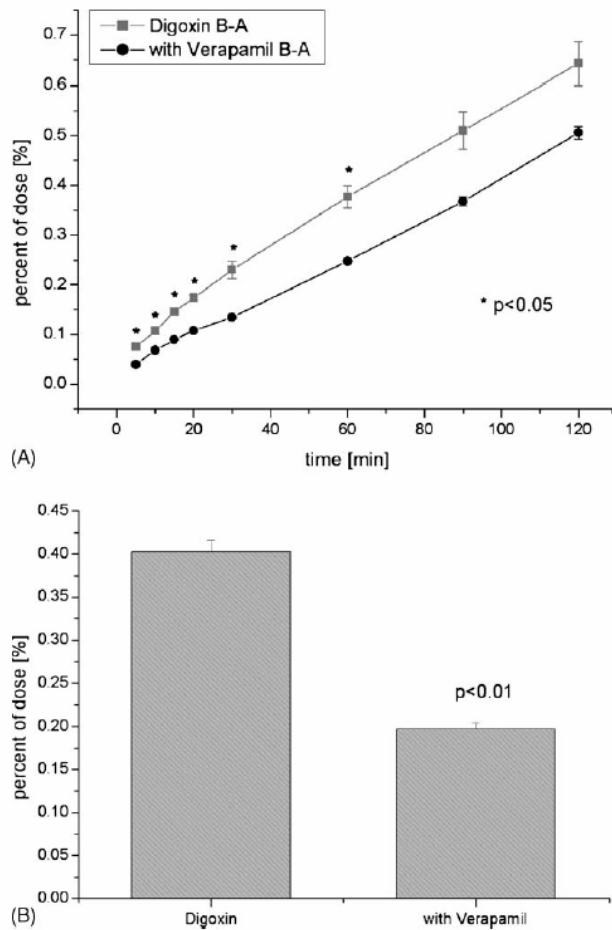


**Figure 2.5** – (A) Transport of 8.55nM digoxin with and without 100 $\mu$ M verapamil from basolateral-to-apical. (B) Uptake of digoxin at the basolateral side with and without 100 $\mu$ M verapamil after 2h.

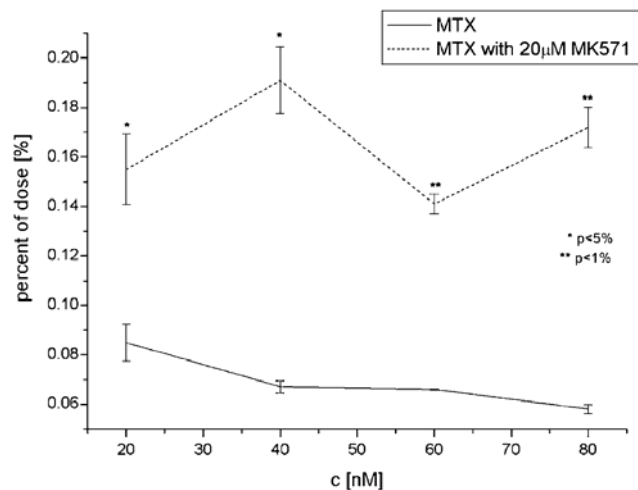


**Figure 2.6** - Uptake in cells at the apical side after 45 min with different MTX concentrations.

## 2.6. Discussion

### 2.6.1. Expression of transporters on mRNA level

The PCR bands of *slc15a1* (pPEPT1) and *slc22a8* (pOAT3) were located lower than they should be (634bp for pPEPT1 and 701 for pOAT3, Fig. 2.2). Therefore the PCR products of pPEPT1 and pOAT3 were sequenced and amplification of the right product was confirmed.

The mRNA expression of porcine *slc5a2* (SGLT2) and *slc15a1* (PEPT1) was shown by RT-PCR and on a functional level. *Slc5a2* and *slc15a1* are restricted to proximal tubular cells only [111, 122]. Therefore, we conclude that the isolation procedure provided us with proximal tubular cells. In the kidney, *slc5a2* and *slc15a1* are restricted to the S1 segment, whereas *slc5a1* (SGLT1) and *slc15a2* (PEPT2) are restricted to the S3 segment [5, 111]. We did not screen our cells for porcine *slc5a1*, *slc15a2*, *abcc3-6* and *slc22a4/5* for mRNA expression since there is a lack of genetic information on these transporters in pigs.

*Slc4a4* (NBC1) is exclusively expressed at the basolateral side of the proximal tubular cells [37, 125]. Its specific staining provided further evidence for the proximal tubular origin of our cells.

Since information about the porcine gene sequences of *abcb1* (P-gp), *abcc1* (MRP1), *abcc2* (MRP2), *slc15a1* (PEPT1), *slc5a2* (SGLT2), *slc22a1* (OCT1), *slc22a6* (OAT1), *slc22a8* (OAT3), *slc4a4* (NBC1) and *slco1a2* (OATP-A) was available, only mRNA expression of these genes was investigated in our cells. In freshly isolated cells mRNA expression of each of these transporters was demonstrated. *Slc22a6* and *slc22a1* mRNA expression was down-regulated in culture. A possibility to reach the „*in vivo* like“ expression of *slc22a6* and *slc22a1* is to induce *slc22a6* gene expression with triiodothyronine [130], dexamethasone [131] or AST-120 [132] and *slc22a1* gene expression with dexamethasone [133]. Another possibility is to use fresh isolated proximal tubular cells without culturing them for days. By this means a down regulation of transporters could be avoided. This should be investigated in a further series of experiments.

Furthermore, *abcb1*, *abcc1* and *abcc2* mRNA expression was determined quantitatively showing a remarkable variability for *abcc1* and *abcc2*, while *abcb1* appeared to be constantly expressed in different isolations (Fig. 2.3). During culturing, *abcc1* and *abcc2* were up- and down-regulated, respectively.

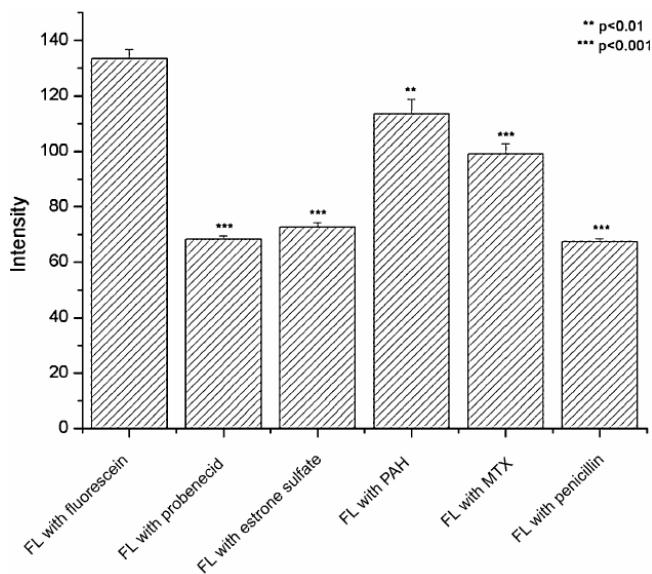


**Figure 2.7** - Intensity values from uptake of 1µM fluorescein after 30min, with 200µM probenecid, 200µM estrone sulfate, 200µM PAH, 100µM MTX and 10mM penicillin.

### 2.6.2. Protein expression

The expression of *slc4a4*, *abcb1*, *abcc1* and *abcc2* on protein level was shown by immunocytochemistry (Fig. 2.8A-D). However, *abcc3* and *abcc5* were not detected in our cells (Fig. 2.8E, F). This could be due to a lack of homology between human and porcine as we used antibodies against human ABCC3 and ABCC5. To date, in pigs there is information available neither about *abcc3* and *abcc5* genes nor the respective protein structures.

*Abcb1* (P-gp) is located apically and *slc4a4* (NBC1) basolaterally [37, 125].

With double-staining for *abcb1* and *slc4a4*, the right spatial orientation of our cells growing on a surface could be confirmed. This gives us further evidence, that the cells are correctly orientated with the basolateral side on the microscope slide.

### 2.6.3. Tightness

By TEER and FITC-dextran transport measurements as a negative control, we could ensure tightness of the monolayers for the transport and uptake assays. For the widely used MDCK cell line, which consists of distal tubular cells, transendothelial resistances were measured resulting in  $\Delta$ TEER between 50-600  $\Omega \cdot \text{cm}^2$  [128, 134-137]. Using dog urine extracts may increase  $\Delta$ TEER in MDCK to values up to 800  $\Omega \cdot \text{cm}^2$  [138]. According to Gallardo et al. [138], transepithelial resistance rises *in vivo* from the proximal tubular cells (5-8  $\Omega \cdot \text{cm}^2$ ) to the distal cells (150-600  $\Omega \cdot \text{cm}^2$ ) and along the collecting duct (860-2000  $\Omega \cdot \text{cm}^2$ ). In the LLC-PK1 cell line, which consists of proximal tubular cells,  $\Delta$ TEER values range between 100-200  $\Omega \cdot \text{cm}^2$  [134, 135, 139], while the interesting cell line HK-2 (immortalised human proximal tubular cells) reaches a tightness of about 110  $\Omega \cdot \text{cm}^2$  [128]. With the primary porcine proximal tubular cells  $\Delta$ TEER values in general between 1500 and 2500  $\Omega \cdot \text{cm}^2$  can be obtained. With values below 900  $\Omega \cdot \text{cm}^2$ , transport assays were not possible: FITC-dextran was transported to a bigger extent indicating that the



monolayers were not confluent anymore. This cell culture model provides a much tighter monolayer than the other commonly used models. A higher transepithelial resistance means reduced paracellular transport (passive diffusion) through tight junctions. This may facilitate the discrimination of transport related from unspecific drug translocation. However, a correlation between *in vivo* and *in vitro* resistances in different parts of the kidney is difficult to establish.

#### 2.6.4. ABCB1 (P-gp)

Expression of porcine *abcb1* could be demonstrated on mRNA, protein and on a functional level. *Abcb1* is located at the apical side (urine side, Fig. 2.1) and seems not to be down or up regulated during cultivation (Fig. 2.3A). Digoxin excretion was reduced with verapamil, a known *abcb1* inhibitor (Fig. 2.5A). In the basolateral-to-apical experiment one would expect accumulation of digoxin in the cells. However, we found contrary results (Fig. 2.5B). Therefore, the mechanism of digoxin uptake into the cell is not completely solved. This may be explained by the inhibition of another not yet defined uptake mechanism of digoxin by verapamil at the basolateral side. One candidate of this uptake may be the human SLCO4C1 or a corresponding porcine transporter [87]. Its inhibition would then result in a decreased digoxin uptake.

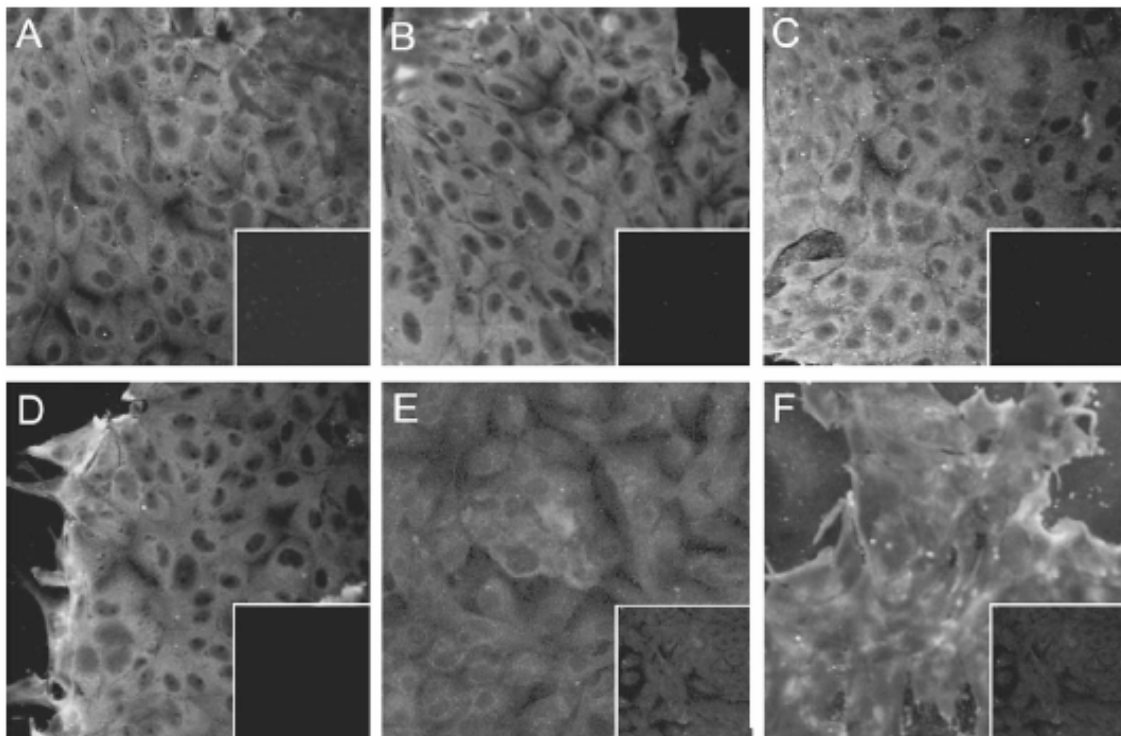


**Figure 2.8** - Immunostaining of transporters, on the right bottom side corresponding negative control. Staining is positive for *slc4a4/NBC1* (A), *ABCB1/P-gp* (B), *ABCC1/MRP1* (C) and *ABCC2/MRP2* (D). For *ABCC3/MRP3* (E) and *ABCC5/MRP5* (F) staining is negative.

#### 2.6.5. *ABCC1-6 (MRP1-6)*

*Abcc1* and *abcc2* mRNA could be shown in primary porcine proximal tubular cells even though *abcc2* is down-regulated during culture as indicated by quantitative RT-PCR (Fig. 2.3C). *Abcc1-6* mediated transport is complex: Each result could be explained either by inhibition of *abcc1* at the basolateral or of *abcc2* at the apical side.

Indomethacin inhibited *abcc1* at the basolateral side, not at the apical side, where *abcc2* is located (Table 2.2). Thus in this model indomethacin can be used as a selective *abcc1* inhibitor, as already described in [107, 140]. Nevertheless the system shows *abcc1-6* activity on both sides, as the uptake is enhanced with MK571 inhibition (Table 2.2), a selective *abcc1-6* inhibitor [141, 142].

Table 2.3 shows that apical-to-basolateral transport of MTX is inhibited with indomethacin which confirms that indomethacin inhibits selectively *abcc1* at the basolateral side.

#### 2.6.6. *Slc22a6/8 (OAT1/3)*

*Slc22a6* and *slc22a8* are expressed in freshly isolated cells, in cultured cells only *slc22a8* was detectable (Fig. 2.2). Fluorescein is a classical model substrate for *slc22a6-8* [143]. They are located at the basolateral side and translocate organic anions into the cells in exchange for  $\alpha$ -ketoglutarate (Fig. 2.1). As a general inhibitor of *slc22a6-8* probenecid is used whereas estrone-sulfate inhibits *slc22a8* selectively and PAH seems to be more selectively inhibiting *slc22a6* [4]. PAH has a high affinity for porcine *slc22a6* ( $K_m = 3.75\mu\text{M}$ ) [144], whereas ES has a high affinity for rat *slc22a8* ( $K_m = 2.3\mu\text{M}$ ) [7]. Although no information on PAH affinity to porcine *slc22a8* was found in the literature, a similar situation was described in rabbit proximal tubular cells where PAH is translocated by rabbit *slc22a6* and not by rabbit *slc22a8* and ES mainly by rabbit *slc22a8* [145]. Also, in human *SLC22A8* transfected *Xenopus laevis* oocytes, ES has a higher affinity than PAH ( $K_m$  3.1 $\mu\text{M}$  for ES and 87.2 $\mu\text{M}$  for PAH) [93]. In many species (from fish to mammals), the organic anion secretion system is expressed and functionally available [146]. Therefore, it is possible that substrate specificity and affinity remain comparable in all species. In the functional assay (Table 2.3), fluorescein transport could only be inhibited by ES and probenecid showed only a weak inhibition. This indicates the functional availability of porcine *slc22a8*. In freshly isolated cells, where *slc22a6* and 8 are expressed, the inhibition with PAH is not as strong as with ES or probenecid (Fig. 2.7). A possible explanation could be that the porcine *slc22a8* analogue has a higher affinity for fluorescein

or that functional activity of *slc22a8* is higher than of porcine *slc22a6*.

Interestingly, penicillin inhibits fluorescein uptake (Fig. 2.7), indicating excretion through *slc22a6-8*. MTX is not only transported through *abcc1-6*, but also by *slc22a6-8* [6], as probenecid, an *slc22a6-8* and *abcc1-6* inhibitor [4], reduced MTX uptake at the basolateral side (Table 2.2). However, the transport of fluorescein, a *slc22a6-8* substrate, could not be inhibited with 100 $\mu$ M MTX (Fig. 2.7). This may be explained by the fact that most data on transport of MTX through *slc22a6-8* were generated in transfected models, where these transporters were over-expressed. Therefore, it is tempting to speculate that in this more complex and physiological model MTX translocation through *slc22a6-8* seems to play only a minor role.

#### 2.6.7. *Slc15a1/2 (PEPT1/2)*

These transporters translocate penicillin and other antibiotics, peptides and peptide-like substances. They are inwardly directed transporters located at the apical side of proximal tubular cells and play – under physiological conditions – an important role for the re-absorption of amino acids and peptides from the urine.

Glycylsarcosine is used as a model substrate for *slc15a1/2*. Whereas *slc15a1* is mainly described as an intestinal transporter, *slc15a2* is described as an renal transporter [122]. Although we could demonstrate *slc15a1* mRNA expression (Fig. 2.2), genetic information on *slc15a2* was to date not available. As both transporters *slc15a1* and *slc15a2* are directed inwardly into the cells at the apical side it is clear that the apical-to-basolateral transport of glycylsarcosine is reduced by penicillin (Table 2.3), an inhibitor of both transporters. On the other side, the basolateral-to-apical transport of glycylsarcosine was slightly enhanced by penicillin (not statistical significant, Table 2.3), as one would have expected.

The uptake of glycylsarcosine at the apical side is inhibited (Table 2.2).

#### 2.6.8. *Slc5a1/2 (SGLT1/2)*

Sodium-dependent glucose transporters are responsible for the re-absorption of glucose and other sugars. Both, *slc5a1* and 2, are located at the apical side and transport sugar from the tubular lumen into the cell [111]. We could show their activity as glucose uptake at the apical membrane is significantly inhibited by phlorizin (Table 2.2), an inhibitor of these two transporters [111].

### 2.6.9. Transporters in other cell lines

Parental HKC, HK-2 and MDCK were investigated for Na/HCO<sub>3</sub> co-transporter (NBC), p-glycoprotein (abcb1) and MRPs (abcc1-6) respectively [147-149]. A lot of information exist on transfected cell lines studying e.g. P-gp (abcb1), MRP2 (abcc2), OATP1B1 (sclo21a6), hOAT1 (SLC22A8) in MDCK [107, 108, 150], but also for LLC-PK1 [105, 106, 151] and HEK293 [109, 110, 118, 152] information is available. These interesting studies have investigated in an isolated manner the function of one to two transfected transporters in one cell line and seem to be useful to study, which drugs could potentially be translocated by the transfected transporters.

*In vivo*, the situation is different, since many transporters are expressed concurrently. Transfecting and over-expressing of one or two drug transporters, lead to a changed *in vitro* system and ignored other possible active drug transporters. We are aware that in primary culture cells, the *in vitro* system is also changed by down- or up-regulation of drug transporters' gene expression. Although we used the cells for a maximum of two weeks, such alteration in gene expression have been observed (see Fig. 2.3). Nevertheless, we could show preservation of functional expression of most of the investigated transporters in our unmodified system. Data on simultaneous functional expression of these drug transporters in parental proximal tubular cell lines, (such as LLC-PK1, HK2 and HEK293), are - as far as we know - to date not available. Despite these possible theoretical advantages of our primary cell culture model, we do not have experimental data to prove superiority over the commonly used cell lines. Therefore, a direct comparison of these models should be done using different model compounds and comparing this with *in vivo* data. However, these kind of experiments were beyond the scope of our capacity and facilities.

### 2.6.10. Final conclusion

Our model is based on a simple isolation of proximal tubular cells from readily available porcine kidneys. We could establish the functional validity of porcine primary proximal tubular cells for *in vitro* study. It might be an interesting tool to study *in vitro* drug elimination, tubular toxicity and drug interactions. Furthermore, it exhibits high transepithelial electrical resistance and thus monolayer tightness was ensured. In addition our model shows functional expression of the most important renal transporters for transport of xenobiotics simultaneously. Therefore, adverse effects resulting from drug-

drug interactions might be investigated and/or predicted. On the other hand, it may allow simulating *in vitro* physiological processes more realistically.

As already mentioned, primary cell cultures seem to have certain advantages compared to immortalised cells [103, 104].

Further studies are required, e.g. characterizing primary human proximal tubular cells in order to establish a correlation between human and pig transport activities in kidney. So far, the question concerning ligand specificities between human and pig transporters remains unanswered. However, pig kidney is apparently easy to obtain compared to human kidney and this species seems to be more closely related to human than rat, rabbit or mouse [10].

This *in vitro* model provides a basis to study the regulation of physiological transport processes and tubular toxicity.

### **Acknowledgements**

This work was supported by the Swiss national foundation and Senglet foundation. Great thanks go especially to Ursula Behrens for the excellent technical assistance.

Reprint requests to Professor Juergen Drewe, Department of Clinical Pharmacology and Toxicology, Petersgraben 4, CH-4031 Basel, Switzerland; Phone: +41-61-265 3848; FAX: +41-61-265 8581; email: juergen.drewe@unibas.ch

### 3. Functional expression of BMDP in kidney

Schlatter P., Gutmann H., Drewe J. ,

Department of Clinical Pharmacology and Toxicology, University Hospital of Basel, Basel,  
Switzerland

**Submitted to: Cellular and Molecular Life Sciences**

### 3.1. Abstract

*Background:* Breast cancer resistance protein (BCRP or ABCG2) is one of the multidrug resistance proteins which is currently under investigations. Its porcine homologue was found in brain capillary endothelial cells and therefore called brain multidrug resistance protein (BMDP). BCRP has shown to be responsible for chemotherapy resistances to various anti-cancer drugs, such as topotecan, irinotecan and mitoxantrone. To date, BCRP protein expression was found in several organs such as in lungs, pancreas, liver, placenta, intestine, urogenital system and kidney (tubular cells). The aim of this study was to investigate, if BMDP is functionally expressed in primary porcine proximal tubular cells (PPPTC). Furthermore, we wanted to investigate, if functional discrimination between BMDP and another multidrug resistant protein (P-gp, ABCB1) is possible. Finally, various drugs (antiepileptic agents, nonsteroidal anti-inflammatory drugs, proton pump inhibitors, caffeine, thalidomide, theophylline and dotatoc) were screened for an inhibitory effect on BMDP function.

*Methods:* PPPTC were isolated from porcine kidneys. Expression of BMDP was measured at the mRNA level by quantitative RT-PCR. Protein expression of BCRP was verified with immunohistochemistry and Western blot analysis. Functional studies included uptake assays with the fluorescent BCRP substrate mitoxantrone and prazosin as inhibitor and various other drugs as well as the P-gp substrate digoxin with verapamil inhibitor.

*Results:* In porcine proximal tubular cells, BMDP was found to be expressed at mRNA and protein level. Prazosin enhanced mitoxantrone uptake at the apical (urine) side, whereas verapamil did not show any inhibitory effect on BMDP. P-gp was functionally active, too. The discrimination of P-gp and BMDP activity was possible. Prazosin inhibited both, BMDP and P-gp function. From the tested drugs, only phenytoin inhibited BMDP.

*Conclusion:* Functional expression of BMDP was shown in PPPTC. This transporter could potentially be involved in renal drug-drug interactions and excretion of drugs. Our study provides an in-vivo model based on primary porcine proximal tubular cell, which can now be used to test drug transport in the kidney with respect to BMDP and P-gp function.

### 3.2. Introduction

The breast cancer resistance protein (BCRP) is a member of the ABCG family and has a molecular weight of 72kDa [29, 153, 154], respectively around 70kDa [155] and authors in [156] even state a molecular weight of 65kDa. The porcine homologue of the human

BCRP was found in brain capillary endothelial cells and was named brain multidrug resistance protein (BMDP) with a sequence homology of 86% to the human BCRP [28].

BCRP (ABCG2) belongs, similar to P-gp (ABCB1 alias P-glycoprotein), to the multidrug resistance proteins, which were first found over-expressed in tumour cells from patients with impaired chemotherapy [32]. Typical BCRP substrates are camptothecin derivatives (topotecan, irinotecan and its active metabolite SN-38, which are topoisomerase I inhibitors), flavopiridol, anthracyclines, the food carcinogen PhIP and the topoisomerase II inhibitor mitoxantrone, but not the typical P-gp substrates such as paclitaxel or vinca alkaloids [29, 32]. ABCG2 has been found in various normal human tissues such as intestine, pancreas, kidney cortex, hepatocytes and alveolar pneumocytes [30]. Interestingly, in human jejunum of healthy subjects the mRNA level of ABCG2 is about three times higher than that of P-gp [35]. Although a correlation between mRNA level and functional expression of the protein is difficult to establish, the latter finding indicates the importance of BCRP in multidrug resistance. In pig, BMDP expression was found in various tissues with highest expression in brain, kidney and lung [28].

ABCG2 seem to have, similar to other multidrug resistance proteins, a protective function: Jonker et al. could show in [33] that *Abcg2* knock-out mice developed severe to lethal phototoxic lesions upon ingestion of pheophorbide, a break-down product of chlorophyll, which occurs in plant-derived foods and food supplements. This protective function is also assumed for the brain, as BCRP is expressed at the blood-brain barrier [32]. Phenobarbital, phenytoin, ethosuximide, primidone, valproate, carbamazepine, clonazepam, and lamotrigine were investigated in a BCRP over-expressed MDCKII cell line, which is originally derived from distal tubular cells from dog, and these tested drugs showed no interactions with BCRP [157]. The authors conclude, that BCRP seems not to be responsible for therapy resistance of the tested antiepileptic drugs at the blood-brain barrier.

As mentioned above, BCRP seems to be expressed in human kidney cortex. In mice, *bcrp* was found to be expressed in the brush border membrane of proximal tubules (apical side/urine side) [31]. Therefore, the aim of this study was to investigate if the porcine homologue BMDP is functionally expressed in primary porcine proximal tubular cells. This was investigated by quantitative RT-PCR, Western blot analysis and immunocytochemistry. For functional studies, the fluorescent BCRP substrate mitoxantrone and the inhibitor prazosin was used. Furthermore, we investigated, if we could discriminate P-gp and BCRP activity by using the P-gp substrate digoxin with



verapamil, prazosin and combination of both substances. Finally, we tested various antiepileptic drugs for BMDP interaction, most of them known to be excreted via the kidney: carbamazepine, carbamazepine-epoxide, gabapentin, lamotrigine, vigabatrine, phenytoin, felbamate and topiramate. Other substances were also tested which could be potentially excreted via kidney: acetylsalicylic acid, diclofenac, ibuprofen, indomethacin, fluvoxamine, clomipramine, imipramine, the proton-pump inhibitors ome-, lanso-, rabe- and pantoprazole, coffein, thalidomide, theophylline, yttrium- and gallium-dotatoc (dotatoc stands for [1,4,7,10-tetraazacyclododecane-N,N''',N''''-tetraacetic-acid-D-Phe1-Tyr3]-octreotide, a somatostatin analogue).

### **3.3. Methods**

#### *3.3.1. Materials*

MEM Eagle D-valine w/L-glutamine was purchased from Lucerna Chem AG (Luzern, Switzerland), Dulbecco's MEM / Nut Mix F-12 (DMEM/F12), Fetal calf serum (FCS) and penicillin/streptomycin from Gibco Life Sciences (Basel, Switzerland), cell flask 75cm<sup>2</sup> and 24-well plates from BD (Franklin Lakes, USA), Fumitremorgin C from Alexis (Lausen, Switzerland). All other substances were purchased from Sigma/Fluka in highest quality.

#### *3.3.2. Cell Culture*

Porcine proximal tubular cells were isolated and seeded as described previously [158]. Cells were first seeded ( $1.5 \cdot 10^6$  cells in 75cm<sup>2</sup> flask) in 50ml of 9.6g/1000ml MEM D-Val, 10% FCS and 100U/ml penicillin/streptomycin and cultured for 5 days (after the first 48h media was changed every day). Then culturing was continued with DMEM/F12 with 10% FCS and 100U/ml penicillin/streptomycin until confluency was reached (about 3 days, media was changed every second day). The cells were incubated at 37°C in 95% air and 5% CO<sub>2</sub>. For passaging, the monolayer was trypsinised with 10 ml (trypsin EDTA from Gibco) for 15 min. Then 10 ml of DMEM/F12 was added and centrifuged. After removing supernatant, the cell pellet was diluted in DMEM/F12. For uptake studies cells were transferred onto uncoated 24-well plates .

#### *3.3.3. RT-PCR for BMDP standards*

Total RNA was isolated from confluent monolayers using the RNeasy Mini Kit (Qiagen, Hilden, Germany). RNA was quantified with a Nanodrop Spectrophotometer (Witeg AG, Littau-Luzern, CH). The purity of the RNA preparations was high, as demonstrated by the

260nm/280nm ratio (range, 1.8 - 2.0). After DNase I digestion (Invitrogen, Basel, Switzerland) 1µg of total RNA was reverse transcribed by SuperScript II RT-Kit (Gibco) according to the manufacturer's protocol using random hexamers (Perkin-Elmer) as primers. Gene amplification for generation of standards was performed by PCR in four 25µl reaction units using AmpliTaq Gold DNA polymerase 1.25U (Applied Biosystems, Foster City, USA), dNTPs 200mM (Promega, Catalys AG, Wallisellen, Switzerland), 35ng cDNA (or DNA digested RNA for negative control), forward and reverse primers 0.4µM. The primer sequences and conditions used for BMDP (Accession no.: AJ420927) and for GAPDH (Accession no.: AF017079) are: BMDP forward 5'-CTTCTCATGACCATCTCGTTTGTG-3', BMDP reverse 5'-CCCAAGCGGAGAGACTGATG-3', GAPDH forward 5'-CTTTGCCCGCGATCTAA-3' and GAPDH reverse 5'-ACGATGCCGAAGTTGTCATG-3'.

PCR was performed with Mastercycler personal (Eppendorf AG, Hamburg, Germany) using the following program: 1. step: 95°C over 10min, 2. step: 95°C over 30s, 3. step: annealing temperature.: 60°C for BMDP and 52°C for GAPDH, 4. step: 72°C over 1 min, 5. step: 72°C over 10 min, 6. step: cooling at 4°C. Steps 2 - 4 were repeated 44 respectively 39 times. PCR products were detected with agarose-gel electrophoresis using an agarose concentration of 1.5% (w/v) (Invitrogen) and 0.5µg/ml ethidium bromide. The gel was run at 120V for 50min.

#### *3.3.4. Real-time Polymerase Chain Reaction (TaqMan® Assay)*

At the end of the culture period, medium was removed, total RNA was extracted and reverse transcribed as described above. TaqMan analysis was carried out on an Abi Prism 7900 Sequence Detection System (Applied Biosystems, Rotkreuz, Switzerland). PCR conditions were 10min at 95°C followed by 40 cycles of 15s at 95 °C and 1min at 60°C. Each TaqMan reaction contained 10ng of cDNA in a total volume of 10µl. TaqMan Universal PCR Mastermix from Eurogentec (Geneva, Switzerland) was used. The concentrations of primers and probes were 900nM and 225nM, respectively. Primers and probes were designed according to the guidelines of Applied Biosystems with help of the Primer Express 2.0 software. Primers were synthesised by Invitrogen (Basel, Switzerland), probes by Eurogentec (Seraing, Belgium). All samples were run in triplicates. A standard curve was generated by serial dilutions of cDNA. The dilution of the latter cDNA was expressed by the respective dilution value. Ct (threshold cycle) values of standards were plotted against the log of the respective dilution factors. Slope and y-intercept of the

standard curve line were then calculated by linear regression and used to calculate the input amount for unknown samples for respective genes. To standardise the amount of sample cDNA added to the reaction the calculated amount of the gene of interest was divided by the calculated amount of the constitutively expressed glyceraldehydes-3-phosphate dehydrogenase (GAPDH) gene in the sample. These normalised amounts were then used to compare the relative amount of target in different samples. All samples expressed GAPDH at same Ct values ( $20.18 \pm 0.08$ ). GLP-1R standard was generated using the respective Taqman primers without probe. PCR product was detected as described above on a 3% agarose gel.

Following Taqman primers and probe have been used: GAPDH probe 5'-CGCCTGGTCACCAGGGCTGC-3', GAPDH forward 5'-GTTGAAGGTCGGAGTGAACG-3', GAPDH reverse 5'-CGACAATGTCCACTTTGCCA-3', BMDP probe 5'-CGTCACAACAAACAATAC-3', BMDP forward 5'-AACTTCTGCCCGGGACTCA-3, BMDP reverse 5'-GCCAGTACATATTGCGAAGCTACA-3.

### 3.3.5. Sequencing of GAPDH and BMDP PCR products

PCR was performed as described above. After detecting the bands on an agarose gel, they were cut out with a sterile scalpel. The PCR product was then extracted from the gel slice with the Qiaquick Gel extraction kit (Qiagen, Hilden, Germany) according to the manufacturer's description. After quantification of DNA with Quant-iT™ Picogreen dsDNA Assay Kit (Molecular Probes, Leiden, The Netherlands), the probes were sent to Microsynth AG (Balgach, Switzerland) for sequencing. Correct sequences were confirmed by nucleotide-nucleotide blast at [www.ncbi.nlm.nih.gov/BLAST/](http://www.ncbi.nlm.nih.gov/BLAST/) (data not shown).

### 3.3.6. Confocal microscopy

For immunostaining, cells grown in Chamberslides® (Nalge Nunc International, Rochester, NY, USA) were used. Cells were washed 3x with PBS and fixed for 20 minutes with 4% (w/v) paraformaldehyde in PBS. After washing 3x with PBS, tissues were permeabilised for 5min with 0.5% (v/v) Triton X-100 in PBS. For immunostaining, cells were incubated for one hour at 37°C in a humid chamber with the primary antibody dissolved in PBS supplemented with 3% (v/v) FCS (foetal calf serum). After washing three times with PBS, the fluorochrome conjugated secondary antibody dissolved in PBS supplemented with 3% FCS was added for one hour at room temperature, in a dark chamber. Stained cells were then washed three times with PBS and mounted with FluorSave® (Calbiochem, San

Diego, CA). Fluorescence stained cells were examined on a confocal Zeiss LSM 150 inverted laser scanning microscope (Carl Zeiss, Oberkochen, Germany). The image was 400x magnified. Fluorescence was detected with a wavelength for excitation at 488 nm and for emission between 505-550nm.

Monoclonal antibody to human BCRP from mouse (BXP-21) used for these experiments was purchased from Alexis (Lausen, Switzerland). The dilution ratio was 1:50 in PBS with 3% FCS.

The following secondary fluorescent antibody was used (Jackson Immuno Research) and diluted in PBS with 3% FCS: CY2 AffiniPure goat anti mouse IgG (H+L) with a dilution rate of 1:50 and a final concentration of 5 µg/ml.

### 3.3.7. *Western blot analysis*

Proximal tubular cells were cultured in a 25cm<sup>2</sup> cell culture flask from BD (Franklin Lakes, USA) until confluency was reached. Then proteins were extracted with 300µl protein extraction buffer (20mM Tris-HCl, 1% Igepal CA-630, 0.5mM sodium orthovanadate) including 1mM phenylmethylsulfonyl fluoride (Sigma-Aldrich, St. Louis, MO, USA) and protease inhibitor cocktail tablet, Complete Mini (Roche Diagnostics, Germany). The quantification of the protein content was performed with the BCA protein assay kit (Pierce Chemical, Rockford, IL, USA). Protein concentration was determined by measuring the absorbance at 562nm with Spectra MAX 250 Microplate Spectrophotometer (Molecular Devices Corporation, California, USA).

For immunoblotting, lane A: 66µg, lane B: 35µg and lane C: 100µg (Fig. 3.2) of total protein extract was mixed with Laemmli sample buffer (Bio Rad Laboratories, Reinach, Switzerland) and transferred to the polyacrylamide gel. Gel electrophoresis was performed with a Mini Protean 3 Electrophoresis Cell (Bio Rad) applying 80V for 15min for the stacking gel (4% polyacrylamide) and 120V for 1hour for the separating gel (7.5% polyacrylamide). After electrophoresis, proteins were blotted to the nitrocellulose membrane (250mA for 2.5 hours) using a Mini Trans-Blot Cell (Bio Rad). Protein transfer was verified by Ponceau S staining. The membrane was blocked overnight at 4°C with PBS containing 5% milk powder and 0.05% Tween 20. After washing three times for 15 minutes (0.05% Tween and 1% milk powder in PBS), the membrane was incubated for 2 hours at 37°C with the primary, mouse anti-human antibody against BCRP, 5µg/ml (Alexis, Lausen, Switzerland) diluted 1:200 in PBS containing 0.05% Tween and 1% milk powder. After the first incubation, the membrane was washed three times for 15min and then incubated with the secondary, horseradish peroxidase-conjugated rabbit anti-mouse IgG

(Dako, Santa Barbara, CA) diluted 1:500. Secondary antibody incubation was performed for one hour at room temperature. Membranes were washed, and BCRP detection was performed with the enhanced chemiluminescence system (ECL-Detection-Kit, Amersham). The molecular weight was identified by using molecular weight Precision Plus Protein Dual Colour Standard (Bio Rad).

### 3.3.8. Functional assays

For functional assays, 24-well plates were used (BD). At time  $t = -30\text{min}$ , pre-warmed HBSS (Gibco) with 1mM MEM sodium pyruvate (Gibco), pH 7.4, with and without inhibitor was added to the well (apical side facing the solution). The whole system was kept at constant temperature ( $37^{\circ}\text{C}$ ). At time<sub>1</sub> = 0min, media was changed, containing HBSS with 1mM sodium pyruvate, mitoxantrone with and without inhibitor. After two hours, media was removed and cells were washed twice with HBSS/sodium pyruvate and incubated for 30min with 5% Triton-X. Then supernatant was removed and transferred into a 96well plate (Perkin Elmer, Schwerzenbach, Switzerland). Fluorescence detection of mitoxantrone was performed with SpectraMax Gemini XS with Softmax Pro 3.1 from Molecular Devices (California, USA) at a excitation wavelength of 610nm, emission filter at 685.

### 3.3.9. Statistical analysis

Statistical significance was investigated with t-test (two-tailed distribution with unequal variances). A probability of  $p < 0.05$  was defined as statistically significant. All transport studies were performed with primary cells obtained from two pigs. Each transport assay was performed in triplicate if not mentioned otherwise. Results are represented as the mean  $\pm$  SEM.

## 3.4. Results

Expression of the brain multidrug resistance protein (BMDP) in porcine proximal tubular cells was detected by means of quantitative RT-PCR (Fig. 3.1). Interestingly, after incubation of cell culture (two weeks), the BMDP mRNA expression was down-regulated and, at the end of the third week, expression reached the initial expression level again.

Protein expression was confirmed by Western blot analysis: A band of approximately 72kDa, corresponding to the expected molecular mass for the monomeric ABCG2, was detected (Fig. 3.2, lane A and B). As positive control, we used the human brain capillary

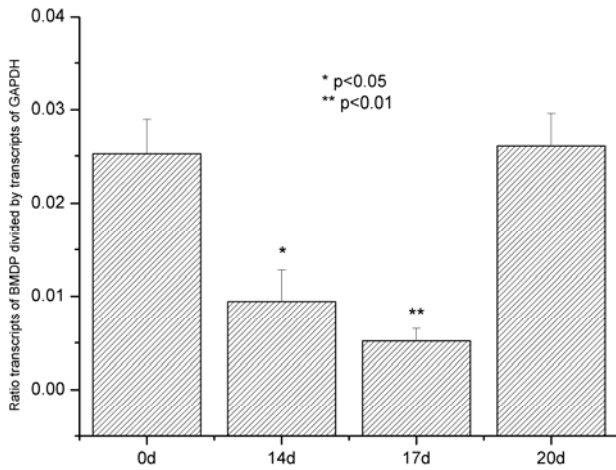


**Figure 3.1** - Quantitative PCR (Taqman): absolute quantification of BMDP mRNA in porcine proximal tubular cells at different days. 0d: freshly isolated cells without seeding them for culturing. Expression of mRNA was normalised to GAPDH. Data were pooled from two independent experiments, n=6.

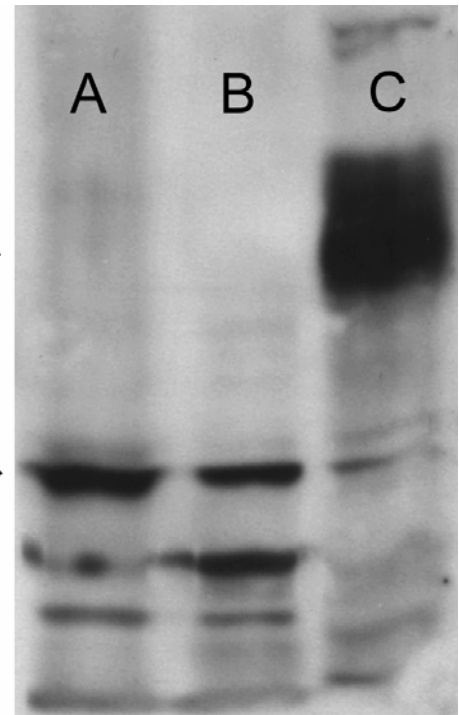


**Figure 3.2** - Western blot analysis of BCRP. Lane A and B: porcine proximal tubular cells, derived from two different isolations, lane C represents proteins from the human BB19 cell line. The monomeric form of BCRP has a molecular weight of around 70kDa.

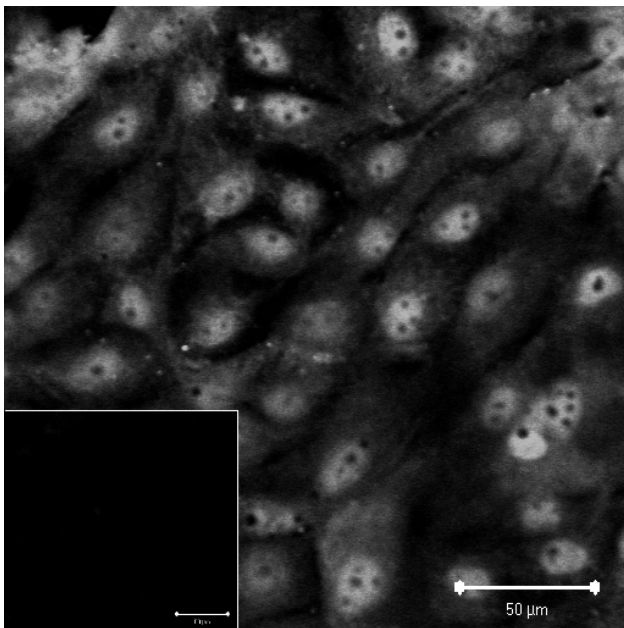


**Figure 3.3** - Confocal microscopy: Immunostaining of BCRP with CY2 (green) and negative control. Size bar represents 50 μm

endothelial cell line BB19 (Fig. 3.2, lane C). The detected band at 140kDa represents the dimeric form of ABCG2. Further evidence for protein expression in proximal tubular cells was given by immunohistochemistry (Fig. 3.3). Functional activity of the breast cancer resistance protein (BCRP) respectively BMDP was shown by enhanced mitoxantrone uptake with the BCRP inhibitor prazosin (Fig. 3.4). No effect

was detected with the P-gp inhibitor verapamil and the other BCRP inhibitor fumitremorgin C (FTC). The results in Fig. 3.5 show, as expected, an enhanced digoxin uptake with verapamil. However, the higher digoxin uptake with prazosin was somewhat surprising, which was even slightly higher in combination with verapamil (Fig. 3.5). The difference in inhibition between 100μM verapamil and 50μM prazosin was statistically significant (p<0.01), whereas the combination of prazosin and verapamil gave a slightly stronger

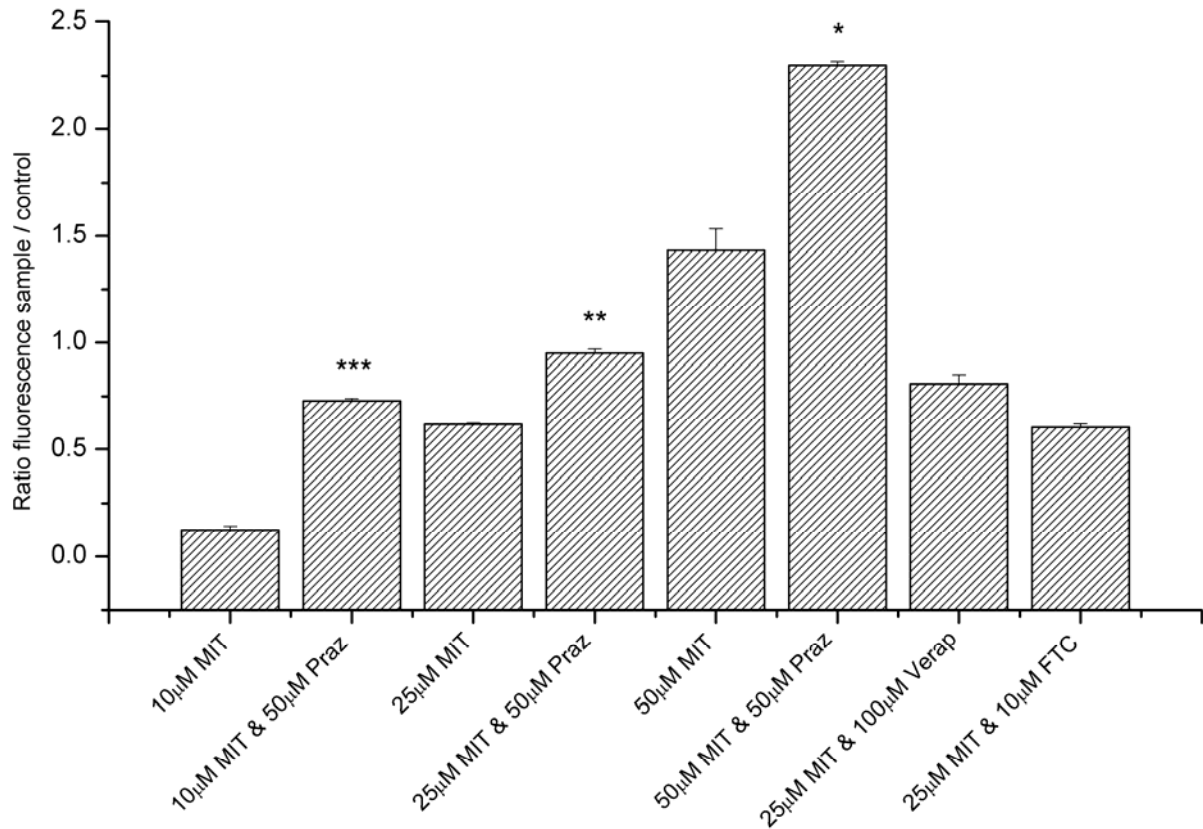


**Figure 3.4** - Mitoxantrone uptake at the apical side after 2h, cells were pre-incubated with the inhibitors for 30 minutes. MIT = mitoxantrone, Praz = prazosin, Verap = verapamil, FTC = fumitremorgin C, \*  $p < 0.05$ , \*\*  $p < 0.01$ , \*\*\*  $p < 0.001$ .

inhibition of P-gp than prazosin alone, but this difference was statistically not significant ( $p=0.48$ ).

Screening of various antiepileptic agents for BCRP respectively BMDP inhibition showed only for phenytoin an effect (Fig. 3.6). Other substances, such as non-steroidal anti-inflammatory drugs (NSAIDs), anti-depressants, and proton-pump inhibitors (PPIs), showed no significant inhibitory effect on BMDP, although a tendency was seen for ibuprofen, indomethacin and fluvoxamine (Fig. 3.7). Contrary to expectations, co-incubation with diclofenac, caffeine, thalidomide, theophylline and gallium-dotatoc lead to a reduction of mitoxantrone concentration in the cells. This might be explained by inhibition of mitoxantrone uptake through an unknown transport mechanism.

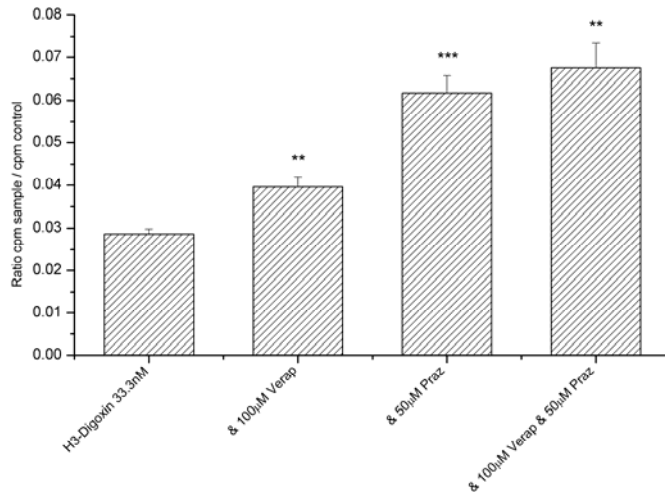


**Figure 3.5** - H<sup>3</sup>-Digoxin uptake at the apical side after 2h, cells were pre-incubated with the inhibitors verapamil (Verap), prazosin (Praz) and combined for 30 minutes. Cpm = counts per minute, \*\* p<0.01, \*\*\* p<0.001, n=6.

### 3.5. Discussion

In mice and human, evidence exists for BCRP expression at the apical side of renal proximal tubules [31, 33, 159, 160]. The objective of this study was to investigate, if primary porcine proximal tubules do express the porcine homologue of BCRP, namely BMDP, at mRNA, protein level and if BMDP is functionally active.

Expression at mRNA level was confirmed by quantitative RT-PCR, showing first a down-regulation of

mRNA BMDP expression in the first 17 days during culturing and then reaching the initial level after 20 days (Fig. 3.1). If one can assume a correlation between mRNA and protein expression, it would have been optimal to perform functional assays either with fresh cells, which is difficult to perform without a confluent monolayer or cells which have been cultured around 20 days. Uptake experiments were performed between day 12-15, two experiments at day 24. At day 17, the effects were less pronounced. However, in cultured cells, protein expression was confirmed by Western blot analysis (Fig. 3.2) and by immunohistochemistry (Fig. 3.3). BCRP is known to be functional as a homodimer with disulfide bonds in between and a molecular weight of 130 respectively 140kDa. Accordingly, the BCRP monomer (“half transporter”) has a molecular weight of 65 respectively 70kDa [156, 161]. Interestingly, the porcine proximal tubular cells seem to express the BMDP monomer, as the Western blot analysis was performed under non-reducing conditions (Fig. 3.2 lane A and B). However, the BB19 cells seem to express mainly the dimer protein at 140kDa (Fig. 3.2 lane C). Intriguingly, [Arg<sup>482</sup>] ABCG2 is capable of translocating methotrexate even in presence of 10mM mercaptoethanol, a reducing agent breaking the disulfide bonds, indicating that ABCG2 may be to a certain extent functional as a monomer [162]. This latter finding seem to be the case in porcine proximal tubular cells, although it can not be excluded, that the half transporter BMDP spontaneously builds dimers in the membrane prior translocating substrates.



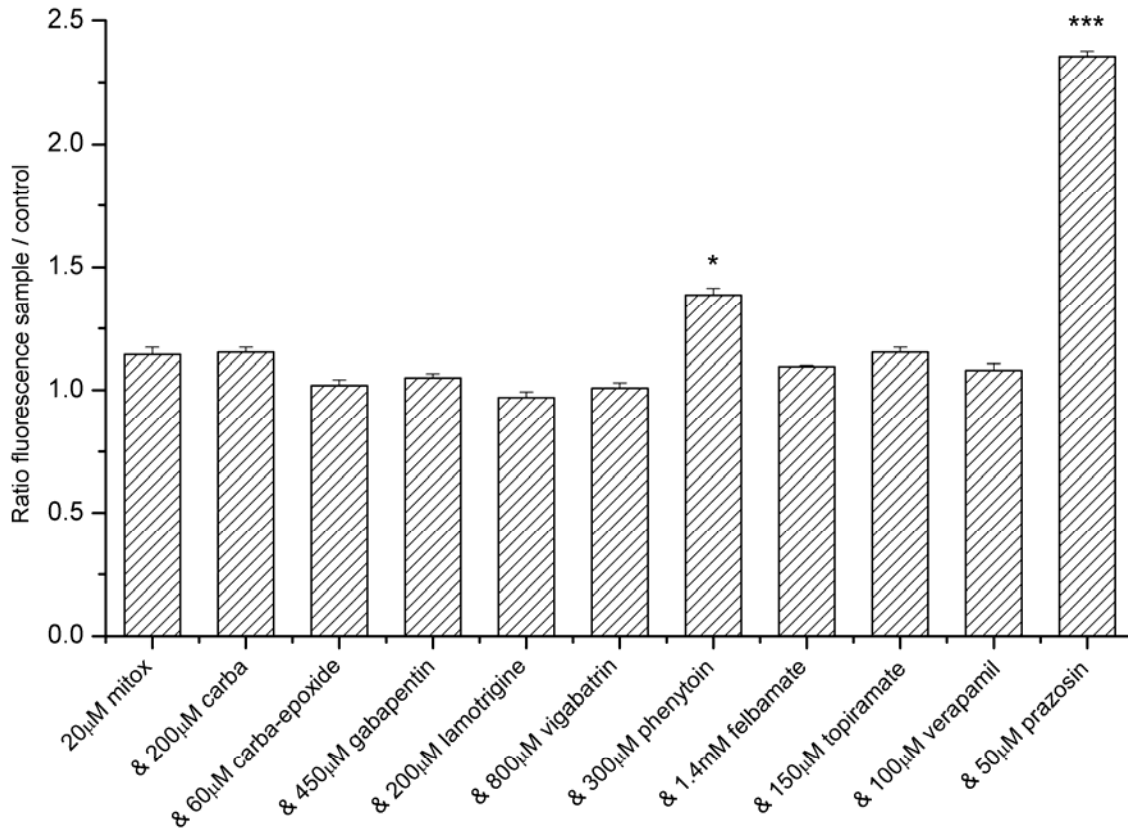


**Figure 3.6** - Mitoxantrone uptake at the apical side after 2h, cells were pre-incubated with anti-epileptic agents for 30 minutes. Mitox = mitoxantrone, carba = carbamazepine, carba-epoxide = carbamazepine-10, 11-epoxide, \*  $p < 0.05$ , \*\*\*  $p < 0.001$ ,  $n = 5$ .

In order to test whether BMDP is functional available, the known BCRP substrate mitoxantrone was used in different concentrations with prazosin as inhibitor. In various cell lines, mitoxantrone was used in a concentration of  $20\mu\text{M}$  [163]. Therefore, we used 50, 25 and  $10\mu\text{M}$  mitoxantrone for the first screening (Fig. 3.4). In literature, prazosin was used as an ABCG2 inhibitor with concentrations ranging from 1- $50\mu\text{M}$  [156, 164-166]. We used prazosin at the highest concentration of  $50\mu\text{M}$ . As mentioned in the beginning, in humans and in mice, BCRP is located at the apical side of the proximal tubules. Therefore, we assumed the same location in porcine tubules. All uptakes were performed in well plates, thus the apical side of these cells faces the solution, as already shown in [158]. The authors showed in [31], that in mice bcrp is involved in renal secretion of organic sulphates. Taking this into account, an inhibition of this transporter at the apical side would result in a reduced secretion of the substrates and accumulation in the tubule cells and in blood.

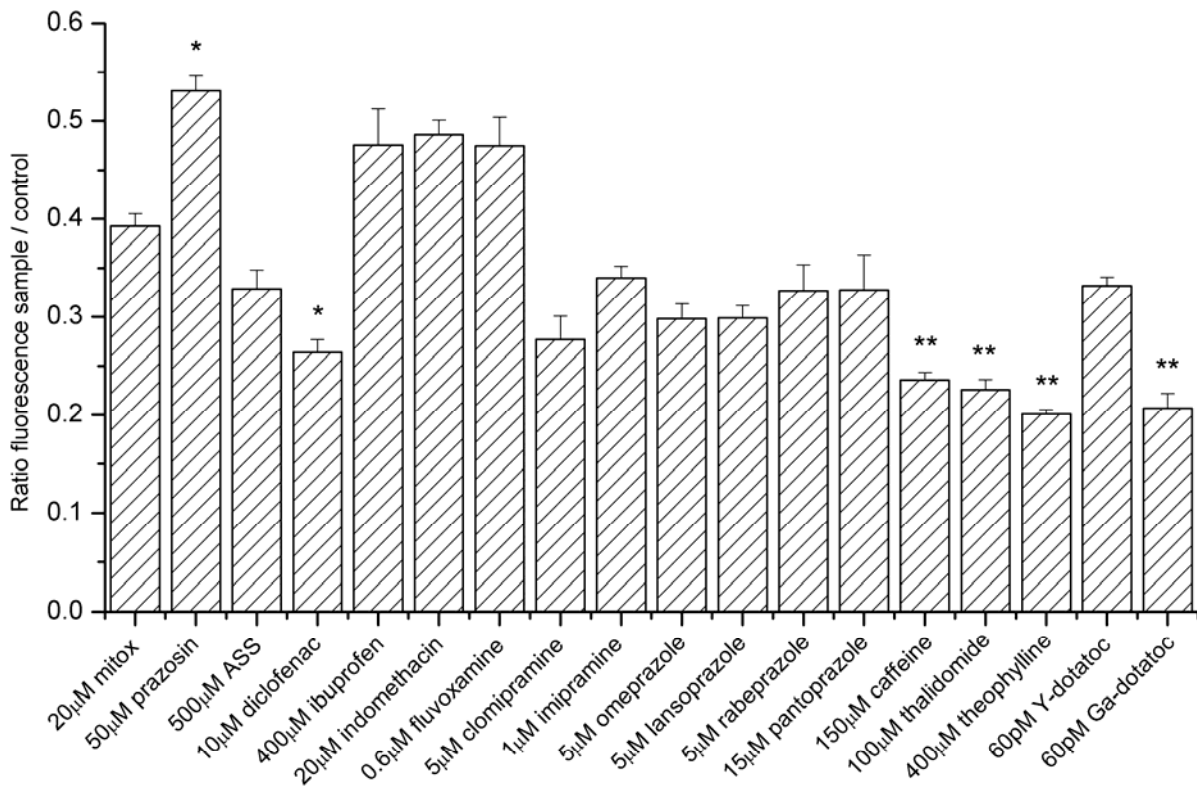


**Figure 3.7** - Mitoxantrone uptake at the apical side after 2h, cells were pre-incubated with various drugs for 30 minutes. Mitox = mitoxantrone, ASS = acetylsalicylic acid, Y = yttrium, Ga = gallium, \*  $p < 0.05$ , \*\*  $p < 0.01$ ,  $n = 4$ .

In Fig. 3.4, it is shown, that mitoxantrone accumulated in porcine proximal tubular cells in the presence of prazosin, indicating the apical localisation of BMDP extruding substrates into lumen respectively into urine. Verapamil was given at a concentration of 100µM to exclude a P-gp mediated effect on mitoxantrone uptake, as verapamil is a known P-gp inhibitor, but no inhibitor of BCRP [160]. Fumitremorgin C (FTC), is reported to be likewise a BCRP inhibitor (Fig. 3.4) [167, 168]. One possible explanation could be, that FTC does not bind to the porcine BMDP. However, in other cell lines with human origin (BB19 and Caco) an inhibitory effect of FTC on BCRP could not be observed (data not shown). These cell lines were not over-expressing BCRP, another possible explanation for the lacking effect, that findings for FTC as a BCRP inhibitor was established mostly in over-expressing cells. Finally, the affinity of mitoxantrone to BMDP could be higher than that of FTC, thus preventing the expected interaction.

The inhibitory effect of prazosin on BMDP seems to be maximal below 25µM mitoxantrone. Therefore, we performed further evaluation uptake assays with 20µM, 10µM mitoxantrone and 50µM prazosin (data not shown). We have chosen 20µM mitoxantrone,

due to the better signal to noise ratio than with 10 $\mu$ M. Therefore, we decided to use 20 $\mu$ M mitoxantrone as final concentration for further experiments.

As already shown in [158], P-gp is located at the apical side of porcine proximal tubules. Therefore, the principles of uptake and its inhibition are similar to BCRP: P-gp extrudes drugs out of the cell into urine. Inhibition of this transporter with verapamil resulted in an accumulation of digoxin in the cells, as shown in figure 3.5. Interestingly, prazosin was capable of inhibiting extrusion of digoxin much stronger than verapamil. It was shown, that digoxin is not translocated by BCRP although digoxin can inhibit BCRP [155]. Therefore, it can be excluded that the inhibitory effect of prazosin could be due to translocation of digoxin by BCRP. Furthermore, verapamil seems to be a relatively selective inhibitor for P-gp compared to BCRP [160] and mitoxantrone uptake was not influenced by verapamil (Fig. 3.4). Prazosin again is not translocated by P-gp (as well as mitoxantrone) but prazosin could inhibit digoxin transport through P-gp as shown in Fig. 3.5 [165]. Interestingly, combination of verapamil and prazosin increased digoxin uptake slightly more than with prazosin alone, although this effect was not statistically significant. However, this latter finding is indicative that prazosin inhibits both P-gp and BCRP.

In order to test a possible interaction of antiepileptic agents with BMDP in proximal tubular cells, we used concentrations of these drugs which are four-fold higher than the highest therapeutic blood concentrations. Although data already exists regarding BCRP and antiepileptic agents, we extended the “drug list” with some other not yet tested drugs which could be of potential relevance in the renal excretion [157]. Prazosin served as positive control for BCRP activity, whereas verapamil excluded a possible P-gp effect of mitoxantrone (Fig. 3.6). Only phenytoin showed an increased uptake of mitoxantrone indicating the possibility to inhibit BCRP/BMDP at least at high concentrations. With 100 $\mu$ M phenytoin, no inhibitory effect could be shown (data not shown). We elucidated the possibility, that phenytoin is not only an inhibitor but also a substrate of BMDP. However, this hypothesis could not be confirmed with apical to basolateral transport (data not shown). Therefore, these results are in accordance with [157] and identify further antiepileptic drugs which are not inhibiting BCRP/BMDP (carbamazepine-10, 11-epoxide, gabapentin, vigabatrin, felbamate and topiramate).

In the next step, we tried to screen for further substances that might interact with BMDP/BCRP in proximal tubular cells (Fig. 3.7). So far, the tested NSAIDs, antidepressants, PPIs, caffeine, theophylline, thalidomide and both dotatocs showed no effect. Solely, ibuprofen, indomethacin and fluvoxamine showed a tendency to enhance mitoxantrone uptake, but this was not statistically significant. Interestingly, some substances were able to inhibit mitoxantrone uptake significantly (diclofenac, caffeine, thalidomide, theophylline and gallium-dotatoc). However, the mechanism of apical mitoxantrone uptake into proximal tubular cells is not yet completely resolved.

In summary, our study could show for the first time expression of the porcine analogue of BCRP, the so called BMDP, in primary proximal tubular cells at mRNA, protein and functional level. In this porcine model, as described in [158], the concurrent expression of a further drug transporter enhances the possibility to reach a more realistic in vitro model as various drug transporters are expressed simultaneously. In order to compare the functional activity of the porcine transporter with the human BCRP, further investigations should be performed with the known BCRP substrates PhIP and prazosin. Then, possible interactions of drugs due to BMDP/BCRP in this in-vitro model must be compared with the in-vivo situation. Therefore clinical studies in human subjects are necessary.

However, with this model it is now possible to screen various drugs regarding BCRP/BMDP and P-gp activity.

### **Acknowledgments**

This work was supported by the Swiss national foundation. We express our gratitude for Ursula Behrens for the excellent technical assistance.

#### 4. Glucagon-like peptide 1 receptor expression in primary porcine proximal tubular cells

Schlatter P<sup>1</sup>., Beglinger C<sup>2</sup>., Drewe J. <sup>1</sup>, Gutmann H<sup>1</sup>.

<sup>1</sup> Department of Clinical Pharmacology and Toxicology, University Hospital of Basel, Basel, Switzerland

<sup>2</sup> Division of Gastroenterology, University Hospital of Basel, Basel, Switzerland

**Submitted to: Regulatory Peptides**

#### **4.1. Abstract**

*Background:* GLP-1 is secreted into the circulation after food intake. The main biological effects of GLP-1 include stimulation of glucose dependent insulin secretion and induction of satiety feelings. Recently, it was demonstrated in rats and humans that GLP-1 can stimulate renal excretion of sodium. Based on these data, the existence of a renal GLP-1 receptor (GLP-1R) was postulated. However, the exact localisation of the GLP-1R and the mechanism of this GLP-1 action have not yet been investigated.

*Methods:* Primary porcine proximal tubular cells were isolated from porcine kidneys. Expression of GLP-1R was measured at the mRNA level by quantitative RT-PCR. Protein expression of GLP-1R was verified with immunocytochemistry, immunohistochemistry and Western blot analysis. Functional studies included transport assessments of sodium and glucose using three different GLP-1 concentrations (200pM, 2nM and 20nM), 200pM exendin-4 (GLP-1 analogue) and an inhibitor of the dipeptidylpeptidase IV (DPPIV) enzyme (P32/98 at 10 $\mu$ M). Finally, the expression of NHE3, the predominant Na<sup>+</sup>/H<sup>+</sup> exchanger in proximal tubular cells, was also investigated.

*Results:* GLP-1R, NHE3 and DPPIV were expressed at the mRNA level in porcine proximal tubular kidney cells. GLP-1R expression was confirmed at the protein level. Staining of human and pig kidney cortex revealed that GLP-1R was predominantly expressed in proximal tubular cells. Functional assays demonstrated an inhibition of sodium re-absorption with GLP-1 after three hours of incubation. Exendin-4 and GLP-1 in combination with P32/98 co-administration had no clear influence on glucose and sodium uptake and transport.

*Conclusion:* GLP-1R is functionally expressed in porcine proximal tubular kidney cells. Addition of GLP-1 to these cells resulted in a reduced sodium re-absorption. GLP-1 had no effect on glucose re-absorption. We conclude that GLP-1 modulates sodium homeostasis in the kidney most likely through a direct action via its GLP-1R in proximal tubular cells.

## 4.2. Introduction

Glucagon-like peptide 1 (GLP-1) is a hormone secreted from intestinal L-cells after food intake. The peptide is synthesised as a pre-proglucagon molecule that is subsequently metabolised to GLP-1 [169-171]. Different molecular forms of GLP-1 exist: GLP-1 7-36 and 7-37 amide are bioactive forms [172], whereas GLP-1 9-36 and 9-37 amide are inactive metabolites [173]. In the following, we refer to the bioactive form GLP-1(7-36), if not stated otherwise. The GLP-1 receptor (GLP-1R) is a class B heptahelical G-protein-coupled receptor with a molecular weight between 62-65kDa [174-180]. Upon GLP-1 binding, adenylate cyclase is activated and intracellular cAMP is generated [180].

The main effect of GLP-1 is stimulation of glucose-dependent insulin secretion from pancreatic  $\beta$ -cells thereby lowering blood glucose levels [181]. *In vivo*, GLP-1 is rapidly degraded by dipeptidylpeptidase IV (DPP-IV) resulting in a short half-life of about two minutes [182]. Interestingly, DPP-IV is highly expressed in renal proximal tubular cells and, therefore, can be used as a specific marker for these cells [183-186].

Further effects of GLP-1 include induction of satiety and reduction of energy intake, both in healthy volunteers and in patients with diabetes type 2 [173, 187, 188].

Furthermore, in rats and humans, exogenous administration of GLP-1 has a natriuretic effect [188-190]. In the kidney, about 60-70% of excreted sodium is re-absorbed in the proximal nephron, mainly by paracellular pathway and by a  $\text{Na}^+/\text{H}^+$  exchanger (NHE3; SLC9A3) [191]. NHE3 exists in multimeric complexes with DPP-IV at the apical side of the proximal tubular cells [57, 58], but the exact mechanism for this action has not been elucidated.

The aim of the study was therefore 1) to screen human, pig kidney cortex and porcine proximal tubular cells for GLP-1R expression, 2) to characterise the effect of GLP-1 on porcine kidney cells on sodium and glucose re-absorption. Primary porcine proximal tubular cells were used to characterise GLP-1R expression by means of RT-PCR for the detection at mRNA level and immunoassays (Western-blot, immunohisto- and cytochemistry) for the detection at protein-level. For sodium transport measurements a fluorescence marker was used and for glucose transport measurements radioactive labelled  $^3\text{H}$ -Glucose.

### **4.3. Materials and Methods**

#### *4.3.1. Materials*

MEM Eagle D-valine w/L-glutamine was purchased from Lucerna Chem AG (Luzern, Switzerland), Dulbecco's MEM/Nut Mix F-12 (DMEM/F12), Fetal calf serum (FCS) and penicillin/streptomycin from Gibco Life Sciences (Basel, Switzerland), cell flask 75cm<sup>2</sup> from BD (Franklin Lakes, USA), GLP-1 7-36 from Bachem (Bubendorf, Switzerland). P32/98 was a kind gift from Dr. H.-U. Demuth from Probiodrug (Halle/Saale, Germany). All other substances were purchased from Sigma/Fluka in highest quality.

#### *4.3.2. Cell Culture*

Porcine proximal tubular cells were isolated and seeded as described previously [158]. Cells were first seeded ( $1.5 \cdot 10^6$  cells in 75cm<sup>2</sup> flask) in 50ml of 9.6g/1000ml MEM D-Val, 10% FCS and 100U/ml penicillin/streptomycin and cultured for 5 days (after the first 48h media was changed every day). Then culturing was continued with DMEM/F12 with 10% FCS and 100 U/ml penicillin/streptomycin until confluency was reached (about 3 days, media was changed every second day). The cells were incubated at 37°C in 95% air and 5% CO<sub>2</sub>. For passaging, the monolayer was trypsinised with 10 ml (trypsin EDTA from Gibco) for 15 min. Then 10ml of DMEM/F12 was added and centrifuged. After removing supernatant the cell pellet was diluted in DMEM/F12. For transport studies cells were transferred on uncoated Transwell filter cell culture systems and for incubation studies on uncoated 6-well plates. In order to investigate the effect of glucose on the mRNA expression, cells were incubated, after passaging, in MEM D-Val, 10% FCS and 100U/ml penicillin/streptomycin containing 5mM Glucose and 15.6mM Glucose (corresponding glucose concentration of DMEM/F12) by adding from a 5M sterile filtered glucose solution.

#### *4.3.3. RT-PCR*

For quantitative RT-PCR standards were generated for the genes NHE3 and DPPIV. Therefore, total RNA was isolated from confluent monolayers using the RNeasy Mini Kit (Qiagen, Hilden, Germany). RNA was quantified with a Nanodrop Spectrophotometer (Witeg AG, Littau-Luzern, CH). The purity of the RNA preparations was high, as



**Table 4.1** - Sequences of porcine primers and probes

Gene	Accession no.	Forward primer
<b>RT-PCR Primers</b>		
GAPDH	<u><a href="#">AF017079</a></u>	5'-AGATCATCAGCAATGCCTCCTG-3' 5'-GAGCTTGACAAAGTGGTCGTTG-3'
DPPIV	<u><a href="#">AY198323</a></u>	5'-TCCTACCAAATCGTTCCTCCG-3' 5'-GCTAAGGCACGTCACCTTTGTGTA-3'
slc9a3	<u><a href="#">AF123280</a></u>	5'-AAGTACGTGAAGGCCAACATCTC-3' 5'-TTCTCCTTGACCTTGTCTCGTC-3'
<b>Gene Taqman primers and probes</b>		
Gene	Accession no.	Forward primer
Taqman primers and probes		Reverse primer
		Probe
GAPDH	<u><a href="#">AF017079</a></u>	5'-GTTGAAGGTCGGAGTGAACG-3' 5'-CGACAATGTCCACTTTGCCA-3' 5'-CGCCTGGTCACCAGGGCTGC-3'
GLP-1R	<u><a href="#">CV871385</a></u>	5'-TACTTCTGGCTGCTGGTGGAG-3' 5'-ACCCAGCCTATGCTCAGGTA-3' 5'-ACCTGTACACGCTGCTGGCCCTGTC-3'
DPPIV	<u><a href="#">AY198323</a></u>	5'-ATTTCTCAGTGGCCCGG-3' 5'-TCTGCAGGCCTAAATCTTCCA-3' 5'-AACACATTGAAATCAGTACCACTGGCTGGG-3'
slc9a3	<u><a href="#">AF123280</a></u>	5'-GGACCCGCTCATCTGGAA-3' 5'-ACCCGGTACACGGAGATAAAGAC-3' 5'-AACACAGCCTTTGTGCTCCTGACGC-3'

demonstrated by the 260/280nm ratio (range, 1.8 - 2.0). After DNase I digestion (Invitrogen, Basel, Switzerland) 1µg of total RNA was reverse transcribed by SuperScript II RT-Kit (Gibco) according to the manufacturer's protocol using random hexamers (Perkin-Elmer) as primers. Gene amplification for generation of standards (except GLP-1R, see under Real Time PCR) was performed by PCR in four 25µl reaction units using AmpliTaq Gold DNA polymerase 1.25U (Applied Biosystems, Foster City, USA), dNTPs 200mM (Promega, Catalys AG, Wallisellen, Switzerland), 35ng cDNA (or DNA digested RNA for negative control), forward and reverse primers 0.4µM. The primer sequences, which were designed with Primer Express V 2.0 from Applied Biosystems, are displayed in table 4.1. Mg<sup>2+</sup> concentration was 3mM for SLC9A3, DPPIV and GAPDH (glyceraldehyde 3-phosphate dehydrogenase).

PCR was performed with Mastercycler personal (Eppendorf AG, Hamburg, Germany) using the following program: 1. step: 95 °C over 10 min, 2. step: 95 °C over 30 s, 3. step: annealing temperature.: 55 °C, 4. step: 72 °C over 1 min, 5. step: 72 °C over 10 min, 6. step: cooling at 4 °C. Steps 2 - 4 were repeated 44 times. PCR products were detected

with agarose-gel electrophoresis using an agarose concentration of 1.5% (w/v) (Invitrogen) and 0.5µg/ml ethidium bromide. The gel was run at 120V for 50min.

#### *4.3.4. Real-time Polymerase Chain Reaction (TaqMan® Assay)*

At the end of the culture period, medium was removed, total RNA was extracted and reverse transcribed as described above. TaqMan analysis was carried out on an Abi Prism 7900 Sequence Detection System (Applied Biosystems, Rotkreuz, Switzerland). PCR conditions were 10min at 95°C followed by 40 cycles of 15s at 95°C and 1min at 60°C. Each TaqMan reaction contained 10ng of cDNA in a total volume of 10µl. TaqMan Universal PCR Mastermix from Eurogentec (Geneva, Switzerland) was used. The concentrations of primers and probes were 900nM and 225nM, respectively. Primers and probes were designed according to the guidelines of Applied Biosystems with help of the Primer Express 2.0 software (Table 4.1). Primers were synthesised by Invitrogen (Basel, Switzerland), probes by Eurogentec (Seraing, Belgium). All samples were run in triplicates. A standard curve was generated by serial dilutions of cDNA. The dilution of the latter cDNA was expressed by the respective dilution value. Ct values of standards were plotted against the log of the respective dilution factors. Slope and y-intercept of the standard curve line were then calculated by linear regression and used to calculate the input amount for unknown samples for respective genes. To standardise the amount of sample cDNA added to the reaction the calculated amount of the gene of interest was divided by the calculated amount of the constitutively expressed glyceraldehydes-3-phosphate dehydrogenase (GAPDH) gene in the sample. These normalised amounts were then used to compare the relative amount of target in different samples. All samples expressed GAPDH at same CT values ( $20.18 \pm 0.08$ ). GLP-1R standard was generated using the respective Taqman primers without probe. PCR product was detected as described above on a 3% agarose gel.

#### *4.3.5. Sequencing of SLC9A3 (NHE3), DPPIV, GLP-1R and GAPDH PCR products*

PCR was performed as described above. After detecting the bands on an agarose gel, they were cut out with a sterile scalpel. The PCR product was then extracted from the gel slice with the Qiaquick Gel extraction kit (Qiagen, Hilden, Germany) according to the manufacturer's description. After quantification of DNA with Quant-iT™ Picogreen dsDNA Assay Kit (Molecular Probes, Leiden, The Netherlands), the probes were sent to

Microsynth AG (Balgach, Switzerland) for sequencing. Correct sequences were confirmed by nucleotide-nucleotide blast at [www.ncbi.nlm.nih.gov/BLAST/](http://www.ncbi.nlm.nih.gov/BLAST/) (data not shown).

#### *4.3.6. Confocal microscopy*

For immunostaining, cells grown in Chamberslides® (Nalge Nunc International, Rochester, NY, USA) were used. Cells were washed 3x with PBS and fixed for 20 minutes with 4% (w/v) paraformaldehyde in PBS. After washing three times with PBS, tissues were permeabilised for 5min with 0.5% (v/v) Triton X-100 in PBS. For immunostaining, cells were incubated for one hour at 37°C in a humid chamber with the primary antibody dissolved in PBS supplemented with 3% (v/v) FCS (foetal calf serum). After washing twice with PBS, the fluorochrome conjugated secondary antibody dissolved in PBS supplemented with 3% FCS with or without 60µg/ml propidium iodide was added for one hour at room temperature, in a dark chamber. Stained cells were then washed three times with PBS and mounted with FluorSave® (Calbiochem, San Diego, CA). Fluorescence stained cells were examined on a confocal Zeiss LSM 150 inverted laser scanning microscope (Carl Zeiss, Oberkochen, Germany). All pictures are 400x magnified. Fluorescence was detected with wavelengths for excitation at 488nm (CY2) and 543nm (propidium iodide), for emission between 505-550nm and 560-615nm, respectively.

Polyclonal antibody to human GLP-1R from rabbit used for these experiments was purchased from Acris Antibodies (Hiddenhausen, Germany). Dilution ratio was 1:100 in PBS with 3% FCS.

The following secondary fluorescent antibody was used (Jackson Immuno Research) and diluted in PBS with 3% FCS: GLP-1R CY2 AffiniPure Goat Anti Rabbit IgG (H+L) with a dilution rate of 1:25.

#### *4.3.7. Immunohistochemistry*

Formalin-fixed, paraffin embedded specimens were used for the immunohistochemical analysis by the avidin-biotin-peroxidase complex method (ABC Vectastain, Vector Laboratories, Burlingame, CA, USA).

For experiments, 5 µm sections of kidney cortex were dewaxed and rehydrated in UltraClear (J.T. Baker, Deventer, Holland) for 30min, in 100, 96, 70% ethanol (each step

2-3min) and afterwards put into methanol with 0.3% H<sub>2</sub>O<sub>2</sub> for 30min. After washing with PBS, protein kinase K 0.05% was applied for 5 min. As blocking agent horse serum was used for GLP-1R and BSA 1% in PBS for DPPIV and co-staining. Further steps were conducted according to manufacturer's description. Negative controls for immunostaining were obtained by substituting the primary antibodies for PBS. Chromogenic detection was performed with 3,3-diaminobenzidine (DAB) for GLP-1R using horse radish peroxidase and fast red for DPPIV using alkaline phosphatase. Counterstaining was briefly performed with Mayer's hematoxylin. The sections were dehydrated in ethanol 70%, 96%, 100% (each step 2-3 min) and finally in Ultra Clear. Mounting was performed with UltraKit Mounting Medium (J.T. Baker, Deventer, Holland).

#### 4.3.8. Western blot analysis

Proximal tubular cells were cultured in a 25cm<sup>2</sup> cell culture flask from BD (Franklin Lakes, USA) until confluency was reached. Then proteins were extracted with 300µl protein extraction buffer (20mM Tris-HCl, 1% Igepal CA-630, 0.5mM sodium orthovanadate) including 1mM phenylmethylsulfonyl fluoride (Sigma-Aldrich, St. Louis, MO, USA) and protease inhibitor cocktail tablet, Complete Mini (Roche Diagnostics, Germany). The quantification of the protein content was performed with the BCA protein assay kit (Pierce Chemical, Rockford, IL, USA). Protein concentration was determined by measuring the absorbance at 562nm with Spectra MAX 250 Microplate Spectrophotometer (Molecular Devices Corporation, California, USA). The same procedure was performed with a piece of human kidney cortex, received from the department of pathology of the university hospital in Basel.

For immunoblotting, 100µg (Fig. 4.4) respectively 150µg (Fig. 4.5) of total protein extract was mixed with Laemmli sample buffer (Bio Rad Laboratories, Reinach, Switzerland) and transferred to the polyacrylamide gel. Gel electrophoresis was performed with a Mini Protean 3 Electrophoresis Cell (Bio Rad) applying 80V for 15min for the stacking gel (4% polyacrylamide) and 120V for 1h for the separating gel (7.5% respectively 10% polyacrylamide). After electrophoresis, proteins were blotted to the nitrocellulose membrane (250mA for 2.5 hours) using a Mini Trans-Blot Cell (Bio Rad). Protein transfer was verified by Ponceau S staining. The membrane was blocked overnight at 4°C with PBS containing 5% milk powder and 0.05% Tween 20. After washing three times for 15 minutes (0.05% Tween and 1% milk powder in PBS), the membrane was incubated for 2 hours at 37°C with the primary, rabbit anti-human antibody against GLP-1R, 1mg/ml (Acris

Antibodies, Hiddenhausen, Germany) diluted 1:500 in PBS containing 0.05% Tween and 1% milk powder. After the first incubation the membrane was washed three times for 15min and then incubated with the secondary, horseradish peroxidase-conjugated, donkey anti-rabbit IgG (Amersham, Buckinghamshire, UK) diluted 1:500. Secondary antibody incubation was performed for 1 hour at room temperature. Membranes were washed, and GLP-1R detection was performed with the enhanced chemiluminescence system (ECL-Detection-Kit, Amersham). The molecular weight was identified by using molecular weight Precision Plus Protein Dual Colour Standard (Bio Rad).

#### 4.3.9. Functional assays

For functional assays the Transwell Costar 3460 system was used (Corning Incorporation, NY, USA). For sodium transport, cells were preincubated with 200pM, 2nM, 20nM GLP-1, 200pM Exendin-4, 10µM P32/98 and a combination of 200pM Exendin-4 or 200pM GLP-1 with P32/98, for three hours. Both sides of the diffusion cells were filled with pre-warmed buffer (see below). The whole system was kept at constant temperature (37 °C). At time  $t = 0$ , HBSS (Gibco) with 1mM MEM sodium pyruvate (Gibco), pH 7.4 with or without GLP-1 was added to the donor chamber (apical). Acceptor media (basolateral) contained 150mM choline chloride, 10mM HEPES, 2mM MgCl<sub>2</sub>, 2mM CaCl<sub>2</sub> and 1µM cell impermeant Sodium Green (Invitrogen, Basel, Switzerland) in sodium free water (Sigma Aldrich, Basel, Switzerland). At defined time intervals, samples were drawn from the acceptor chamber and analysed. [<sup>14</sup>C]PEG4000 (11000Bq/well) was used for monitoring the monolayer integrity (max. 0.2% of applied dose was transported).

For glucose transport assays, pre-incubation was performed with 200pM, 2 and 20nM GLP-1 for three, 24, 48 and 72 hours. In both chambers of the Transwell Costar 3460 HBSS was used with MEM sodium pyruvate as mentioned above. 3H-Glucose (11000Bq/well) was used in combination with 6.5µM glucose. Samples were drawn at 5, 10, 15, 20, 30, 60, 90 and 120 minutes. To test monolayer integrity Fitc-dextran in a concentration of 250µg/ml was used (max. 0.8% of applied dose was transported).

Glucose uptake was performed for three hours in 6-well plates with pre-incubation of GLP-1, exendin-4, P32/98 and its combinations as mentioned above.

For detection of radioactive substances Packard 1900TR liquid scintillation counter was used. The samples were diluted in 3ml Insta-Gel Plus (Perkin-Elmer, Schwerzenbach, Switzerland). Detection of Sodium Green and Fitc-dextran was carried out with Perkin-

Elmer HTS 7000 Bio Assay Reader with the following parameters: excitation at 485nm, emission 535nm.

#### *4.3.10. Cytotoxicity assay*

The effect of GLP-1, exendin-4 and P32/98 on cell viability was assessed using the sulforhodamine-B (SRB) colorimetric assay. Aliquots of primary porcine proximal tubular cells suspension were seeded onto 96-well plates. In order to test toxicity after three hours of incubation, cells were first incubated for 24 hours in blank medium and then treated with different concentrations of drugs in the culture medium.

Toxicity was also tested for 96 hours changing the media with different concentrations of drugs every 24 hours. After incubation, cells were washed with medium and fixed with 5% trichloroacetic acid in medium for one hour at 4°C. Subsequently cells were washed with water, air dried and stained with 0.4% SRB in 1% acetic acid for 15 minutes. Then the plate was again air dried, 10mM TRIS (pH=10.5) was applied for 5 minutes and absorption was measured at 540nm in Spectra Max 250 plate reader (Molecular Devices Corporation, CA, USA). Each condition was performed in five wells.

#### *4.3.11. Statistical analysis*

Statistical significance was investigated with t-test (two-tailed distribution with unequal variances). A probability of  $p < 0.05$  was defined as statistically significant. All transport studies were performed with primary cells obtained from two pigs. Each transport assay was performed in triplicate. Results are expressed as the mean  $\pm$  SEM.

### **4.4. Results**

Glucagon like peptide 1 receptor (GLP-1R), dipeptidyl-peptidase IV (DPPIV) and Na<sup>+</sup>/H<sup>+</sup> exchanger isoform 3 (NHE3) mRNA expression was investigated by quantitative RT-PCR (Fig. 4.1). Glucose had no significant effect on the expression of these three genes (Fig. 4.1).

GLP-1R expression at the protein level was confirmed in primary porcine proximal tubular cells (Fig 4.2, 4.3D-F and 4.5) by immunocytochemistry, immunohistochemistry and Western blot analysis. In Fig. 4.4 homogenised kidney cortex slices from human (right lane) and pig (left lane) were used, whereas in Fig. 4.5 isolated porcine proximal tubular

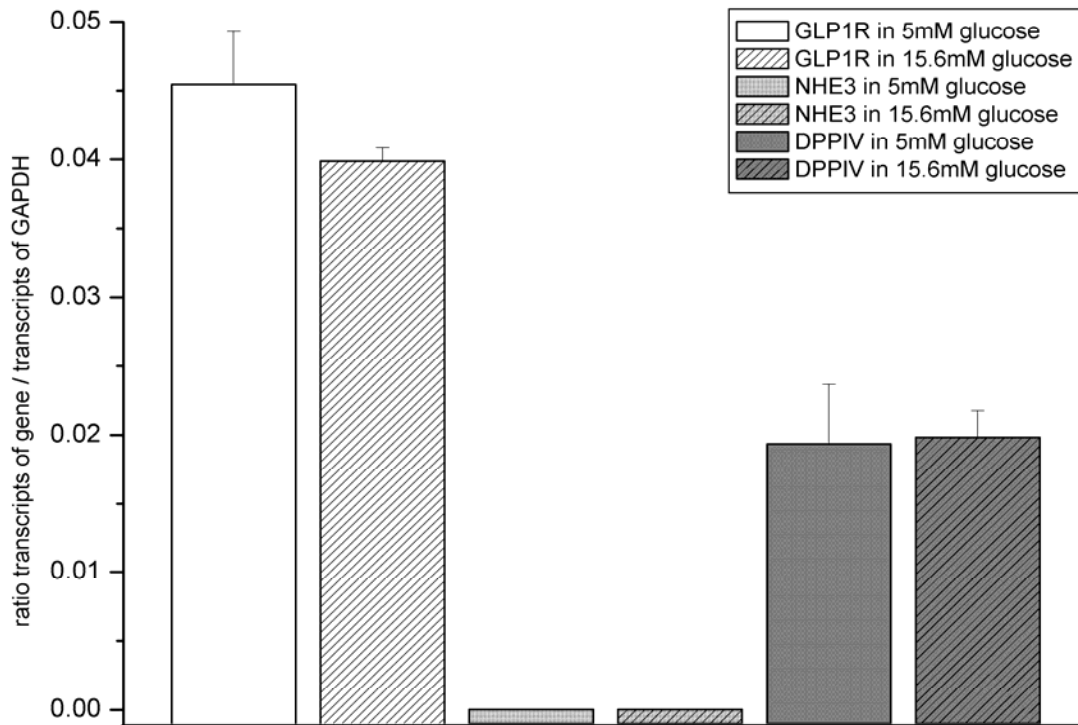


**Figure 4.1** - Quantitative RT-PCR (Taqman): Absolute quantification of GLP-1R (Glucagon like peptide receptor), NHE3 (Na<sup>+</sup>/H<sup>+</sup> exchanger isoform 3) and DPPIV (dipeptidyl-peptidase IV) mRNA in media containing two different glucose concentrations. Incubation was over 96 h. Expression of mRNA was normalized to GAPDH and 1µg RNA.

cells were analysed. The acrylamid concentration of the gel in Fig. 4.4 is 7.5%, whereas in Fig. 4.5 the gel consists of 10% acrylamid.

GLP-1R seems to be localised throughout the cell and a high staining was observed intracellular, near the nucleus (Fig. 4.2A). To assess the intracellular localisation of GLP-1R expression in proximal tubular cells, a co-staining with propidium iodide was performed, as propidium iodide stains DNA respectively the nucleus (Fig. 4.2B, D).

For immunohistochemistry and Western blot analysis, human kidney cortex was used as positive control (Fig. 4.3B and 4.4). DPPIV staining was performed in order to identify proximal tubular cells both in human and pig kidney cortex (Fig. 4.3A, D). In kidney cortex, GLP-1R seems to be expressed predominantly in proximal tubular cells, since staining of DPPIV (pink) and GLP-1R (brown) were overlapping (Fig. 4.3C, F).

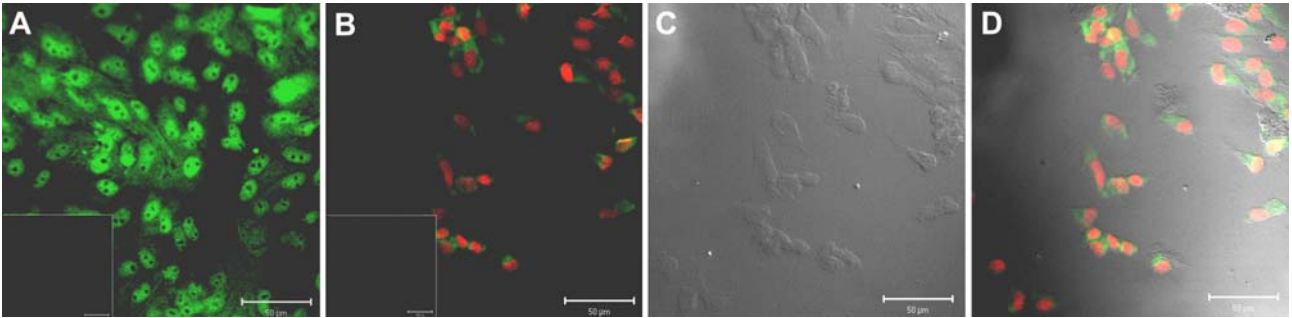


**Figure 4.2** - Confocal microscopy: Immunostaining of GLP1R with CY2 (green) (A), costained with propidium iodide (red) (B), transmission picture (C) and superposed (D). Size bar represents 50 µm. Negative control is placed in the lower left corner.

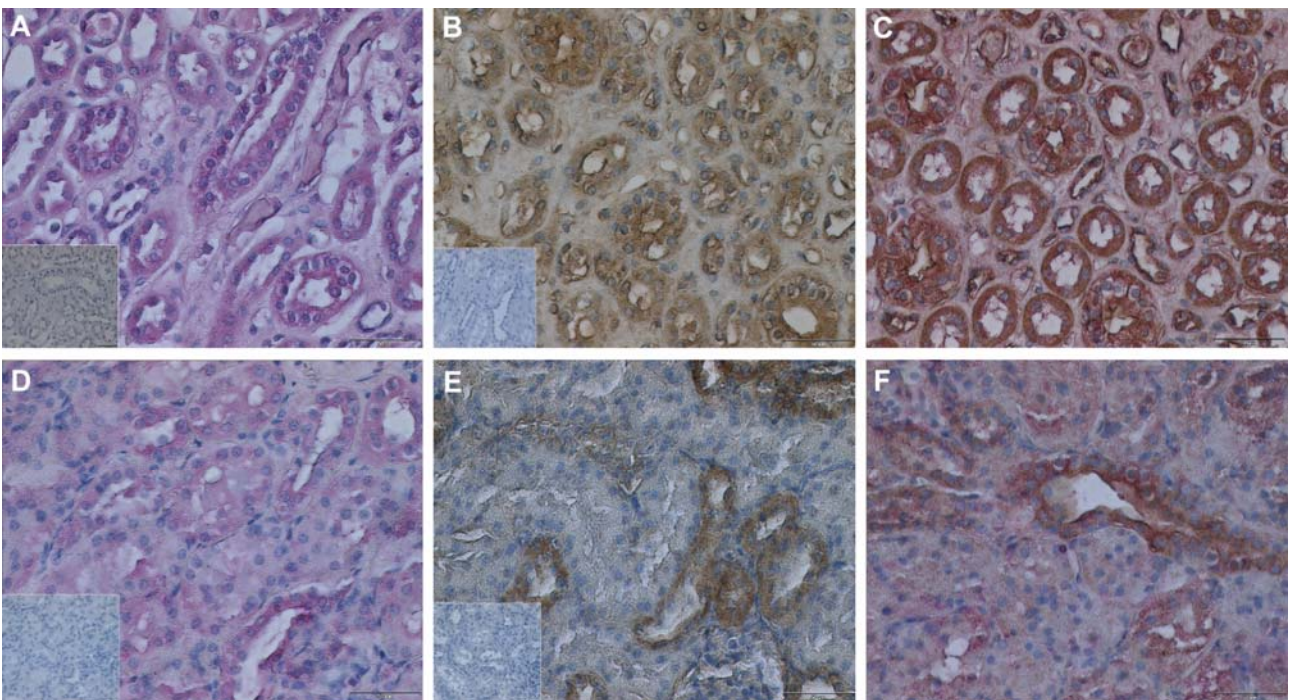


**Figure 4.3** - Immunocytochemistry: **A-C** human kidney cortex, **D-F** pig kidney cortex. **A** and **D**: staining for DPPIV (specific proximal tubular marker); **B** and **E**: staining for GLP-1R, **C** and **F**: double staining DPPIV and GLP-1R. Size bar represents 50µm.

For sodium transport assays, cells were pre-incubated with 200pM, 2nM and 20nM GLP-1, 200pM Exendin-4, 10µM P32/98 and combination of 200pM Exendin-4 or 200pM GLP-1 with P32/98, for three hours. These conditions were chosen to have a comparison with a clinical study in healthy subjects and in insulin resistant obese men [188]. After 30, 60 and 90min, apical-to-basolateral transport of sodium (corresponding to re-absorption) was significantly inhibited with 20nM GLP-1 (Fig. 4.6). Lower GLP-1 concentrations showed a



slight, but statistically not significant inhibition. 10 $\mu$ M P32/98 alone and in combination with 200pM Exendin-4 or 200pM GLP-1 showed no inhibition (data not shown).

Glucose transport assays from apical to basolateral were performed with 200pM, 2 and 20nM GLP-1 without any differences (data not shown). Glucose uptake with GLP-1, exendin-4, P32/98 and its combinations showed inconclusive results (data not shown).

All drugs used did not show any toxicity after three or ninety-six hours at the mentioned concentrations (data not shown).

#### **4.5. Discussion**

Renal effects of GLP-1 have been documented *in vivo*, both in healthy subjects and in obese persons [188]. The findings were supported by animal data in anaesthetised rats. When the animals received GLP-1 infusion, a remarkable 13-fold increase of sodium excretion was observed [189]. The authors postulated that the inhibitory effect of GLP-1 on sodium re-absorption was a direct action on the proximal tubules and not due to a change in renal hemodynamics.

*In vitro* investigations have confirmed the tissue distribution of GLP-1R in rat and mouse at mRNA level [192-196]. With one exception [195], GLP-1R expression was always found in the kidney.

Though information is available on the expression of GLP-1R in the human kidney at mRNA level [197], the intrarenal distribution of GLP-1R has not clearly been defined yet nor has it been investigated whether in particular proximal tubular cells express GLP-1R. Therefore, it was the objective of this study, to confirm renal expression of GLP-1R and to evaluate, whether this expression was confined to proximal tubular cells in kidney cortex. Furthermore, we tried to show the cellular distribution and the regulation of expression of GLP-1R as well as the effect of GLP-1 administration on proximal tubular cell sodium re-absorption.

In the first experiments, GLP-1R mRNA expression was shown in renal tissue by RT-PCR. In previous studies we have observed GLP-1 effects on renal sodium re-absorption in obese subjects with impaired glucose tolerance. In the following experiments, we therefore investigated the effect of glucose on GLP-1R mRNA expression. The expression levels of

GLP-1R, DPPIV and NHE3 were not dependent on glucose concentrations (5.0 and 15.6mM) (Fig. 4.1). However, using a high glucose concentration (22mM) in a mouse pancreatic beta cell line (MIN6), an up-regulation of GLP-1R expression was observed [195]. We can only speculate on the physiological importance of this latter finding. Furthermore, the lack of induction of GLP-1R expression at mRNA level in primary porcine proximal tubules may be explained by the lower (more clinically relevant) glucose concentrations used in this study or by species differences (pigs versus mice). In addition, we have shown that GLP-1, exendin-4 and P32/98 did not influence the mRNA expression of GLP-1R, DPPIV, NHE3, sodium- dependent glucose transporter slc5a1, slc5a2 (SGLT1, 2) after incubation over 96 hours (data not shown).

GLP-1R expression was confirmed on the protein level using immunohistochemistry, immunocytochemistry and Western blot analysis (Fig. 4.2-4.5). This analysis showed that GLP-1R protein was found in the kidney cortex, predominantly in proximal tubular cells. This was proven by co-staining with DPPIV, which is exclusively expressed in proximal

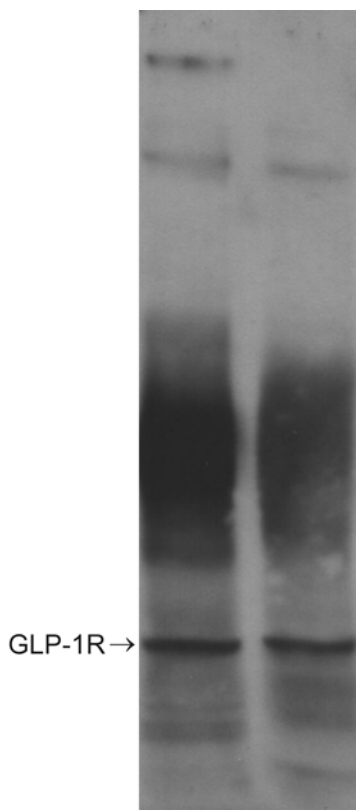


**Figure 4.4** - Western blot of GLP-1R **left lane:** pig kidney cortex, **right lane:** human kidney cortex run on a 7.5% polyacrylamide gel.

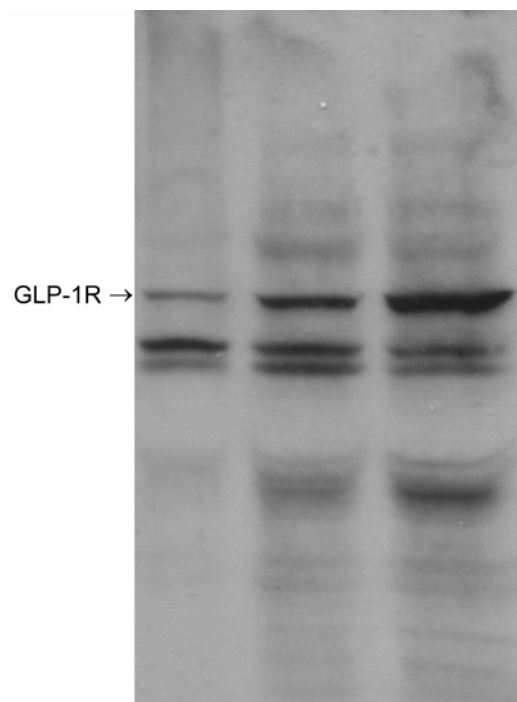


**Figure 4.5** - Western blot of three different samples of primary porcine proximal tubular cells from two different isolations, each isolation derived from kidneys of two pigs. Gel run on a 10% polyacrylamide gel.

tubular cells (Fig. 4.3). Interestingly, Fig. 4.3E shows a distribution of GLP-1R throughout the cells, although we would have expected a concentration of GLP-1R protein expression at the apical side, as GLP-1 influenced sodium transport there. Authors in [177] deliver an possible explanation for the distribution of GLP-1R in the cells: The receptor is internalised upon GLP-1 binding. Afterwards endosomal membrane fractions was found to be enriched with GLP-1R. Furthermore, the authors could show a cycling of the receptor between endosomal compartments and plasma membrane. However, our preparation for immunocytochemistry was performed without GLP-1 application. Additional experiments are required in order to clarify the intracellular protein distribution and function.

For our functional experiments, higher GLP-1 concentrations were applied (significantly higher than those observed physiologically). These concentrations were chosen, since GLP-1 is very rapidly (half-life of 2min) degraded *in vivo* by DPPIV [182]. DPPIV represents the major renal catabolic pathway for GLP-1 [198]. Therefore, in order to measure the direct effects of GLP-1 on primary porcine proximal tubular cells, either supra-physiological concentrations of GLP-1 need to be applied and/or DPPIV has to be blocked by specific inhibitors (such as P32/98). In patients with type 2 diabetes, supraphysiological GLP-1 serum concentrations of 50 to 120pM have been shown to lower glucose plasma concentrations. These concentrations are 3-5 fold higher than those reached after a meal or oral glucose intake [173].

Since our *in vitro* model consists of proximal tubular cells and DPPIV is abundantly expressed at the cell surface (apical side) in proximal tubular cells (and used as a marker for these cells) [183-186], a high activity of DPPIV is expected.

We therefore used high GLP-1 concentrations of 200pM to 20nM. The experiments of GLP-1 were compared with exendin-4 (200pM), a GLP-1 receptor agonist with a prolonged half-life of 2-4 hours [173], which was shown to be active in concentrations above 12pM [199]. To study inhibition of DPPIV, P32/98, a specific blocker of this enzyme was used at a concentration of 10µM, a concentration, which was effective in opossum kidney proximal tubule cells [58].

With 20nM GLP-1, we could show a significant inhibition of sodium re-absorption without using a DPPIV inhibitor (Fig. 4.6). Lower concentrations were ineffective although there

was a trend towards inhibition. However, 200pM GLP-1 and 10 $\mu$ M P32/98 given alone and in combination also failed to show a significant inhibition of sodium re-absorption (data not shown, n=6). A possible explanation of the latter finding could be that P32/98 does not bind to porcine DPPIV. Furthermore, in opossum kidney cells, even a complete inhibition of DPPIV with P32/98 resulted in only a 45% inhibition of NHE3 [58]. It is possible that the expression pattern of the five existing Na<sup>+</sup>/H<sup>+</sup> exchanger isoforms differs somewhat between pig and opossum that a partial inhibition of NHE3 isn't sufficient enough to influence the overall sodium re-absorption in porcine proximal tubular cells.

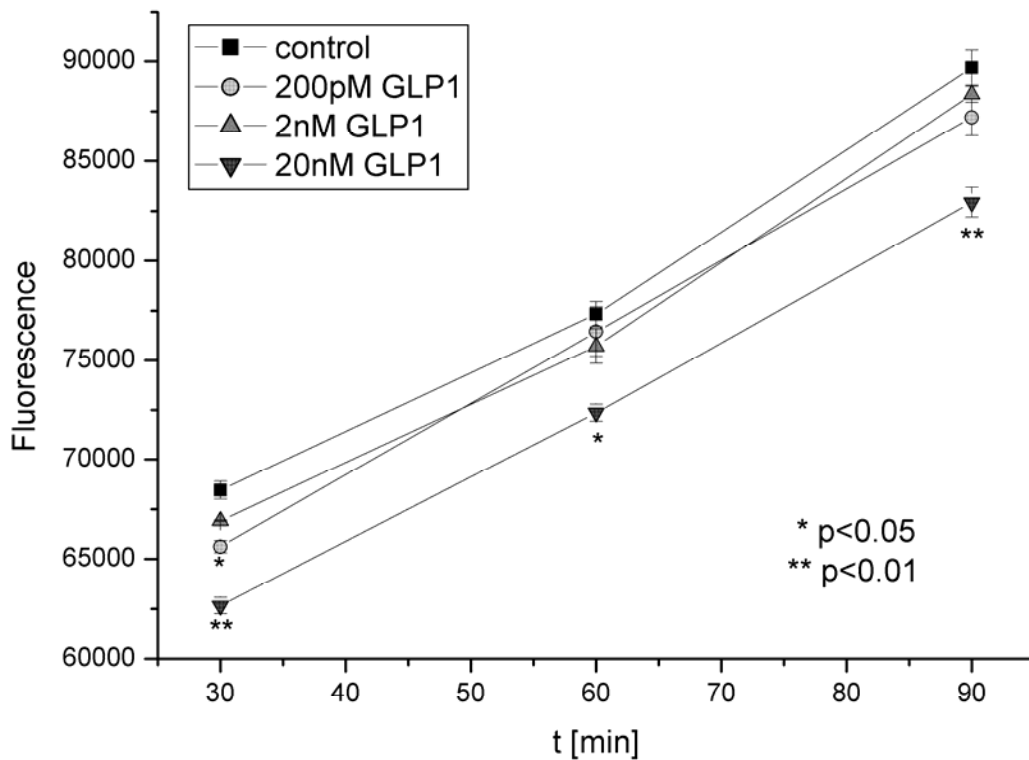


**Figure 4.6** - Sodium transport after 3h incubation from apical to basolateral (n=3), representative for three independent experiments. Sodium is measured with sodium green indicator (tetramethylammonium salt) by fluorescence.

When we used the DPPIV resistant GLP-1 analog exendin-4, a concentration of 200 pM with and without additional administration of 10 $\mu$ M P32/98 had also no effect on sodium re-absorption (data not shown, n=6). This lack of effect is somewhat surprising. Although exendin-4 has only a 53% amino acid sequence homology with human GLP-1 [200], exendin-4 binds *in vitro* (rat and human) with similar affinity to the pancreatic GLP-1

receptor as GLP-1 [201]. On the other hand, exendin-4 does not mimic all GLP-1 effects such as suppressing gastric acid secretion or activating hepatic vagal afferent nerves [202]. Recent findings even indicate that exendin-4 exerts additional effects, which are not mediated by GLP-1 receptor activation [201]. Further alternative explanations may be 1) a GLP-1 metabolite is necessary for this effects or 2) exendin-4 does not bind to the porcine GLP-1 receptor.

Inhibition of sodium transport from apical-to-basolateral (urine to blood) indicates enhanced secretion of sodium from blood to urine compartment. This fact corresponds with a clinical study: a significantly increased natriuresis was seen in men receiving intravenous GLP-1 for three hours [188]. Since the clinical data demonstrated, that plasma glucose levels were lowered by GLP-1 infusion, we also checked a possible effect of GLP-1 on glucose re-absorption in porcine proximal tubular cells. However, glucose transport was not affected with 200pM, 2 and 20nM GLP-1. Uptake with GLP-1, exendin-4, P32/98 and its combinations showed inconclusive results (data not shown).

The mechanism of the observed inhibition of sodium re-absorption is still not clear. A possible explanation could be a conformational change of the NHE3-DPPIV complex by GLP-1, resulting in a reduced transport activity of NHE3. This transporter is critical for the proximal tubular sodium re-absorption [191]. On the other hand, it is not yet resolved, which isoform of NHE is responsible in our cell line model, as mRNA expression of NHE3 was very low. Therefore, it may be speculated that such a conformational effect of GLP1 on the NHE3-DPPV complex would be independent of GLP-1R activation. Another possibility could be that the GLP-1 mediated increase in intracellular cAMP concentrations could influence the activity of the different NHE isoforms in the kidney. Indirect evidence for this explanation comes from experiments with intestinal cells, which showed that an intracellular rise of cGMP inhibits sodium absorption notably through inhibition of NHE transporters [203].

Finally, further investigations are required in order to elucidate 1. GLP-1R expression in other parts of the kidney and to which part it would contribute to physiology, 2. the effect of GLP-1 on intracellular cAMP production.

In conclusion, we have found further evidence for a direct renal action of GLP-1 in a porcine primary cell culture model of proximal tubules. These *in vitro* findings are in

agreement with findings in animals, and clinical observations in healthy volunteers and patients. Although the cellular mechanisms of this GLP-1 action remain unclear, this work demonstrates that GLP-1 has a direct effect on sodium re-absorption in primary cultures of porcine proximal tubular cells.

#### Acknowledgments

This work was supported by the Swiss National Science Foundation (grant #3200-065588.04/1) and the Senglet foundation, Basel, Switzerland. We express our gratitude to Ursula Behrens for the valuable technical support.

Great thanks go especially to Brigitte Schneider for the excellent technical assistance in immunohistochemistry.

## 5. Conclusion and outlook

Development of one successful pharmaceutical lasts about 10 years and costs, according to pharmaceutical companies around 800-1000 million US-Dollars (includes also costs for unsuccessful projects) [204]. Therefore it is of great interest to filter potentially “dangerous” pharmaceuticals in an early stage of drug discovery and development in order to prevent the costly and awkward situation of withdrawing a drug from market after 10 years of development due to a drug-drug interaction. Various “filtering” systems do exist. One of them is to use predictive in-vitro models, preferentially with high throughput screening capacities. In addition, an advantageous validated system can reduce costly and unnecessary animal tests.

In this thesis, we provide a new validated in-vitro model, which expresses various drug transporters functionally and simultaneously. Many drugs are often transported not only by one specific transporter (chapter 2.2). Therefore, this in-vitro model can now be used to test substances for tubular toxicity or to screen for possible drug-drug interactions in proximal tubules with the advantage to have various drug transporters available in one system without altering it by e.g. transfection. We are aware, that the definitive confirmation, whether this in-vitro model has more advantages compared to other established cell lines (LLC-PK1, HK2, HEK293, etc.), is yet to be performed. Even if the mentioned benefits are more theoretical, though plausible, we believe to provide an interesting tool for further studies. One of them would be to compare porcine with human transporter properties either by isolating these cells from human kidney or to confirm future findings in the porcine model with human clinical studies. Furthermore, evidence has to be supplied for high throughput screening capacities. Under certain conditions, such as using fluorescence markers (e.g. mitoxantrone) in 96 wells for uptake measurements, high throughput screening could be possible.

In addition, this system expresses genes, which are currently of great interest in diabetes research regarding GLP-1, its analogues and inhibitors of the degrading enzyme DPPIV. Therefore, in this part of the kidney, it is now possible to investigate the effect of these substances, which will be soon launched onto market.

## 6. References

1. Junqueira LC: *Histologie*, 4 ed. Berlin Heidelberg, Springer, 1996
2. Hediger MA, Romero MF, Peng JB, Rolfs A, Takanaga H, Bruford EA. The ABCs of solute carriers: physiological, pathological and therapeutic implications of human membrane transport proteins. *Pflugers Arch* 2004;447:465-8.
3. Daniel H, Kottra G. The proton oligopeptide cotransporter family SLC15 in physiology and pharmacology. *Pflugers Arch* 2004;447:610-8.
4. Van Aubel RA, Masereeuw R, Russel FG. Molecular pharmacology of renal organic anion transporters. *Am J Physiol Renal Physiol* 2000;279:F216-32.
5. You G. Structure, function, and regulation of renal organic anion transporters. *Med Res Rev* 2002;22:602-16.
6. Lee W, Kim RB. Transporters and renal drug elimination. *Annu Rev Pharmacol Toxicol* 2004;44:137-66.
7. Inui KI, Masuda S, Saito H. Cellular and molecular aspects of drug transport in the kidney. *Kidney Int* 2000;58:944-58.
8. Koepsell H. Polyspecific organic cation transporters: their functions and interactions with drugs. *Trends Pharmacol Sci* 2004;25:375-81.
9. Sawada K, Terada T, Saito H, Hashimoto Y, Inui K. Effects of glibenclamide on glycylsarcosine transport by the rat peptide transporters PEPT1 and PEPT2. *Br J Pharmacol* 1999;128:1159-64.
10. Kruidering M, Maasdam DH, Prins FA, de Heer E, Mulder GJ, Nagelkerke JF. Evaluation of nephrotoxicity in vitro using a suspension of highly purified porcine proximal tubular cells and characterization of the cells in primary culture. *Exp Nephrol* 1994;2:324-44.
11. Sai Y. Biochemical and molecular pharmacological aspects of transporters as determinants of drug disposition. *Drug Metab Pharmacokinet* 2005;20:91-9.
12. Ambudkar SV, Kim IW, Xia D, Sauna ZE. The A-loop, a novel conserved aromatic acid subdomain upstream of the Walker A motif in ABC transporters, is critical for ATP binding. *FEBS Lett* 2006;580:1049-55.
13. Dean M: *The Human ATP-Binding Cassette (ABC) Transporter Superfamily*. Bethesda (MD), National Library of Medicine (US), NCBI, 2002
14. Dean M, Hamon Y, Chimini G. The human ATP-binding cassette (ABC) transporter superfamily. *J Lipid Res* 2001;42:1007-17.
15. Kakumoto M, Sakaeda T, Takara K, Nakamura T, Kita T, Yagami T, et al. Effects of carvedilol on MDR1-mediated multidrug resistance: comparison with verapamil. *Cancer Sci* 2003;94:81-6.
16. Ding R, Tayrouz Y, Riedel KD, Burhenne J, Weiss J, Mikus G, et al. Substantial pharmacokinetic interaction between digoxin and ritonavir in healthy volunteers. *Clin Pharmacol Ther* 2004;76:73-84.
17. Hoffmeyer S, Burk O, von Richter O, Arnold HP, Brockmoller J, John A, et al. Functional polymorphisms of the human multidrug-resistance gene: multiple sequence variations and correlation of one allele with P-glycoprotein expression and activity in vivo. *Proc Natl Acad Sci U S A* 2000;97:3473-8.
18. Bodo A, Bakos E, Szeri F, Varadi A, Sarkadi B. The role of multidrug transporters in drug availability, metabolism and toxicity. *Toxicol Lett* 2003;140-141:133-43.
19. Nies AT, Keppler D. The apical conjugate efflux pump ABCC2 (MRP2). *Pflugers Arch* 2006.



20. Paulusma CC, Bosma PJ, Zaman GJ, Bakker CT, Otter M, Scheffer GL, et al. Congenital jaundice in rats with a mutation in a multidrug resistance-associated protein gene. *Science* 1996;271:1126-8.
21. Wada M, Toh S, Taniguchi K, Nakamura T, Uchiumi T, Kohno K, et al. Mutations in the canalicular multispecific organic anion transporter (cMOAT) gene, a novel ABC transporter, in patients with hyperbilirubinemia II/Dubin-Johnson syndrome. *Hum Mol Genet* 1998;7:203-7.
22. van Aubel RA, Smeets PH, Peters JG, Bindels RJ, Russel FG. The MRP4/ABCC4 gene encodes a novel apical organic anion transporter in human kidney proximal tubules: putative efflux pump for urinary cAMP and cGMP. *J Am Soc Nephrol* 2002;13:595-603.
23. Smeets PH, van Aubel RA, Wouterse AC, van den Heuvel JJ, Russel FG. Contribution of multidrug resistance protein 2 (MRP2/ABCC2) to the renal excretion of p-aminohippurate (PAH) and identification of MRP4 (ABCC4) as a novel PAH transporter. *J Am Soc Nephrol* 2004;15:2828-35.
24. Nies AT, Spring H, Thon WF, Keppler D, Jedlitschky G. Immunolocalization of multidrug resistance protein 5 in the human genitourinary system. *J Urol* 2002;167:2271-5.
25. Le Saux O, Urban Z, Tschuch C, Csiszar K, Bacchelli B, Quagliano D, et al. Mutations in a gene encoding an ABC transporter cause pseudoxanthoma elasticum. *Nat Genet* 2000;25:223-7.
26. Wang J, Near S, Young K, Connelly PW, Hegele RA. ABCC6 gene polymorphism associated with variation in plasma lipoproteins. *J Hum Genet* 2001;46:699-705.
27. Annilo T, Tammur J, Hutchinson A, Rzhetsky A, Dean M, Allikmets R. Human and mouse orthologs of a new ATP-binding cassette gene, ABCG4. *Cytogenet Cell Genet* 2001;94:196-201.
28. Eisenblatter T, Galla HJ. A new multidrug resistance protein at the blood-brain barrier. *Biochem Biophys Res Commun* 2002;293:1273-8.
29. Mao Q, Unadkat JD. Role of the breast cancer resistance protein (ABCG2) in drug transport. *Aaps J* 2005;7:E118-33.
30. Fetsch PA, Abati A, Litman T, Morisaki K, Honjo Y, Mittal K, et al. Localization of the ABCG2 mitoxantrone resistance-associated protein in normal tissues. *Cancer Lett* 2006;235:84-92.
31. Mizuno N, Suzuki M, Kusuhara H, Suzuki H, Takeuchi K, Niwa T, et al. Impaired renal excretion of 6-hydroxy-5,7-dimethyl-2-methylamino-4-(3-pyridylmethyl) benzothiazole (E3040) sulfate in breast cancer resistance protein (BCRP1/ABCG2) knockout mice. *Drug Metab Dispos* 2004;32:898-901.
32. Cervenak J, Andrikovics H, Ozvegy-Laczka C, Tordai A, Nemet K, Varadi A, et al. The role of the human ABCG2 multidrug transporter and its variants in cancer therapy and toxicology. *Cancer Lett* 2006;234:62-72.
33. Jonker JW, Buitelaar M, Wagenaar E, Van Der Valk MA, Scheffer GL, Scheper RJ, et al. The breast cancer resistance protein protects against a major chlorophyll-derived dietary phototoxin and protoporphyria. *Proc Natl Acad Sci U S A* 2002;99:15649-54.
34. van Herwaarden AE, Jonker JW, Wagenaar E, Brinkhuis RF, Schellens JH, Beijnen JH, et al. The breast cancer resistance protein (Bcrp1/Abcg2) restricts exposure to the dietary carcinogen 2-amino-1-methyl-6-phenylimidazo[4,5-b]pyridine. *Cancer Res* 2003;63:6447-52.
35. Taipalensuu J, Tornblom H, Lindberg G, Einarsson C, Sjoqvist F, Melhus H, et al. Correlation of gene expression of ten drug efflux proteins of the ATP-binding

- cassette transporter family in normal human jejunum and in human intestinal epithelial Caco-2 cell monolayers. *J Pharmacol Exp Ther* 2001;299:164-70.
36. Pushkin A, Kurtz I. SLC4 base (HCO<sub>3</sub><sup>-</sup>, CO<sub>3</sub><sup>2-</sup>) transporters: classification, function, structure, genetic diseases, and knockout models. *Am J Physiol Renal Physiol* 2006;290:F580-99.
  37. Aalkjaer C, Frische S, Leipziger J, Nielsen S, Praetorius J. Sodium coupled bicarbonate transporters in the kidney, an update. *Acta Physiol Scand* 2004;181:505-12.
  38. Muller-Berger S, Ducoudret O, Diakov A, Fromter E. The renal Na-HCO<sub>3</sub>-cotransporter expressed in *Xenopus laevis* oocytes: change in stoichiometry in response to elevation of cytosolic Ca<sup>2+</sup> concentration. *Pflugers Arch* 2001;442:718-28.
  39. Gross E, Hawkins K, Pushkin A, Sassani P, Dukkipati R, Abuladze N, et al. Phosphorylation of Ser(982) in the sodium bicarbonate cotransporter kNBC1 shifts the HCO<sub>3</sub><sup>(-)</sup>: Na<sup>(+)</sup> stoichiometry from 3: 1 to 2: 1 in murine proximal tubule cells. *J Physiol* 2001;537:659-65.
  40. Abuladze N, Lee I, Newman D, Hwang J, Boorer K, Pushkin A, et al. Molecular cloning, chromosomal localization, tissue distribution, and functional expression of the human pancreatic sodium bicarbonate cotransporter. *J Biol Chem* 1998;273:17689-95.
  41. Igarashi T, Inatomi J, Sekine T, Cha SH, Kanai Y, Kunimi M, et al. Mutations in SLC4A4 cause permanent isolated proximal renal tubular acidosis with ocular abnormalities. *Nat Genet* 1999;23:264-6.
  42. Wood IS, Trayhurn P. Glucose transporters (GLUT and SGLT): expanded families of sugar transport proteins. *Br J Nutr* 2003;89:3-9.
  43. Lee WS, Kanai Y, Wells RG, Hediger MA. The high affinity Na<sup>+</sup>/glucose cotransporter. Re-evaluation of function and distribution of expression. *J Biol Chem* 1994;269:12032-9.
  44. Kanai Y, Lee WS, You G, Brown D, Hediger MA. The human kidney low affinity Na<sup>+</sup>/glucose cotransporter SGLT2. Delineation of the major renal reabsorptive mechanism for D-glucose. *J Clin Invest* 1994;93:397-404.
  45. Diez-Sampedro A, Eskandari S, Wright EM, Hirayama BA. Na<sup>+</sup>-to-sugar stoichiometry of SGLT3. *Am J Physiol Renal Physiol* 2001;280:F278-82.
  46. Tazawa S, Yamato T, Fujikura H, Hiratochi M, Itoh F, Tomae M, et al. SLC5A9/SGLT4, a new Na<sup>+</sup>-dependent glucose transporter, is an essential transporter for mannose, 1,5-anhydro-D-glucitol, and fructose. *Life Sci* 2005;76:1039-50.
  47. Zhao FQ, Zheng YC, Wall EH, McFadden TB. Cloning and expression of bovine sodium/glucose cotransporters. *J Dairy Sci* 2005;88:182-94.
  48. Roll P, Massacrier A, Pereira S, Robaglia-Schlupp A, Cau P, Szepetowski P. New human sodium/glucose cotransporter gene (KST1): identification, characterization, and mutation analysis in ICCA (infantile convulsions and choreoathetosis) and BFIC (benign familial infantile convulsions) families. *Gene* 2002;285:141-8.
  49. Turk E, Zabel B, Mundlos S, Dyer J, Wright EM. Glucose/galactose malabsorption caused by a defect in the Na<sup>+</sup>/glucose cotransporter. *Nature* 1991;350:354-6.
  50. Kong CT, Yet SF, Lever JE. Cloning and expression of a mammalian Na<sup>+</sup>/amino acid cotransporter with sequence similarity to Na<sup>+</sup>/glucose cotransporters. *J Biol Chem* 1993;268:1509-12.
  51. Calado J, Loeffler J, Sakallioğlu O, Gok F, Lhotta K, Barata J, et al. Familial renal glucosuria: SLC5A2 mutation analysis and evidence of salt-wasting. *Kidney Int* 2006;69:852-5.

52. Sugawara-Yokoo M, Suzuki T, Matsuzaki T, Naruse T, Takata K. Presence of fructose transporter GLUT5 in the S3 proximal tubules in the rat kidney. *Kidney Int* 1999;56:1022-8.
53. Linden KC, DeHaan CL, Zhang Y, Glowacka S, Cox AJ, Kelly DJ, et al. Renal expression and localization of the facilitative glucose transporters GLUT1 and GLUT12 in animal models of hypertension and diabetic nephropathy. *Am J Physiol Renal Physiol* 2006;290:F205-13.
54. de Silva MG, Elliott K, Dahl HH, Fitzpatrick E, Wilcox S, Delatycki M, et al. Disruption of a novel member of a sodium/hydrogen exchanger family and DOCK3 is associated with an attention deficit hyperactivity disorder-like phenotype. *J Med Genet* 2003;40:733-40.
55. Nakamura N, Tanaka S, Teko Y, Mitsui K, Kanazawa H. Four Na<sup>+</sup>/H<sup>+</sup> exchanger isoforms are distributed to Golgi and post-Golgi compartments and are involved in organelle pH regulation. *J Biol Chem* 2005;280:1561-72.
56. Orłowski J, Grinstein S. Diversity of the mammalian sodium/proton exchanger SLC9 gene family. *Pflugers Arch* 2004;447:549-65.
57. Gonzalez-Gronow M, Misra UK, Gawdi G, Pizzo SV. Association of plasminogen with dipeptidyl peptidase IV and Na<sup>+</sup>/H<sup>+</sup> exchanger isoform NHE3 regulates invasion of human 1-LN prostate tumor cells. *J Biol Chem* 2005;280:27173-8.
58. Girardi AC, Knauf F, Demuth HU, Aronson PS. Role of dipeptidyl peptidase IV in regulating activity of Na<sup>+</sup>/H<sup>+</sup> exchanger isoform NHE3 in proximal tubule cells. *Am J Physiol Cell Physiol* 2004;287:C1238-45.
59. Vallon V, Schwark JR, Richter K, Hropot M. Role of Na<sup>(+)</sup>/H<sup>(+)</sup> exchanger NHE3 in nephron function: micropuncture studies with S3226, an inhibitor of NHE3. *Am J Physiol Renal Physiol* 2000;278:F375-9.
60. Wang T, Hropot M, Aronson PS, Giebisch G. Role of NHE isoforms in mediating bicarbonate reabsorption along the nephron. *Am J Physiol Renal Physiol* 2001;281:F1117-22.
61. Pang T, Su X, Wakabayashi S, Shigekawa M. Calcineurin homologous protein as an essential cofactor for Na<sup>+</sup>/H<sup>+</sup> exchangers. *J Biol Chem* 2001;276:17367-72.
62. Pang T, Wakabayashi S, Shigekawa M. Expression of calcineurin B homologous protein 2 protects serum deprivation-induced cell death by serum-independent activation of Na<sup>+</sup>/H<sup>+</sup> exchanger. *J Biol Chem* 2002;277:43771-7.
63. Biemesderfer D, DeGray B, Aronson PS. Active (9.6 s) and inactive (21 s) oligomers of NHE3 in microdomains of the renal brush border. *J Biol Chem* 2001;276:10161-7.
64. Weinman EJ, Steplock D, Wang Y, Shenolikar S. Characterization of a protein cofactor that mediates protein kinase A regulation of the renal brush border membrane Na<sup>(+)</sup>-H<sup>+</sup> exchanger. *J Clin Invest* 1995;95:2143-9.
65. Yun CH, Oh S, Zizak M, Steplock D, Tsao S, Tse CM, et al. cAMP-mediated inhibition of the epithelial brush border Na<sup>+</sup>/H<sup>+</sup> exchanger, NHE3, requires an associated regulatory protein. *Proc Natl Acad Sci U S A* 1997;94:3010-5.
66. Booth IW, Stange G, Murer H, Fenton TR, Milla PJ. Defective jejunal brush-border Na<sup>+</sup>/H<sup>+</sup> exchange: a cause of congenital secretory diarrhoea. *Lancet* 1985;1:1066-9.
67. Ledoussal C, Lorenz JN, Nieman ML, Soleimani M, Schultheis PJ, Shull GE. Renal salt wasting in mice lacking NHE3 Na<sup>+</sup>/H<sup>+</sup> exchanger but not in mice lacking NHE2. *Am J Physiol Renal Physiol* 2001;281:F718-27.
68. Schultheis PJ, Clarke LL, Meneton P, Miller ML, Soleimani M, Gawenis LR, et al. Renal and intestinal absorptive defects in mice lacking the NHE3 Na<sup>+</sup>/H<sup>+</sup> exchanger. *Nat Genet* 1998;19:282-5.

69. Ogihara H, Saito H, Shin BC, Terado T, Takenoshita S, Nagamachi Y, et al. Immuno-localization of H<sup>+</sup>/peptide cotransporter in rat digestive tract. *Biochem Biophys Res Commun* 1996;220:848-52.
70. Shen H, Smith DE, Yang T, Huang YG, Schnermann JB, Brosius FC, 3rd. Localization of PEPT1 and PEPT2 proton-coupled oligopeptide transporter mRNA and protein in rat kidney. *Am J Physiol* 1999;276:F658-65.
71. Knutter I, Rubio-Aliaga I, Boll M, Hause G, Daniel H, Neubert K, et al. H<sup>+</sup>-peptide cotransport in the human bile duct epithelium cell line SK-ChA-1. *Am J Physiol Gastrointest Liver Physiol* 2002;283:G222-9.
72. Smith DE, Pavlova A, Berger UV, Hediger MA, Yang T, Huang YG, et al. Tubular localization and tissue distribution of peptide transporters in rat kidney. *Pharm Res* 1998;15:1244-9.
73. Berger UV, Hediger MA. Distribution of peptide transporter PEPT2 mRNA in the rat nervous system. *Anat Embryol (Berl)* 1999;199:439-49.
74. Groneberg DA, Doring F, Theis S, Nickolaus M, Fischer A, Daniel H. Peptide transport in the mammary gland: expression and distribution of PEPT2 mRNA and protein. *Am J Physiol Endocrinol Metab* 2002;282:E1172-9.
75. Groneberg DA, Nickolaus M, Springer J, Doring F, Daniel H, Fischer A. Localization of the peptide transporter PEPT2 in the lung: implications for pulmonary oligopeptide uptake. *Am J Pathol* 2001;158:707-14.
76. Sakata K, Yamashita T, Maeda M, Moriyama Y, Shimada S, Tohyama M. Cloning of a lymphatic peptide/histidine transporter. *Biochem J* 2001;356:53-60.
77. Kottra G, Stamford A, Daniel H. PEPT1 as a paradigm for membrane carriers that mediate electrogenic bidirectional transport of anionic, cationic, and neutral substrates. *J Biol Chem* 2002;277:32683-91.
78. Steel A, Nussberger S, Romero MF, Boron WF, Boyd CA, Hediger MA. Stoichiometry and pH dependence of the rabbit proton-dependent oligopeptide transporter PepT1. *J Physiol* 1997;498 (Pt 3):563-9.
79. Chen XZ, Zhu T, Smith DE, Hediger MA. Stoichiometry and kinetics of the high-affinity H<sup>+</sup>-coupled peptide transporter PepT2. *J Biol Chem* 1999;274:2773-9.
80. Covitz KM, Amidon GL, Sadee W. Human dipeptide transporter, hPEPT1, stably transfected into Chinese hamster ovary cells. *Pharm Res* 1996;13:1631-4.
81. Sugawara M, Ogawa T, Kobayashi M, Miyazaki K. Uptake of dipeptide and beta-lactam antibiotics by the basolateral membrane vesicles prepared from rat kidney. *Biochim Biophys Acta* 2003;1609:39-44.
82. Ganapathy ME, Prasad PD, Mackenzie B, Ganapathy V, Leibach FH. Interaction of anionic cephalosporins with the intestinal and renal peptide transporters PEPT 1 and PEPT 2. *Biochim Biophys Acta* 1997;1324:296-308.
83. Buyse M, Tsocas A, Walker F, Merlin D, Bado A. PepT1-mediated fMLP transport induces intestinal inflammation in vivo. *Am J Physiol Cell Physiol* 2002;283:C1795-800.
84. Merlin D, Si-Tahar M, Sitaraman SV, Eastburn K, Williams I, Liu X, et al. Colonic epithelial hPepT1 expression occurs in inflammatory bowel disease: transport of bacterial peptides influences expression of MHC class 1 molecules. *Gastroenterology* 2001;120:1666-79.
85. Sekine T, Miyazaki H, Endou H. Molecular physiology of renal organic anion transporters. *Am J Physiol Renal Physiol* 2006;290:F251-61.
86. Hagenbuch B, Meier PJ. The superfamily of organic anion transporting polypeptides. *Biochim Biophys Acta* 2003;1609:1-18.

87. Mikkaichi T, Suzuki T, Onogawa T, Tanemoto M, Mizutamari H, Okada M, et al. Isolation and characterization of a digoxin transporter and its rat homologue expressed in the kidney. *Proc Natl Acad Sci U S A* 2004;101:3569-74.
88. Kusuhara H, Sugiyama Y. Active efflux across the blood-brain barrier: role of the solute carrier family. *NeuroRx* 2005;2:73-85.
89. Lahjouji K, Mitchell GA, Qureshi IA. Carnitine transport by organic cation transporters and systemic carnitine deficiency. *Mol Genet Metab* 2001;73:287-97.
90. Tamai I, China K, Sai Y, Kobayashi D, Nezu J, Kawahara E, et al. Na(+)-coupled transport of L-carnitine via high-affinity carnitine transporter OCTN2 and its subcellular localization in kidney. *Biochim Biophys Acta* 2001;1512:273-84.
91. Koepsell H, Endou H. The SLC22 drug transporter family. *Pflugers Arch* 2004;447:666-76.
92. Koepsell H, Schmitt BM, Gorboulev V. Organic cation transporters. *Rev Physiol Biochem Pharmacol* 2003;150:36-90.
93. Cha SH, Sekine T, Fukushima JI, Kanai Y, Kobayashi Y, Goya T, et al. Identification and characterization of human organic anion transporter 3 expressing predominantly in the kidney. *Mol Pharmacol* 2001;59:1277-86.
94. Fromm MF, Kim RB, Stein CM, Wilkinson GR, Roden DM. Inhibition of P-glycoprotein-mediated drug transport: A unifying mechanism to explain the interaction between digoxin and quinidine [see comments]. *Circulation* 1999;99:552-7.
95. Sakaeda T, Nakamura T, Okumura K. MDR1 genotype-related pharmacokinetics and pharmacodynamics. *Biol Pharm Bull* 2002;25:1391-400.
96. Sekine T, Watanabe N, Hosoyamada M, Kanai Y, Endou H. Expression cloning and characterization of a novel multispecific organic anion transporter. *J Biol Chem* 1997;272:18526-9.
97. Sweet DH, Wolff NA, Pritchard JB. Expression cloning and characterization of ROAT1. The basolateral organic anion transporter in rat kidney. *J Biol Chem* 1997;272:30088-95.
98. Sekine T, Cha SH, Tsuda M, Apiwattanakul N, Nakajima N, Kanai Y, et al. Identification of multispecific organic anion transporter 2 expressed predominantly in the liver. *FEBS Lett* 1998;429:179-82.
99. Tahara H, Kusuhara H, Chida M, Fuse E, Sugiyama Y. Is the monkey an appropriate animal model to examine drug-drug interactions involving renal clearance? Effect of probenecid on the renal elimination of H2 receptor antagonists. *J Pharmacol Exp Ther* 2006;316:1187-94.
100. Tahara H, Kusuhara H, Endou H, Koepsell H, Imaoka T, Fuse E, et al. A species difference in the transport activities of H2 receptor antagonists by rat and human renal organic anion and cation transporters. *J Pharmacol Exp Ther* 2005;315:337-45.
101. Tahara H, Shono M, Kusuhara H, Kinoshita H, Fuse E, Takadate A, et al. Molecular cloning and functional analyses of OAT1 and OAT3 from cynomolgus monkey kidney. *Pharm Res* 2005;22:647-60.
102. Timchalk C. Comparative inter-species pharmacokinetics of phenoxyacetic acid herbicides and related organic acids. evidence that the dog is not a relevant species for evaluation of human health risk. *Toxicology* 2004;200:1-19.
103. Taub M, Han HJ, Rajkhowa T, Allen C, Park JH. Clonal analysis of immortalized renal proximal tubule cells: Na(+)/glucose cotransport system levels are maintained despite a decline in transport function. *Exp Cell Res* 2002;281:205-12.
104. Ip MM, Darcy KM. Three-dimensional mammary primary culture model systems. *J Mammary Gland Biol Neoplasia* 1996;1:91-110.

105. Imai Y, Tsukahara S, Asada S, Sugimoto Y. Phytoestrogens/flavonoids reverse breast cancer resistance protein/ABCG2-mediated multidrug resistance. *Cancer Res* 2004;64:4346-52.
106. Flanagan SD, Cummins CL, Susanto M, Liu X, Takahashi LH, Benet LZ. Comparison of furosemide and vinblastine secretion from cell lines overexpressing multidrug resistance protein (P-glycoprotein) and multidrug resistance-associated proteins (MRP1 and MRP2). *Pharmacology* 2002;64:126-34.
107. Wein S, Fauroux M, Laffitte J, de Nadai P, Guaini C, Pons F, et al. Mediation of annexin 1 secretion by a probenecid-sensitive ABC-transporter in rat inflamed mucosa. *Biochem Pharmacol* 2004;67:1195-202.
108. Zalups RK, Aslamkhan AG, Ahmad S. Human organic anion transporter 1 mediates cellular uptake of cysteine-S conjugates of inorganic mercury. *Kidney Int* 2004;66:251-61.
109. Baldes C, Koenig P, Neumann D, Lenhof HP, Kohlbacher O, Lehr CM. Development of a fluorescence-based assay for screening of modulators of human Organic Anion Transporter 1B3 (OATP1B3). *Eur J Pharm Biopharm* 2005.
110. Wielinga P, Hooijberg JH, Gunnarsdottir S, Kathmann I, Reid G, Zelcer N, et al. The human multidrug resistance protein MRP5 transports folates and can mediate cellular resistance against antifolates. *Cancer Res* 2005;65:4425-30.
111. You G, Lee WS, Barros EJ, Kanai Y, Huo TL, Khawaja S, et al. Molecular characteristics of Na(+)-coupled glucose transporters in adult and embryonic rat kidney. *J Biol Chem* 1995;270:29365-71.
112. Gutmann H, Miller DS, Droulle A, Drewe J, Fahr A, Fricker G. P-glycoprotein- and mrp2-mediated octreotide transport in renal proximal tubule. *Br J Pharmacol* 2000;129:251-6.
113. Vellonen KS, Honkakoski P, Urtti A. Substrates and inhibitors of efflux proteins interfere with the MTT assay in cells and may lead to underestimation of drug toxicity. *Eur J Pharm Sci* 2004;23:181-8.
114. Miller DS. Xenobiotic export pumps, endothelin signaling, and tubular nephrotoxics--a case of molecular hijacking. *J Biochem Mol Toxicol* 2002;16:121-7.
115. Khamdang S, Takeda M, Shimoda M, Noshiro R, Narikawa S, Huang XL, et al. Interactions of human- and rat-organic anion transporters with pravastatin and cimetidine. *J Pharmacol Sci* 2004;94:197-202.
116. Hasannejad H, Takeda M, Taki K, Shin HJ, Babu E, Jutabha P, et al. Interactions of human organic anion transporters with diuretics. *J Pharmacol Exp Ther* 2004;308:1021-9.
117. Khamdang S, Takeda M, Noshiro R, Narikawa S, Enomoto A, Anzai N, et al. Interactions of human organic anion transporters and human organic cation transporters with nonsteroidal anti-inflammatory drugs. *J Pharmacol Exp Ther* 2002;303:534-9.
118. Takeda M, Khamdang S, Narikawa S, Kimura H, Hosoyamada M, Cha SH, et al. Characterization of methotrexate transport and its drug interactions with human organic anion transporters. *J Pharmacol Exp Ther* 2002;302:666-71.
119. Masereeuw R, Russel FG, Miller DS. Multiple pathways of organic anion secretion in renal proximal tubule revealed by confocal microscopy. *Am J Physiol* 1996;271:F1173-82.
120. Sweet DH, Chan LM, Walden R, Yang XP, Miller DS, Pritchard JB. Organic anion transporter 3 (Slc22a8) is a dicarboxylate exchanger indirectly coupled to the Na+ gradient. *Am J Physiol Renal Physiol* 2003;284:F763-9.

121. Jonker JW, Schinkel AH. Pharmacological and physiological functions of the polyspecific organic cation transporters: OCT1, 2, and 3 (SLC22A1-3). *J Pharmacol Exp Ther* 2004;308:2-9.
122. Groneberg DA, Doring F, Nickolaus M, Daniel H, Fischer A. Renal assimilation of short chain peptides: visualization of tubular peptide uptake. *Pharm Res* 2002;19:1209-14.
123. Takata K. Glucose transporters in the transepithelial transport of glucose. *J Electron Microscop* (Tokyo) 1996;45:275-84.
124. Heilig C, Zaloga C, Lee M, Zhao X, Riser B, Brosius F, et al. Immunogold localization of high-affinity glucose transporter isoforms in normal rat kidney. *Lab Invest* 1995;73:674-84.
125. Schmitt BM, Biemesderfer D, Romero MF, Boulpaep EL, Boron WF. Immunolocalization of the electrogenic Na<sup>+</sup>-HCO<sub>3</sub><sup>-</sup> cotransporter in mammalian and amphibian kidney. *Am J Physiol* 1999;276:F27-38.
126. Elbling L, Berger W, Weiss RM, Printz D, Fritsch G, Micksche M. A novel bioassay for P-glycoprotein functionality using cytochalasin D. *Cytometry* 1998;31:187-98.
127. Kruidering M, Van de Water B, de Heer E, Mulder GJ, Nagelkerke JF. Cisplatin-induced nephrotoxicity in porcine proximal tubular cells: mitochondrial dysfunction by inhibition of complexes I to IV of the respiratory chain. *J Pharmacol Exp Ther* 1997;280:638-49.
128. Whittin JC, Bhamre S, Tham DM, Cohen HJ. Extracellular glutathione peroxidase is secreted basolaterally by human renal proximal tubule cells. *Am J Physiol Renal Physiol* 2002;283:F20-8.
129. Zhou S, Li Y, Kestell P, Paxton JW. Determination of thalidomide in transport buffer for Caco-2 cell monolayers by high-performance liquid chromatography with ultraviolet detection. *J Chromatogr B Analyt Technol Biomed Life Sci* 2003;785:165-73.
130. Bahn A, Hauss A, Appenroth D, Ebbinghaus D, Hagos Y, Steinmetzer P, et al. RT-PCR-based evidence for the in vivo stimulation of renal tubular para-aminohippurate (PAH) transport by triiodothyronine (T3) or dexamethasone (DEXA) in kidney tissue of immature and adult rats. *Exp Toxicol Pathol* 2003;54:367-73.
131. Fleck C, Hilger R, Jurkutat S, Karge E, Merkel U, Schimske A, et al. Ex vivo stimulation of renal transport of the cytostatic drugs methotrexate, cisplatin, topotecan (Hycamtin) and raltitrexed (Tomudex) by dexamethasone, T3 and EGF in intact human and rat kidney tissue and in human renal cell carcinoma. *Urol Res* 2002;30:256-62.
132. Aoyama I, Enomoto A, Niwa T. Effects of oral adsorbent on gene expression profile in uremic rat kidney: cDNA array analysis. *Am J Kidney Dis* 2003;41:S8-14.
133. Arndt P, Volk C, Gorboulev V, Budiman T, Popp C, Ulzheimer-Teuber I, et al. Interaction of cations, anions, and weak base quinine with rat renal cation transporter rOCT2 compared with rOCT1. *Am J Physiol Renal Physiol* 2001;281:F454-68.
134. Van Itallie CM, Fanning AS, Anderson JM. Reversal of charge selectivity in cation or anion-selective epithelial lines by expression of different claudins. *Am J Physiol Renal Physiol* 2003;285:F1078-84.
135. Contreras RG, Shoshani L, Flores-Maldonado C, Lazaro A, Monroy AO, Roldan ML, et al. E-Cadherin and tight junctions between epithelial cells of different animal species. *Pflugers Arch* 2002;444:467-75.
136. Colegio OR, Van Itallie C, Rahner C, Anderson JM. Claudin extracellular domains determine paracellular charge selectivity and resistance but not tight junction fibril architecture. *Am J Physiol Cell Physiol* 2003;284:C1346-54.

137. Kiely B, Feldman G, Ryan MP. Modulation of renal epithelial barrier function by mitogen-activated protein kinases (MAPKs): mechanism of cyclosporine A-induced increase in transepithelial resistance. *Kidney Int* 2003;63:908-16.
138. Gallardo JM, Hernandez JM, Contreras RG, Flores-Maldonado C, Gonzalez-Mariscal L, Cereijido M. Tight junctions are sensitive to peptides eliminated in the urine. *J Membr Biol* 2002;188:33-42.
139. Clarke H, Soler AP, Mullin JM. Protein kinase C activation leads to dephosphorylation of occludin and tight junction permeability increase in LLC-PK1 epithelial cell sheets. *J Cell Sci* 2000;113 (Pt 18):3187-96.
140. Perloff MD, Von Moltke LL, Marchand JE, Greenblatt DJ. Ritonavir induces P-glycoprotein expression, multidrug resistance-associated protein (MRP1) expression, and drug transporter-mediated activity in a human intestinal cell line. *J Pharm Sci* 2001;90:1829-37.
141. Yang Z, Li CS, Shen DD, Ho RJ. Cloning and characterization of the rat multidrug resistance-associated protein 1. *AAPS PharmSci* 2002;4:E15.
142. Ng KH, Lim BG, Wong KP. Sulfate conjugating and transport functions of MDCK distal tubular cells. *Kidney Int* 2003;63:976-86.
143. Fricker G, Gutmann H, Droulle A, Drewe J, Miller DS. Epithelial transport of anthelmintic ivermectin in a novel model of isolated proximal kidney tubules. *Pharm Res* 1999;16:1570-5.
144. Hagos Y, Bahn A, Asif AR, Krick W, Sendler M, Burckhardt G. Cloning of the pig renal organic anion transporter 1 (pOAT1). *Biochimie* 2002;84:1221-4.
145. Zhang X, Groves CE, Bahn A, Barendt WM, Prado MD, Rodiger M, et al. Relative contribution of OAT and OCT transporters to organic electrolyte transport in rabbit proximal tubule. *Am J Physiol Renal Physiol* 2004;287:F999-1010.
146. Lu R, Chan BS, Schuster VL. Cloning of the human kidney PAH transporter: narrow substrate specificity and regulation by protein kinase C. *Am J Physiol* 1999;276:F295-303.
147. Romiti N, Tramonti G, Chieli E. Influence of different chemicals on MDR-1 P-glycoprotein expression and activity in the HK-2 proximal tubular cell line. *Toxicol Appl Pharmacol* 2002;183:83-91.
148. Hara C, Satoh H, Usui T, Kunimi M, Noiri E, Tsukamoto K, et al. Intracellular pH regulatory mechanism in a human renal proximal cell line (HKC-8): evidence for Na<sup>+</sup>/H<sup>+</sup> exchanger, Cl<sup>-</sup>/HCO<sub>3</sub><sup>-</sup> exchanger and Na<sup>+</sup>-HCO<sub>3</sub><sup>-</sup> cotransporter. *Pflugers Arch* 2000;440:713-20.
149. Aleo MF, Morandini F, Bettoni F, Giuliani R, Rovetta F, Steimberg N, et al. Endogenous thiols and MRP transporters contribute to Hg<sub>2</sub><sup>+</sup> efflux in HgCl<sub>2</sub>-treated tubular MDCK cells. *Toxicology* 2005;206:137-51.
150. Chen C, Mireles RJ, Campbell SD, Lin J, Mills JB, Xu JJ, et al. Differential interaction of 3-hydroxy-3-methylglutaryl-coa reductase inhibitors with ABCB1, ABCC2, and OATP1B1. *Drug Metab Dispos* 2005;33:537-46.
151. Spears KJ, Ross J, Stenhouse A, Ward CJ, Goh LB, Wolf CR, et al. Directional trans-epithelial transport of organic anions in porcine LLC-PK1 cells that co-express human OATP1B1 (OATP-C) and MRP2. *Biochem Pharmacol* 2005;69:415-23.
152. Beljanski V, Soulika A, Tucker JM, Townsend DM, Davis W, Jr., Tew KD. Characterization of the ATPase activity of human ATP-binding cassette transporter-2 (ABCA2). *In Vivo* 2005;19:657-60.
153. Litman T, Jensen U, Hansen A, Covitz KM, Zhan Z, Fetsch P, et al. Use of peptide antibodies to probe for the mitoxantrone resistance-associated protein MXR/BCRP/ABCP/ABCG2. *Biochim Biophys Acta* 2002;1565:6-16.



154. Polgar O, Robey RW, Morisaki K, Dean M, Michejda C, Sauna ZE, et al. Mutational analysis of ABCG2: role of the GXXXG motif. *Biochemistry* 2004;43:9448-56.
155. Pavek P, Merino G, Wagenaar E, Bolscher E, Novotna M, Jonker JW, et al. Human breast cancer resistance protein: interactions with steroid drugs, hormones, the dietary carcinogen 2-amino-1-methyl-6-phenylimidazo(4,5-b)pyridine, and transport of cimetidine. *J Pharmacol Exp Ther* 2005;312:144-52.
156. Ishikawa T, Kasamatsu S, Hagiwara Y, Mitomo H, Kato R, Sumino Y. Expression and functional characterization of human ABC transporter ABCG2 variants in insect cells. *Drug Metab Pharmacokinet* 2003;18:194-202.
157. Cerveny L, Pavek P, Malakova J, Staud F, Fendrich Z. Lack of interactions between breast cancer resistance protein (bcrp/abcg2) and selected antiepileptic agents. *Epilepsia* 2006;47:461-8.
158. Schlatter P, Gutmann H, Drewe J. Primary porcine proximal tubular cells as a model for transepithelial drug transport in human kidney. *Eur J Pharm Sci* 2006;28:141-54.
159. van Herwaarden AE, Schinkel AH. The function of breast cancer resistance protein in epithelial barriers, stem cells and milk secretion of drugs and xenotoxins. *Trends Pharmacol Sci* 2006;27:10-6.
160. Zhang Y, Gupta A, Wang H, Zhou L, Vethanayagam RR, Unadkat JD, et al. BCRP transports dipyrindamole and is inhibited by calcium channel blockers. *Pharm Res* 2005;22:2023-34.
161. Kage K, Fujita T, Sugimoto Y. Role of Cys-603 in dimer/oligomer formation of the breast cancer resistance protein BCRP/ABCG2. *Cancer Sci* 2005;96:866-72.
162. Mitomo H, Kato R, Ito A, Kasamatsu S, Ikegami Y, Kii I, et al. A functional study on polymorphism of the ATP-binding cassette transporter ABCG2: critical role of arginine-482 in methotrexate transport. *Biochem J* 2003;373:767-74.
163. Robey RW, Honjo Y, van de Laar A, Miyake K, Regis JT, Litman T, et al. A functional assay for detection of the mitoxantrone resistance protein, MXR (ABCG2). *Biochim Biophys Acta* 2001;1512:171-82.
164. Bhatia A, Schafer HJ, Hrycyna CA. Oligomerization of the human ABC transporter ABCG2: evaluation of the native protein and chimeric dimers. *Biochemistry* 2005;44:10893-904.
165. Cisternino S, Mercier C, Bourasset F, Roux F, Scherrmann JM. Expression, up-regulation, and transport activity of the multidrug-resistance protein Abcg2 at the mouse blood-brain barrier. *Cancer Res* 2004;64:3296-301.
166. Islam MO, Kanemura Y, Tajria J, Mori H, Kobayashi S, Hara M, et al. Functional expression of ABCG2 transporter in human neural stem/progenitor cells. *Neurosci Res* 2005;52:75-82.
167. Rabindran SK, Ross DD, Doyle LA, Yang W, Greenberger LM. Fumitremorgin C reverses multidrug resistance in cells transfected with the breast cancer resistance protein. *Cancer Res* 2000;60:47-50.
168. Zhou XF, Yang X, Wang Q, Coburn RA, Morris ME. Effects of dihydropyridines and pyridines on multidrug resistance mediated by breast cancer resistance protein: in vitro and in vivo studies. *Drug Metab Dispos* 2005;33:1220-8.
169. Holst JJ, Orskov C, Nielsen OV, Schwartz TW. Truncated glucagon-like peptide I, an insulin-releasing hormone from the distal gut. *FEBS Lett* 1987;211:169-74.
170. Kreymann B, Williams G, Ghatei MA, Bloom SR. Glucagon-like peptide-1 7-36: a physiological incretin in man. *Lancet* 1987;2:1300-4.
171. Mojsov S, Heinrich G, Wilson IB, Ravazzola M, Orci L, Habener JF. Preproglucagon gene expression in pancreas and intestine diversifies at the level of post-translational processing. *J Biol Chem* 1986;261:11880-9.

172. Valverde I, Wang GS, Burghardt K, Kauri LM, Redondo A, Acitores A, et al. Bioactive GLP-1 in gut, receptor expression in pancreas, and insulin response to GLP-1 in diabetes-prone rats. *Endocrine* 2004;23:77-84.
173. Nauck MA, Meier JJ. Glucagon-like peptide 1 and its derivatives in the treatment of diabetes. *Regul Pept* 2005;128:135-48.
174. Goke R, Cole T, Conlon JM. Characterization of the receptor for glucagon-like peptide-1(7-36)amide on plasma membranes from rat insulinoma-derived cells by covalent cross-linking. *J Mol Endocrinol* 1989;2:93-8.
175. Lankat-Buttgereit B, Goke R, Stockmann F, Jiang J, Fehmann HC, Goke B. Detection of the human glucagon-like peptide 1(7-36) amide receptor on insulinoma-derived cell membranes. *Digestion* 1994;55:29-33.
176. Van Eyll B, Goke B, Wilmen A, Goke R. Exchange of W39 by A within the N-terminal extracellular domain of the GLP-1 receptor results in a loss of receptor function. *Peptides* 1996;17:565-70.
177. Widmann C, Dolci W, Thorens B. Agonist-induced internalization and recycling of the glucagon-like peptide-1 receptor in transfected fibroblasts and in insulinomas. *Biochem J* 1995;310 (Pt 1):203-14.
178. Widmann C, Dolci W, Thorens B. Desensitization and phosphorylation of the glucagon-like peptide-1 (GLP-1) receptor by GLP-1 and 4-phorbol 12-myristate 13-acetate. *Mol Endocrinol* 1996;10:62-75.
179. Wilmen A, Van Eyll B, Goke B, Goke R. Five out of six tryptophan residues in the N-terminal extracellular domain of the rat GLP-1 receptor are essential for its ability to bind GLP-1. *Peptides* 1997;18:301-5.
180. Holz GG. New insights concerning the glucose-dependent insulin secretagogue action of glucagon-like peptide-1 in pancreatic beta-cells. *Horm Metab Res* 2004;36:787-94.
181. Weir GC, Mojsov S, Hendrick GK, Habener JF. Glucagonlike peptide I (7-37) actions on endocrine pancreas. *Diabetes* 1989;38:338-42.
182. Vilsboll T, Agerso H, Krarup T, Holst JJ. Similar elimination rates of glucagon-like peptide-1 in obese type 2 diabetic patients and healthy subjects. *J Clin Endocrinol Metab* 2003;88:220-4.
183. Stange T, Kettmann U, Holzhausen HJ. Immunoelectron microscopic demonstration of the membrane proteases aminopeptidase N/CD13 and dipeptidyl peptidase IV/CD26 in normal and neoplastic renal parenchymal tissues and cells. *Eur J Histochem* 2000;44:157-64.
184. Helbert MJ, Dauwe SE, Van der Biest I, Nouwen EJ, De Broe ME. Immunodissection of the human proximal nephron: flow sorting of S1S2S3, S1S2 and S3 proximal tubular cells. *Kidney Int* 1997;52:414-28.
185. Baer PC, Tunn UW, Nunez G, Scherberich JE, Geiger H. Transdifferentiation of distal but not proximal tubular epithelial cells from human kidney in culture. *Exp Nephrol* 1999;7:306-13.
186. Stange T, Kettmann U, Holzhausen HJ. Immunoelectron microscopic single and double labelling of aminopeptidase N (CD 13) and dipeptidyl peptidase IV (CD 26). *Acta Histochem* 1996;98:323-31.
187. Gutzwiller JP, Drewe J, Göke B, Schmidt H, Rohrer B, Lareida J, et al. Glucagon-like peptide-1 promotes satiety and reduces food intake in patients with diabetes mellitus type 2. *Am J Physiol* 1999;276:R1541-4.
188. Gutzwiller JP, Tschopp S, Bock A, Zehnder CE, Huber AR, Kreyenbuehl M, et al. Glucagon-like peptide 1 induces natriuresis in healthy subjects and in insulin-resistant obese men. *J Clin Endocrinol Metab* 2004;89:3055-61.

189. Moreno C, Mistry M, Roman RJ. Renal effects of glucagon-like peptide in rats. *Eur J Pharmacol* 2002;434:163-7.
190. Yu M, Moreno C, Hoagland KM, Dahly A, Ditter K, Mistry M, et al. Antihypertensive effect of glucagon-like peptide 1 in Dahl salt-sensitive rats. *J Hypertens* 2003;21:1125-35.
191. Greger R. Physiology of renal sodium transport. *Am J Med Sci* 2000;319:51-62.
192. Bullock BP, Heller RS, Habener JF. Tissue distribution of messenger ribonucleic acid encoding the rat glucagon-like peptide-1 receptor. *Endocrinology* 1996;137:2968-78.
193. Campos RV, Lee YC, Drucker DJ. Divergent tissue-specific and developmental expression of receptors for glucagon and glucagon-like peptide-1 in the mouse. *Endocrinology* 1994;134:2156-64.
194. Dunphy JL, Taylor RG, Fuller PJ. Tissue distribution of rat glucagon receptor and GLP-1 receptor gene expression. *Mol Cell Endocrinol* 1998;141:179-86.
195. Yamato E, Ikegami H, Takekawa K, Fujisawa T, Nakagawa Y, Hamada Y, et al. Tissue-specific and glucose-dependent expression of receptor genes for glucagon and glucagon-like peptide-1 (GLP-1). *Horm Metab Res* 1997;29:56-9.
196. Yoo-Warren H, Willse AG, Hancock N, Hull J, McCaleb M, Livingston JN. Regulation of rat glucagon receptor expression. *Biochem Biophys Res Commun* 1994;205:347-53.
197. Wei Y, Mojsov S. Tissue-specific expression of the human receptor for glucagon-like peptide-I: brain, heart and pancreatic forms have the same deduced amino acid sequences. *FEBS Lett* 1995;358:219-24.
198. Ruiz-Grande C, Alarcon C, Alcantara A, Castilla C, Lopez Novoa JM, Villanueva-Penacarrillo ML, et al. Renal catabolism of truncated glucagon-like peptide 1. *Horm Metab Res* 1993;25:612-6.
199. Degn KB, Brock B, Juhl CB, Djurhuus CB, Grubert J, Kim D, et al. Effect of intravenous infusion of exenatide (synthetic exendin-4) on glucose-dependent insulin secretion and counterregulation during hypoglycemia. *Diabetes* 2004;53:2397-403.
200. Ahren B, Schmitz O. GLP-1 receptor agonists and DPP-4 inhibitors in the treatment of type 2 diabetes. *Horm Metab Res* 2004;36:867-76.
201. Nielsen LL, Young AA, Parkes DG. Pharmacology of exenatide (synthetic exendin-4): a potential therapeutic for improved glycemic control of type 2 diabetes. *Regul Pept* 2004;117:77-88.
202. Nielsen LL, Baron AD. Pharmacology of exenatide (synthetic exendin-4) for the treatment of type 2 diabetes. *Curr Opin Investig Drugs* 2003;4:401-5.
203. Sindic A, Schlatter E. Mechanisms of actions of guanylin peptides in the kidney. *Pflugers Arch* 2005;450:283-91.
204. Dickson M, Gagnon JP. Key factors in the rising cost of new drug discovery and development. *Nat Rev Drug Discov* 2004;3:417-29.

# Curriculum vitae

## Particulars

Name: Philipp Schlatter  
Address: Badplatzweg 13  
4323 Wallbach

Phone: home: +41 (0)61 421 34 69  
mobile: +41 (0)79 708 12 52

E-Mail: ph.schlatter@tele2.ch

Date of Birth: 6<sup>th</sup> march 1978  
Citizenship: Switzerland, Basel (former St. Gallen)  
Marital status: Married, 3 children



## Languages

German Native language  
Finnish Native language  
English Very good skills  
French Adequate skills

## Education

Sept. 2003 – Sept. 2006 Dissertation at the University of Basel in **Clinical Pharmacology and Toxicology** supervised by Prof. Jürgen Drewe

- Assay development & validation of an in-vitro primary cell culture
- Screening of drug-drug interaction in kidney cells
- Effect of glucagon like peptide 1 (GLP-1) on proximal tubular cells
- Validation of a new HPLC assay according to FDA guidelines
- Pre-formulation of a herbal extract
- Assistance in two clinical trials (Phase I-II)

February - May 2003 Military school in the **paramedic** troops with education as a specialist, Swiss army

1997 - 2002 University of Basel, study of **pharmacy**, including:

- Apprenticeship of one year in City Pharmacy, Basel (**customer care, dispensing, analytics**)
- Diploma-thesis on polymorphism and crystallisation of Paracetamol at Solvias AG, Basel (Raman, thermo-analysis, basic crystalliser)

1994 - 1997 **Brussels**, grammar school of German School  
1990 - 1994 **Helsinki**, grammar school of German School  
1985 - 1989 **Vienna**, Austrian primary school and grammar school  
1982 - 1985 **Lagos**, kindergarten and primary school of German School  
1981 - 1982 **Beirut**, kindergarten of German School

## Qualifications

November 2004	Basel, Education course with passed exam in “ <b>Key issues in drug discovery &amp; development</b> ”
Sept. – Oct. 2004	Zürich, Education course: <b>Strategies</b> and <b>trends</b> in pharmaceutical development and production
April 2003	Tesserete, specialist for „Behandlungsstelle“ in the <b>paramedic</b> troops, Swiss army
November 2002	University of Basel, <b>Master of pharmacy</b>
September 1997	University of Basel, „eidgenössische Maturitätsergänzungsprüfungen“ in Swiss history and geography
May 1997	Brussels, <b>German Abitur</b>

## Professional training and experiences

from 16.10.2006	<b>Clinical Trial Specialist</b> , Roche Pharma Switzerland, Reinach
May - September 2005	<b>Supervision</b> of diploma thesis, Anne Pulver: Screening of transporters in the porcine proximal tubule cell line LLC-PK1
Feb. - July 2004	<b>Supervision</b> of diploma thesis, Dorina Saurer: Development of a HPLC assay for cannabinoids, extraction of cannabis-ingredients, production of an oral cannabis formulation.
since 1.9.2003	<b>Pharmacist</b> , University Hospital Basel <ul style="list-style-type: none"><li>• Handling and responding to internal &amp; external inquiries about <b>drug safety</b>, interaction potentials</li><li>• Conducting therapeutic drug monitoring including <b>advisory service</b></li><li>• <b>Presentation</b> of interesting and complex cases to medical professionals</li><li>• Mammalian <b>cell cultivation</b>, immunohistochemistry, immunocytochemistry with <b>confocal microscopy</b>, quantitative RT-PCR, Western blot analysis, functional transport activity measurements with radioactive and fluorescent substances</li><li>• <b>Supervision</b> of the practical course in “Pharmacology and Toxicology”</li></ul>
Dec. 2002- Jan. 2003	<b>Pharmacist</b> , part time at Dorf-Pharmacy in Pratteln, Vindonissa-Pharmacy in Windisch and Aare-Pharmacy in Rombach <ul style="list-style-type: none"><li>• Pharmacist <b>in charge</b></li><li>• Customer care</li><li>• Dispensing</li></ul>
2000-2002	<b>Proxy</b> as pharmacist assistant in City-, Tell-, Epa-pharmacies in Basel

## Voluntary services

since July 2004	Honorary <b>supervisor</b> of the young men in church
Oct. 2003 - July 2004	Honorary institute <b>teacher</b> for adults
Aug. 2002- Sept. 2003	Honorary <b>counsellor</b> of the young men in church
Aug. 2001- July 2002	Honorary seminary <b>teacher</b> for the youth
2000-2002	Honorary <b>chair</b> asep (association suisse des étudiants en pharmacie) Achieved goals: <ul style="list-style-type: none"><li>• Strengthened relationship with the <b>Swiss Association of Pharmacists (SAV)</b> and <b>Swiss Society of Industrial Pharmacist (GSIA)</b></li><li>• <b>National promotion</b> for pharmacy studies in cooperation with the Swiss Association of Pharmacists (SAV) including flyers, posters and public advertisements in news papers and cinemas</li></ul>

## Membership in academic society

Since 2000	Swiss Association of Pharmacists
------------	----------------------------------

## Computer literacy

Microsoft Office (Word, Excel, Powerpoint), Outlook Express, Eudora, Opera, Internet Explorer, Endnote, Origin, Isis Draw, Primer Express, NIH Image, Laser Scanning Microscope LSM510 software, Ulead PhotoExpress, Adobe Photoshop, siViewer.

## Publication

Schlatter P, Gutmann H, Drewe J. Primary porcine proximal tubular cells as a model for transepithelial drug transport in human kidney. Eur J Pharm Sci. 2006 May;28(1-2):141-54.

Schlatter P., Beglinger C., Drewe J. , Gutmann H. Glucagon-like peptide 1 receptor expression in primary porcine proximal tubular cells. Submitted to Regulatory Peptides.

Schlatter P., Gutmann H, Drewe J. Functional expression of BMDP in kidney. Submitted to Cellular and Molecular Life Sciences.

## Grant

**Senglet**-foundation „zur Förderung des pharmazeutischen  
Nachwuchses in Basel“, 2004/2005

Wallbach, 9<sup>th</sup> october 2006, \_\_\_\_\_  
Philipp Schlatter